6-3-2011

Antibacterial activity of conjugated electrolytes

Thomas S. Corbitt

Thomas S. Corbitt
Candidate

Chemistry and Chemical Biology
Department

This dissertation is approved, and it is acceptable in quality and form for publication:

Approved by the Dissertation Committee:

_____, Chairperson

_____

_____

_____

_____

_____

_____

_____

_____

ANTIBACTERIAL ACTIVITY
OF
CONJUGATED ELECTROLYTES

BY

THOMAS S. CORBITT

B.S., Chemistry, Valdosta State College, 1990

DISSERTATION

Submitted in Partial Fulfillment of the
Requirements for the Degree of

Doctor of Philosophy
Chemistry and Chemical Biology

The University of New Mexico
Albuquerque, New Mexico

May, 2010

DEDICATION

This work is dedicated to the memory of my parents, Hillman and Menna Lee Corbitt, whose patience, diligence and commitment to God, family and the land provided my secure foundation and yielded a legacy that will persevere.

ACKNOWLEDGMENTS

I am eternally grateful to Dr. David G. Whitten, my research advisor and mentor, for his insuperable patience and unwavering support and encouragement throughout this research project. His approachability and caring promote the human relationship, while his drive for understanding, guidance in research methodology and clear and concise communication style demonstrate that he is a consummate scientist as well.

I am sincerely thankful to Dr. Julia Fulghum for offering me the opportunity to reconnect with the academic world to complete my studies. Her facility in overcoming administrative hurdles and her cheerfulness and undaunted optimism made me realize that it *was* possible after all.

Many thanks also to Dr. David Keller, Dr. Steve Cabaniss and Dr. Kirk Schanze for their encouragement, support and valuable recommendations pertaining to these research studies.

This is obviously not my work alone, but results from the input, guidance and hard work of my mentors and co-workers. I am most grateful to my fellow group members and collaborators, Sireesha Chemburu, Liping Ding, Lance Edens, Eric Hill, Linnea Ista, Eunkyung Ji, Sarah McQuate, Katsu Ogawa, Jonathon Sommer, Yanli Tang, Ying Wang, Kristen Wilde and Zhijun Zhou for the discussion, encouragement and generous supplies of bacteria and conjugated electrolytes. And to the cadre of engineers and scientists in the Center for Biomedical Engineering: thanks for your comradery and those occasional critical loans of equipment, devices, utensils, etc.

To my family, especially my siblings, Steve, Lana and Bruce, and my in-laws Fred and Sharon, who gave me immeasurable support over the years—I can't overstate how important your encouragement has been and how much you are loved and appreciated.

To my loving children, Patricia, Justine and Wesley—you are inspirations to me daily. I look on in awe and amazement at the wonderful persons you are becoming and know that I am so blessed to have you in my life.

To my wife, Heather: you've been patiently waiting for this, all the while encouraging and supporting my endeavors and our marriage. Working together with you through the years, raising our children and planning our dreams together has made me realize what an amazing gift your love is. I can say without reservation, without hesitation, that I would do it all again—with you. (Sounds like there's a song in there somewhere.)

To the others who have touched my life during this journey: Jacqueline Agnew, Mark Alexander, Brett Andrzejewski, Leo Archer, Al Artiaga, Ed Bagwell, Zsolt Bencze, Gordon Boone, Ruth Boone, Clive Chandler, Denise Chavez, Kai L. Chiu, Val Christianson, The Leningrad Cowboys, Dick Crooks, Kevin Cushing, Phil Duran, Debi Evans, Patrick Fleig, Tom Gamble, Tony Garcia, John W. Garvey, Dorothy Gillespie, Aree Hanprasopwattana, Sam Haskins, Julian Haskins, Ron Hooks, Mickey Jojola, Hal Lankford, John L. Lindsey, Gabriel Garcia Marquez, J. Charles McCrea, Christopher Merchant, J.J. Michelitch, Nancy Mobley, Monte Monteith, Don Montoya, Os Morgan, Timothy Morris, Randy Nethers, Eric Nuttall, Paul & Becky O'Brien, Gwen Osaki, Bryan Parisien, Neil Peart, Dean Pershall, Clifford Qualls, Lyle Reece, Rainer Maria Rilke,

Christophe Roger, Jonathan K. Schoer, Guihua Shang, Scott Sharp, Li Sun, Srinivasan Sundararajan, Yanli Tang, Bruce Thompson, Dorothy Treadwell, Nader Vadiee, Karen Vaught-Alexander, and James Wilson. My sincerest apologies to those that I have omitted; your memories are most certainly rattling around amongst my synapses somewhere.

And finally, I am grateful for financial and facilities support from the following sources:

Defense Threat Reduction Agency (DTRA), contract # W911NF-07-1-0079
Bureau of Indian Affairs for leave time
NSF IGERT CORE Fellowship
Office of Naval Research, AASERT and grant # N00014-05-1-0743
The W.M. Keck Confocal Microscopy Facility of the UNM Keck Nanofluidics Laboratory

ANTIBACTERIAL ACTIVITY
OF
CONJUGATED ELECTROLYTES

BY

THOMAS S. CORBITT

ABSTRACT OF DISSERTATION

Submitted in Partial Fulfillment of the
Requirements for the Degree of

Doctor of Philosophy
Chemistry and Chemical Biology

The University of New Mexico
Albuquerque, New Mexico

May, 2010

ANTIBACTERIAL ACTIVITY OF CONJUGATED ELECTROLYTES

by

Thomas S. Corbitt

Center for Biomedical Engineering
Department of Chemistry and Chemical Biology
University of New Mexico

2010

B.S. CHEMISTRY
PH.D. CHEMISTRY & CHEMICAL BIOLOGY

ABSTRACT

A series of water soluble, cationic, anionic and zwitterionic conjugated polyelectrolytes (CPEs) with main chains based on an arylene ethynylene repeat unit structure with tetraalkylammonium and/or alkylsulfonate side groups were found to exhibit significant antibacterial activity. A number of these complexes also showed pronounced light-induced modulation of their effectiveness, with either biocidal enhancement or suppression, depending on such properties as singlet oxygen sensitization potential and lipophilicity.

These collected studies examine the biocidal activity of the CPEs, as determined by Confocal Laser Scanning Microscopy (CLSM) and Flow Cytometry, correlating this activity with the photophysical properties of the polymers. We demonstrate biocidal activity, both in solution and immobilized, of similar ionic conjugated polyelectrolytes. These polymers were tested and shown to be effective in solution, physisorbed or surface grafted on non-porous borosilicate microspheres and grafted on fabrics.

Also, studies with templated hollow spheres formed from polymer multilayers show considerable bacterial sequestration and significant biocidal activity, especially upon light exposure. The effective killing of *Cobetia marina*, *Pseudomonas aeruginosa* and *Bacillus atrophaeus* in these systems is also correlated with a requirement for oxygen suggesting that interfacial generation of singlet oxygen is the crucial step in the light-induced biocidal activity.

This document begins with an introduction to the problem, including a review of literature. This is followed by an experimental section describing in detail the selection, growth and harvesting parameters for the bacteria and a summary of substrate preparation protocols. A number of biocidal experiments using a variety of compounds and substrates and evaluated with confocal microscopy and flow cytometry are then covered, followed by conclusions and future directions.

TABLE OF CONTENTS

LIST OF FIGURES

LIST OF TABLES AND SCHEMA

ACRONYMS & ABBREVIATIONS

µRM	micro“Roach Motels”
AFM	atomic force microscope
AMP	antimicrobial peptide
ATCC	American type culture collection
ATP	adenosine triphosphate
CHDDE	1,3-cyclohexadiene-1,4-diethanoate
CLSM	confocal laser scanning microscope
CPE	conjugated polyelectrolyte
DABCO	diazabicyclooctyl
DMF	dimethylformamide
DMPC	dimyristoylphosphatidylcholine
DMSO	dimethylsulfoxide
DNA	deoxyribonucleic acid
DOPG	dioleoylphosphatidylglycerol
FSC	forward scatter
ICU	intensive care unit
LbL	layer-by-layer
MA	marine agar
MB	marine broth
MBMMG	modified basic marine medium plus glycerol
OPE	oligo-phenylene ethynylene
PAMCM	*Pseudomonas aeruginosa* minimal citrate medium
PAO	phosphate accumulating organism
PBS	phosphate buffered saline
PEM	polyelectrolyte multilayer
PG-1	protegrin-1
PMT	photomultiplier tube
PPE	polyphenylene ethynylene
ROS	reactive oxygen species
SEM	scanning electron microscope
SGCP	surface grafted conjugated polyelectrolyte
SSC	side scatter
SYTO	trade name for Molecular Probes' cell membrane permeant dyes
SYTOX	trade name for Molecular Probes' cell membrane impermeant dyes
TAO	total acronym overload
TEM	transmission electron microscope
TPPS	5,10,15,20-tetrakis(4-sulfonatophenyl)porphyrin
UV	ultraviolet

Chapter 1

The Need for Antimicrobials

Introduction

Since the beginning, presumably, mankind has done battle with the elements of nature, including fellow creatures, both big and small. Some of the tiniest of these have proven to be the greatest foes, with viruses and bacteria killing far more humans than all of our wars. Even now, in an age when our mastery of chemical synthesis and our understanding of biological systems are greater than ever before, we find these enemies to be more adaptable and persistent than anyone would have predicted when antibiotics were first discovered.

The control of these pathogens is a major challenge for the household and community, in the hospital environment and for developing defenses against intentional release by terrorists or in warfare. The appearance of new antibiotic resistant bacterial strains that cannot be defeated by our current arsenal of drugs elevates the problem to another level. The virulence and drug-resistance of some of these (Methicillin Resistant *Staphylococcus aureus* (MRSA), *Clostridium difficile* and *Pseudomonas aeruginosa*, for example) are on the increase.(12, 18, 31, 44, 79, 86, 106, 191) There are several contributing human/social factors: overuse of antibiotics (overprescribed, self-medication, high dosing in animal populations); underuse of antibiotics (lack of access, inadequate dosing, poor adherence to dosing, and substandard antimicrobials); urbanization/overcrowding and poor sanitation among ever-increasing population densities; and an extensive global travel network with increased ease, speed and

interconnectedness of transportation, enabling disease to spread rapidly from distant areas.

As for the microbes themselves, a great number of them have an impressive ability to survive the assaults visited on them by various antibiotics, antimicrobials and disinfectants and emerge with some form of defense which is passed along to their progeny and occasionally even shared with other species. Given their ubiquity and, in many cases, increasing virulence, the ability to destroy the pathogenic organisms that cause infectious disease is a matter of critical concern to human society. Unfortunately, there are now pathogens emerging with resistance to some or all of the "front-line" antibiotic and antibacterial agents. This bacterial resistance to antibiotics is obviously a cause of great concern, especially since the occurrence of nosocomial (hospital-acquired) infections in the U.S. alone now amounts to 2 million new cases annually, resulting in over 90,000 deaths and more than 5 billion dollars of added healthcare costs.(132, 143, 26, 86)

Methods of microbial control

There are numerous approaches to the elimination of microbial agents external to the human body. These can be grouped into two general types: physical/mechanical—heat, filtration, scrubbing (usually with a surfactant to aid in dislodging the microbes)—and chemical, where compounds which are toxic to the organism of interest (and often to other organisms, including humans) are employed (Table 1-1). These may be combined to increase the overall efficacy of the process. Unfortunately, most of these methods involve temporary or intermittent processes that typically require periodic renewal of their components. This leaves a window for resistant microbes to multiply, eventually

increasing in population to a point where the method may be rendered less effective and potentially thwarted.(106, 191, 145, 209, 172, 125, 41).

Table 1-1. Physical and Chemical Antimicrobials (23, 201)

physical	**chemical**
autoclaving	alcohols
desiccation	aldehydes
heat (dry or moist)	halogens
filtration	heavy metals
freezing	organic acids
ionizing radiation (UV/gamma)	oxidizing agents
	penetrating toxic gases
	phenolic compounds
	quaternary ammonium compounds

In the scope of this discussion, our focus will be on chemicals for microbial control and elimination. These chemical agents are called by many names, including biocides, microbicides, antimicrobials, antiseptics, sanitizers, disinfectants, antibacterials. While there may be subtle differences in the meanings of these terms, with biocide being the broadest, most are used somewhat interchangeably, as I have used them throughout this document. Strictly speaking, for our experimental system (having only been tested on bacteria so far), the latter term, antibacterial, is the most appropriate.

Chemical biocides have been employed for centuries, first in the form of naturally occurring agents like salts, vinegar and honey. Later, the halogens (in the form of hypochlorite and iodine tincture) found use as general and wound disinfectants, alcohol as a skin disinfectant and phenol in antiseptic surgery. From there, the field has burgeoned with the use of synthetic antimicrobials from many different chemical families—iodophors, biguanides, bisphenols, aldehydes, isothiazolones, tetracyclines, chloramphenicol, beta-lactams, glycopeptides, and 4-quinolones, just to name a few—

many of which are derived from naturally-occurring sources. Some of these are listed in Scheme 1-1, assembled by Cloete, which groups a number of these agents matched to their active sites/primary mechanisms.

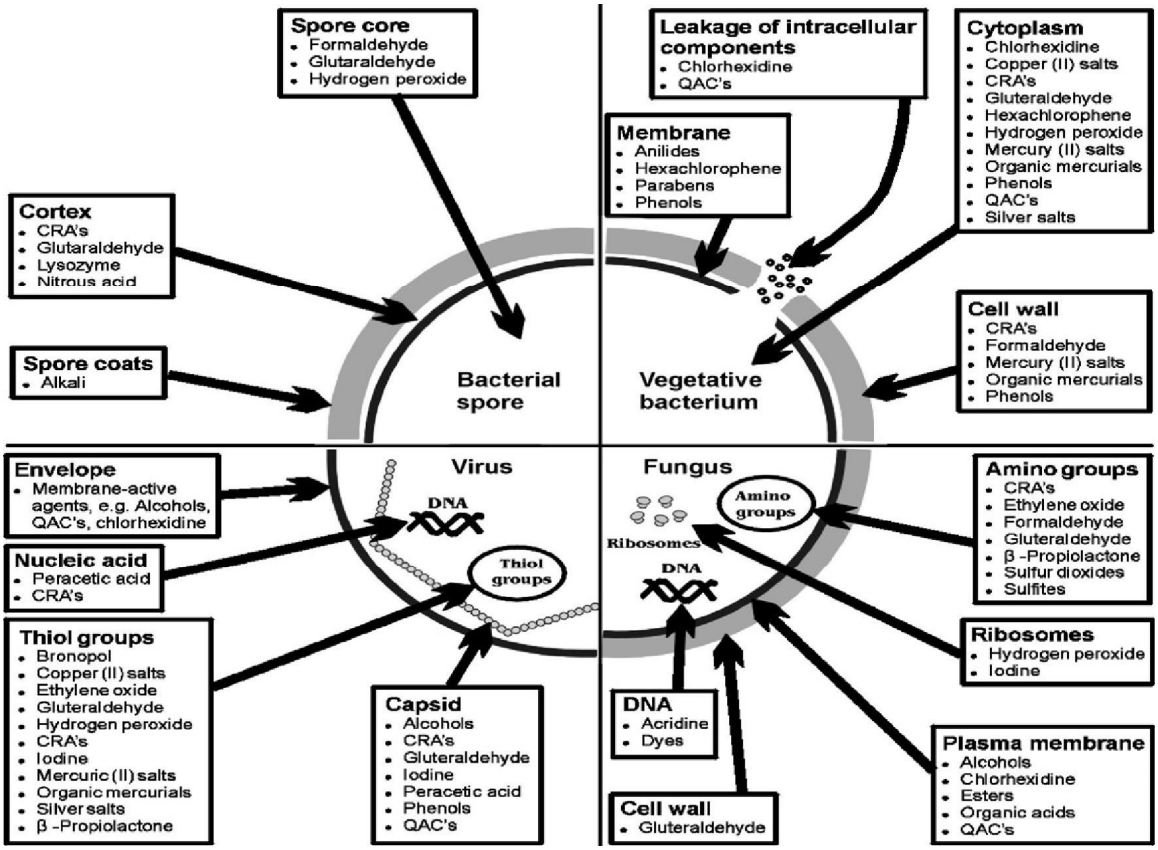

Scheme 1-1. An overview of some commonly used biocides and their active sites in the target organisms. (41)

Much recent research has been directed towards the identification and development of catalytic antimicrobial coatings that can capture, entrap and kill pathogens, especially pathogenic Gram negative bacteria and bacterial spores.(34, 208, 2, 8, 178) These coatings and materials may have important applications in healthcare settings for sterilization of medical devices, disinfection of surfaces and liquids, and skin antisepsis.(200, 218, 117, 131, 128) Several biocidal materials have been developed wherein the biocidal material releases an “active” reagent such as an antibiotic, iodine,

phenols or heavy metals such as silver, tin or mercury. These conventional antimicrobials act by diffusing into the cell and disrupting essential cell functions; this requires the release of the antimicrobial from the matrix.(21, 29, 69, 87, 142, 192) One drawback of these "leachable" biocides is that the reagents have a finite lifetime and are either rendered useless or must be "recharged" once the leachable component has been exhausted.(100, 132) Also, some of the leachable components may themselves become environmental hazards.(24, 88, 123) Another problem with the environmental dissemination of current antimicrobials which target specific cellular metabolic processes is that they provide selective pressure for the development of antibiotic resistance.(57, 74, 180)

These growing problems have led to the need for the development of non-leachable self-sterilizing surfaces(121, 170, 181, 100, 115, 103, 153, 8, 149) and interfacial coatings (solid-liquid and solid-vapor) that exhibit efficient biocidal activity against a variety of bacteria, bacterial spores and other agents.(142, 128) In contrast to the leachable agents, biocides immobilized on a surface can be continuously active or reusable and may prevent uncontrolled material release to the environment.(113, 100, 103, 8) Among the systems that have been proposed and/or developed are metal ion containing formulations (29, 192, 98, 69, 87, 43, 21, 102) (which should be monitored over their lifetimes to ensure that release is minimized, as referenced in the previous paragraph), coated and uncoated semiconductor particles,(29, 69) and polymer blends or surfactants containing pendant reactive organic functionalities (quaternary ammonium groups, hydantoins, tetramisole derivatives or alkyl pyridinium structures) that may or may not require additional reagents for activation of biocidal function.(213, 77, 217, 211,

187, 76, 39, 78, 200, 130, 121, 181, 140, 34, 113) Bacterial killing based on physical interaction (mechanical damage) with carbon nanotubes has also been noted.(94)

As previously mentioned, the defensive mechanisms of pathogenic bacteria are numerous and varied. The formidable barrier of the bacterial cell membranes, metabolically redundant systems, robust repair mechanisms and simple avoidance of harm through quiescence (only rapidly dividing cells are susceptible to metabolic processing of drugs) are difficult to bypass. Other sundry processes that promote antimicrobial resistance include: rapid transfer of resistance genes (plasmid exchange), alteration of target biomolecules or metabolic pathways, antibiotic cleavage (penicillinase), chemical traps and removal processes, such as efflux pumping (active transport—uses ATP) and biofilm formation (initiated by quorum sensing).

Defeating these physico-chemical barriers, including the manifold individual cell membrane components and the higher complexity interactive structures of biofilms, has been a focus of work for our group and several others for a number of years now. Some of the tools for investigating many of the biocidal phenomena have only become widely available and/or more affordable very recently. These include various types of high resolution optical devices, such as laser scanning confocal microscopy. This technique doesn't drastically perturb the system of study, as TEM and SEM tend to do with many biological samples. In addition, the improved specificity and sophistication of stains, the availability and reliability of atomic force microscopy (AFM), and increased understanding of cell structure and metabolism, including the identification and isolation of membrane components, have contributed to these efforts.

Development of new biocides.

One possibility for a persistent, broad-spectrum solution is to create an active surface that can sequester and/or kill the microbes on contact and is not damaged or leached away under mild cleaning conditions.(137, 200, 129, 120, 71) Designing a surface that is robust and long-lived and that is active or can be activated on demand requires understanding and some degree of control over bulk and surface properties. The practice of manipulating materials on ever-decreasing scales has led to the possibility of systematically controlling the architecture of nanostructures using individual molecules as components. In terms of interaction with bacteria, this means that size, functionality, density, and even tertiary structures can be tailored for the purpose of increasing the biocidal characteristics of a given system. This is predicated on having some empirical evidence for disinfection by a class of compounds and/or on the understanding of the biocidal mechanism exhibited.(99, 3, 11, 42, 107) This is a sweeping approach, potentially producing prophylaxes that exhibit biocidal activity which could help to reduce exposures and propagation of the diseases caused by these microbes.

Cationic polymers are one such family of materials found to be effective as long-lasting antimicrobials and biocides. Some of these compounds are increasingly used to reduce environmental impact in certain applications.(199) Among the advantages of such polymers over monomeric and small molecule organic biocides such as glutaraldehyde and chloroxylenol are lower residual toxicity, increased lifetimes and increased specificity.(96) Cationic biocidal polymers are thought to function by associating with negatively charged bacteria, permeating the bacterial cell wall and physically disrupting the underlying cell membrane.(101, 111, 200, 85) The physical mechanism resulting in

membrane disruption has been suggested to involve association of the cationic groups with the phospholipid bilayer membrane followed by an ion exchange process in which the organic cations exchange with inorganic cations resulting in a destabilization of the membrane and subsequent pore formation or collapse.(85, 152)

In order to investigate the mechanism for biocidal activity, a number of researchers have undertaken experiments to build biomimetic membrane systems to probe with potential antimicrobial compounds. Their efforts have yielded model systems for representing membrane bilayers, as well as experiments where those models have been challenged by antimicrobial compounds both natural and synthetic.

Two such naturally occurring compounds are magainin (Figure 1-1) and protegrin-1 (PG-1) which have been dubbed antimicrobial peptides or AMPs. The R-helical magainin (isolated from frogs) and α-sheet PG-1 both fold into secondary structures that concentrate charges and nonpolar groups into separate areas. These unique properties apparently enable them move through the outer lipopolysaccharides and to strongly interact with the phospholipids of Gram negative bacterial cellular membranes, to the point of dispersion and eventual perforation of the cell wall. New families of synthetic compounds that build on the active properties of these natural products are also being developed.(11, 68, 193)

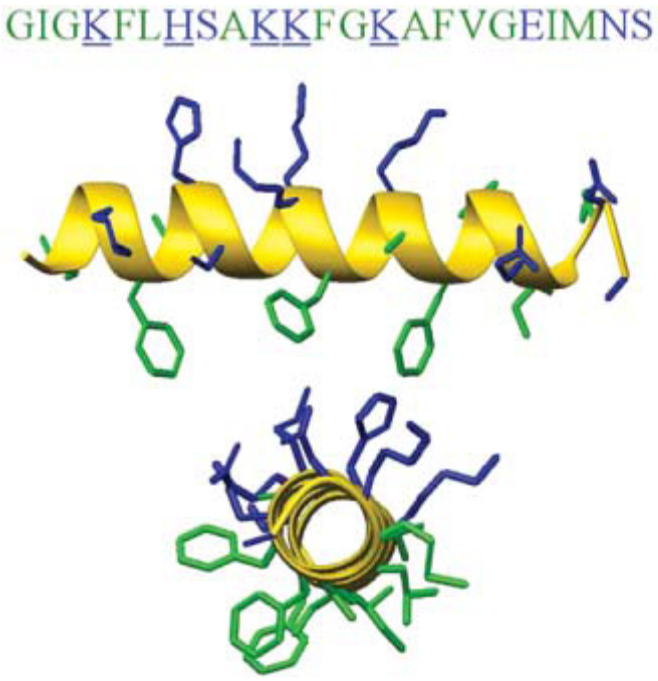

Figure 1-1. Primary sequence of magainin-2 with side and end-on representations based on structures in the protein database. Blue and green side groups represent polar and hydrophobic non-polar amino acids, respectively, with the cationic amino acids underlined. The secondary structure illustrates the facially amphiphilic arrangement of polar and non-polar residues along the helical backbone, which is in yellow. (66) The amino acids of magainin-2 that contribute to its facially amphiphilic properties are: K-lysine, H-histidine, E-glutamic acid, N-asparagine, S-serine, G-glycine, I-isoleucine, F-phenylalanine, L-leucine, A-alanine, V-valine, M-methionine. Of these, K, H and E are charged, while N and S are polar. These are labeled in blue and mostly occupy the upper (as oriented here) surface. The non-polar G, I, F, L, A, V, and M are labeled in green and are consigned to the bottom surface.

Some new families of cationic polymers that are loosely related to the naturally occurring peptides have recently garnered a great deal of interest because of their broad spectrum activity against bacterial agents. This activity arises from the targeting of the lipid bilayers of cell membranes rather than specific protein receptors, leading to the disordering and destabilization of the cell membrane. The characteristic chemical and structural properties of these compounds allow selective interaction and subsequent disruption of bacterial cell membranes. The mechanistic details of pathogenic interaction

of both the naturally-occurring and synthetic polymers are only partially understood and have been the subject of considerable debate in the literature.(32, 41, 42, 54, 101, 122, 159, 172, 208)

Chemical structures and properties

Related work herein is being done with a family of conjugated polyelectrolytes (CPEs), specifically, polyphenylene ethynylene (PPE) based compounds, synthesized at the University of Florida by the Schanze group, and oligo phenylene ethynylene (OPE) compounds, developed here at the University of New Mexico by the Whitten group. Both types of compounds have been spectroscopically characterized and investigated for their biocidal properties. The ability to study antibacterial efficacy of these compounds, establish relevant structure-property relationships and design new polymers or oligomers based on this information is a strength of this team effort.

Conjugated polyelectrolytes have gained significant attention due to their unique materials and photophysical properties.(171, 124, 198, 83, 222) In particular, CPEs are soluble in water and polar organic solvents, and the presence of the ionic solubilizing groups allows the polymers to interact strongly with ions in solution and with charged planar or colloid surfaces. Due to their relatively high carbon atom to ionic group ratio, CPEs can be considered to be amphiphiles. They self-assemble into nanoscale aggregates in aqueous solution and adsorb strongly to charged substrates, forming films that can be tailored on the nanoscale. In addition to these interesting and useful materials properties, CPEs also have favorable photophysical properties such as efficient light harvesting ability (large absorption coefficients), rapid singlet exciton diffusion along the conjugated backbone, high fluorescence quantum yields, and an amplified fluorescence

quenching effect.(222, 40, 195, 196) Such desirable characteristics of CPEs have led to their use a variety of applications including chemo- and bio- sensors(222, 151), photovoltaic devices(90, 197), and light-activated antimicrobial materials.(126, 37, 47, 46)

The commonality between these CPEs and the AMPs is their cationic and/or amphiphilic nature. The CPE polymers (Figure 1-2, Figure 1-3, Figure 1-4 and Figure 1-5), oligomers (Figure 1-6) and polyampholytes (Scheme 8-1) used in these studies are designed to contain both charged groups (quaternary ammonium or sulfonate) and nonpolar groups along a rigid, primarily linear backbone. These studies appear to indicate that a defined secondary structure, such as a helix or sheet, is not essential to the biocidal functionality. In either case, little is known about the direct interaction of the biocidal agents with the cell membrane.

These CPE compounds have an additional property of relevance to their antimicrobial activity: some of them have been found to produce singlet oxygen ($^1O_2^*$) in solution when exposed to visible and near-UV light in the 365-500 nm range. Presumably this energetic species can either directly attack a membrane in proximity or can generate other reactive (and longer-lived) species which ultimately degrade the membrane.(133, 141, 202, 206) These species have also been shown to be effective in destroying viruses, spores and chemical agents (194, 53, 82, 169), making them a potentially broad-spectrum solution for a number of threats, depending on their engineered delivery mechanisms.

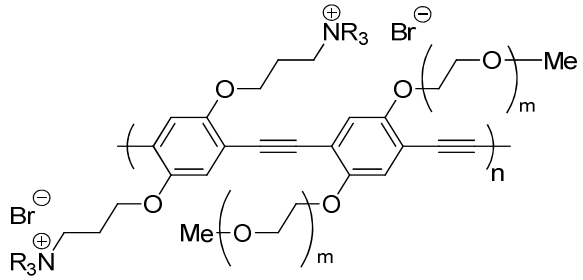

1a : R = Me, m = 2
1b : R = Et, m = 3

Figure 1-2. Structure of polyphenylene ethynylene molecules first used in the antimicrobial studies, referred to as PPE-OR8 (**1a**) and PPE-OR11 (**1b**). These compounds have phenylene units (separated by ethynyls) containing alternate functionalization: oligo ethylene glycols terminated with a methyl group adjacent to a propyl ether terminated with a trialkylammonium group.

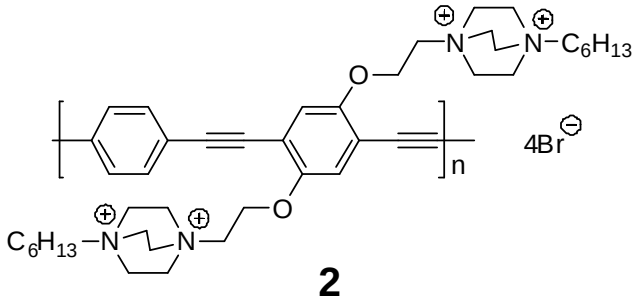

2

Figure 1-3. The structure of compound **2**, referred to as PPE-DABCO, omits the oligo ethylene glycols and has an ether-linked doubly charged diazabicyclooctyl moiety terminated with a hexyl group.

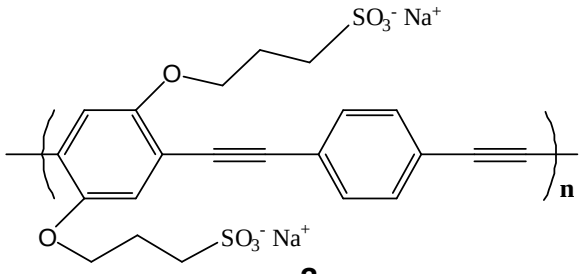

3

Figure 1-4. Polymer compound **3**, a negatively charged polyphenylene ethynylene molecule used in these studies. The structure is somewhat analogous to compound 1, with sulfonate groups instead of the ammoniums and without the alternating oligo ethylene glycols.

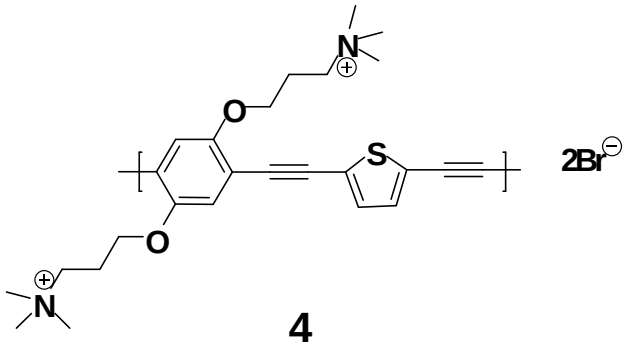

4

Figure 1-5. Structure of CPE **4** with thiophenyl groups alternating with phenylene along the backbone of the polymer. Herein referred to as PPE-Th.

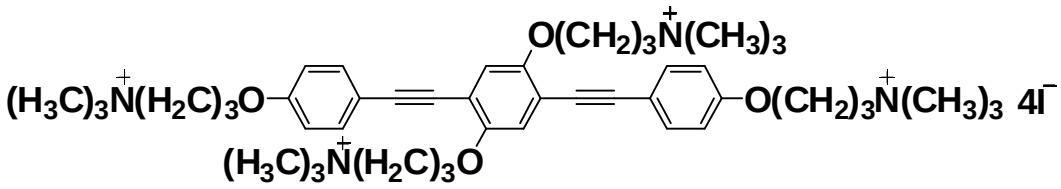

5

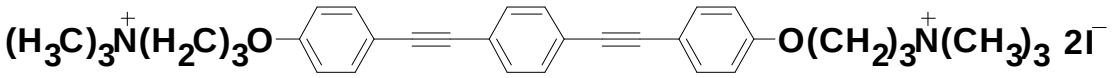

6

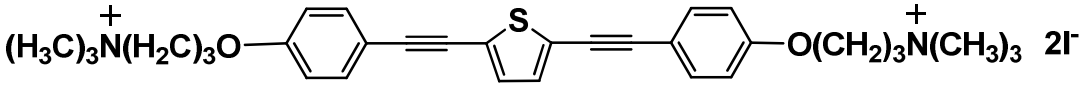

7

Figure 1-6. Structures of three oligomeric compounds, OPE6 (**5**), OPE17 (**6**), and OPE17Th (**7**)which were tested for antibacterial properties.

Biocide effects on membranes.

In general, hydrophilic antibacterial agents are primarily prevented from entering the bacterium through the outer membrane by the lipopolysaccharide layer and the underlying phospholipids, whereas hydrophobic agents are excluded by outer membrane proteins. These components are illustrated in Scheme 1-2.

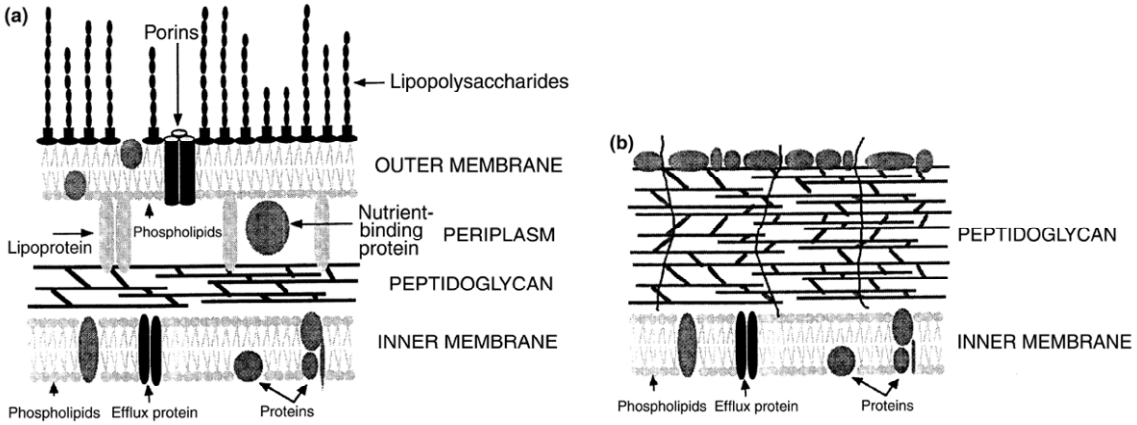

Gram-negative cell membrane

Gram positive cell membrane

Gram- inner membrane (96 proteins)	Gram+ acid-fast cell wall (4 proteins)
Gram- outer membrane (64 proteins)	Gram+ plasma membrane (13 proteins)

Pores: 0.15 to 3 nm

Scheme 1-2. Structure of Gram negative (left) and Gram positive (right) cell walls, with a comparison of their relative complexity.(41)

Most of the compounds under study contain both charged groups and non-polar segments, such as the long nonpolar side chains, that share some of the nature of the typical phospholipids (Figure 1-7) that comprise bacterial cell membranes. This being the case, it would be reasonable to assume that the hydrophilic charged group may act similarly to the phospholipid head group, while the hydrophobic non-polar portions of the molecule could mimic the tail of the phospholipids. It may be that this synergistic combination of elements is able to confuse defensive mechanisms. At a minimum, these factors would certainly contribute to some affinity for interaction with the membranes themselves. Indeed, many studies have been carried out (primarily looking at insertion and transport of drugs) that verify this structure/property relationship (14, 33, 182) and membrane modeling has become a useful tool for design of antimicrobials.(54, 127, 190)

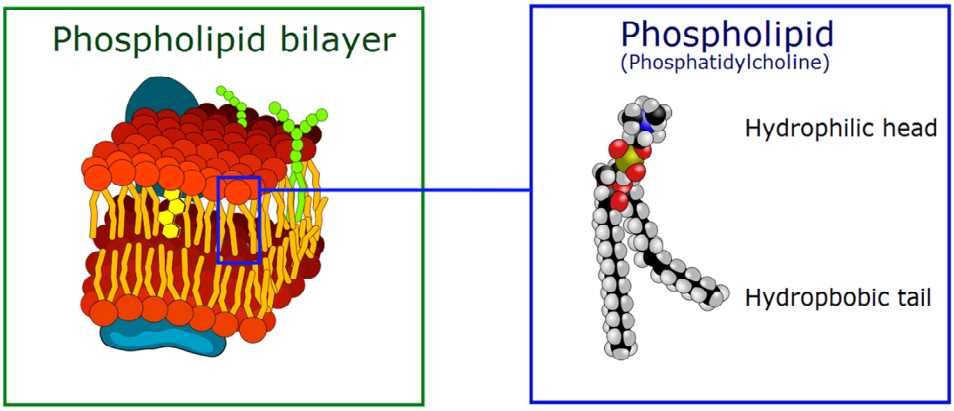

Figure 1-7. Structure of a cellular membrane bilayer (left) and an individual component phospholipid molecule (right).(4)

Changes in model membrane integrity have also been observed with AFM. Due to the high resolution of this technique, it is possible to obtain information on changes in morphology, porosity, layer thickness and area of a true bilayer (instead of the monolayer obtained in a Langmuir trough). Figure 1-8 shows a continuous dimyristoylphosphatidyl-choline (DMPC) bilayer exposed to a dendromeric form of a quaternary ammonium polycationic complex. Over a 19 minute exposure, the film experiences significant loss of integrity, with the development of 100-200 nm holes.

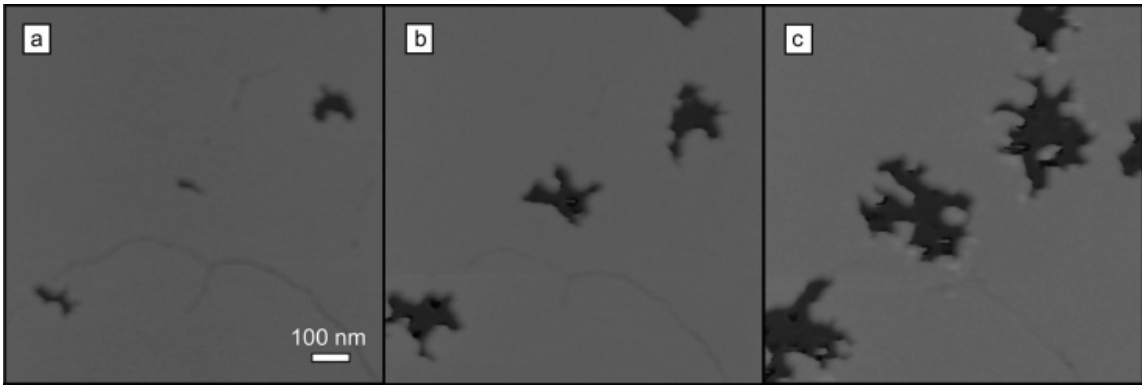

Figure 1-8. AFM height images of the same area of the dimyristoylphosphatidylcholine (DMPC) bilayer (a) 12 to (c) 19 min after exposure to G5-amine. Color height scale: 0-20 nm. (152)

The conditions are reversed in Figure 1-9, where isolated bilayer "islands" are exposed to the protegrin-1 peptide, resulting again in bilayers with disordering, especially at the edges, and porosity increasing with time, up to 15 minutes, by which time the process seems to have reached maximum entropy.

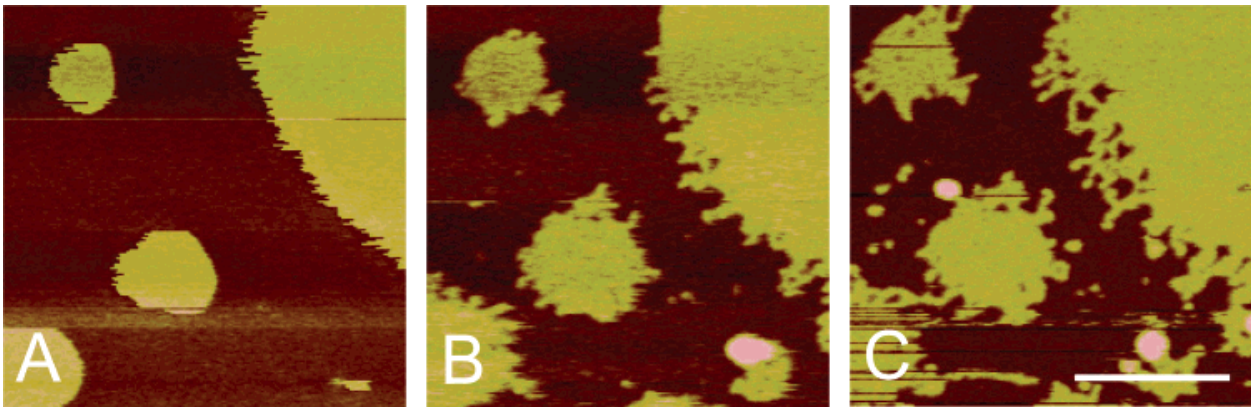

Figure 1-9. AFM images of DMPC bilayer patches (A) before and (B and C) after introducing 2 µg/mL of PG-1 to the superphase. (scale bar = 500 nm) (A) Without PG-1, stable supported bilayer patches maintained smooth boundaries by line tension. (B) After 5 min of incubation in the PG-1 solution, edges were destabilized, and fingerlike structures grew. (C) After 15 min, the destabilization process reached completion, and no further changes were observed. (105)

In terms of the effectiveness of these compounds in the actual killing of bacteria, a number of studies have been undertaken. (2, 39, 104, 218, 114, 47) Fluorescence microscopy and confocal fluorescence microscopy have been used to analyze a number of these trials. This can generate wavelength specific data which can be viewed as color images. Quantitative analysis of these images can be tedious and uncertain because of inhomogeneities in the mounted microscope slides and in the selection of images retained for consideration. Figure 1-10 shows an example of a study where unambiguous results were possible because of the absolute killing over the entire sample. Evolution of a given observable area over time may also be difficult to monitor because of photobleaching of

the stains, inability to re-locate given features after moving the stage, and drying of the sample.

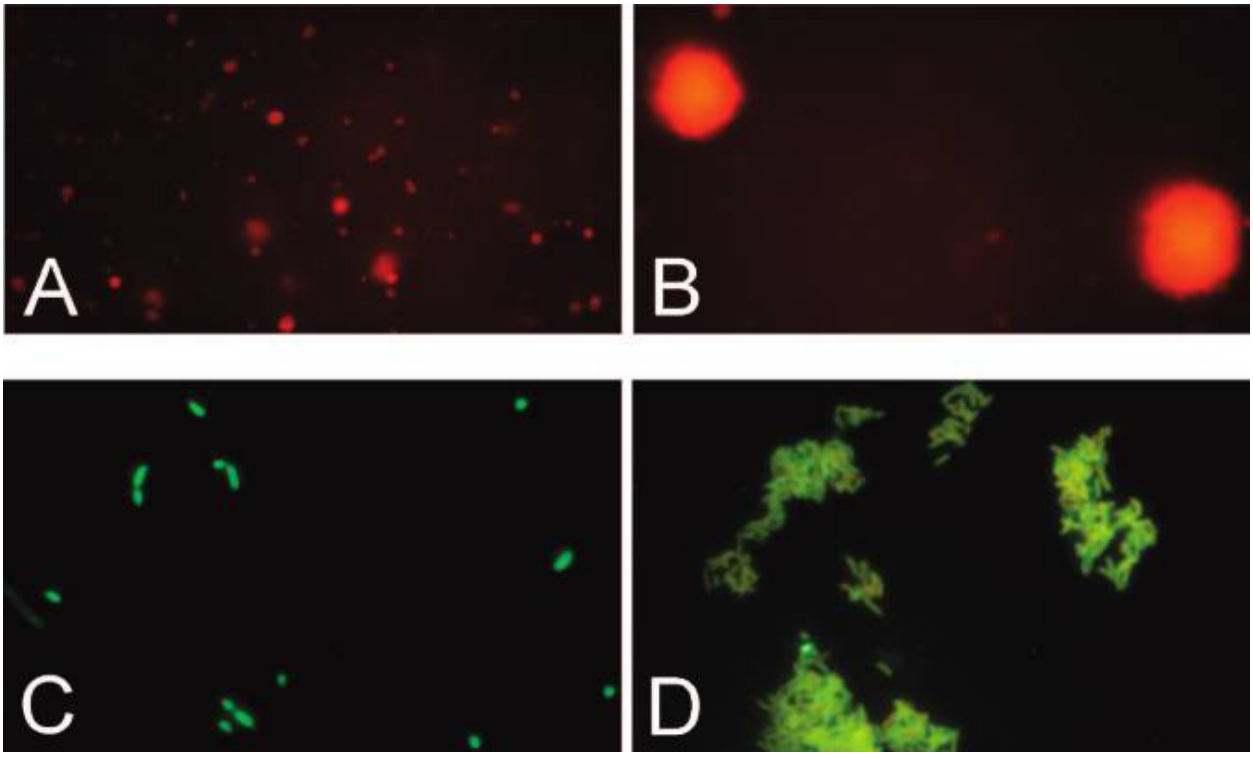

Figure 1-10. Fluorescence microscopy images of (A) Rhodamine labeled vesicles formed from *E. coli* lipid extracts before addition of polymer and (B) after 30 min in the presence of a conjugated norbornene polymer. Vesicles had an approximate diameter of 2-3 μm. (C) Stained bacteria (*E. coli*) before addition of polymer and (D) after 30 min in the presence of polymer. Bacteria were ~1-2 μm in length. (64)

Research Goals

The antimicrobial system currently under study is a family of ethynylene polymers with alternating phenyl and ethynyl groups along the polymeric backbone. This family of polymers is generally stable in air and at elevated temperatures (>150 ºC), both attractive characteristics for materials intended for use in coatings on environmentally-exposed surfaces and in biosensors. Furthermore, these compounds have a straightforward synthesis from relatively inexpensive starting materials.

Compounds **1a** and **1b** (Figure 1-2) and compound **4** (Figure 1-5) are disubstituted on each phenyl group, while compounds **2** (Figure 1-3) and **3** (Figure 1-4) are disubstituted on every other phenyl group. These ether linked substituent groups provide the charge for the polyelectrolyte. The complexes have been shown to have strong absorbance and emission in the visible range, the wavelengths of which may be manipulated by changing branching functional groups, branching chain lengths or conjugation lengths. Studies so far have concentrated mainly on synthetic routes to these complexes and their general spectroscopic qualities. Subsequent studies of the biocidal actions of this class of compounds in our group were reported by Chemburu *et al*.(37) and most recently Corbitt *et al*.(45, 47)

The ability of the CPEs to damage and kill bacteria and spores had been previously established within the research group.(126) In order to further establish proof of concept and begin to quantify this activity, we began testing of the CPEs against laboratory strains of bacteria that were considered relatively benign. Our constraints were initially somewhat facility-dependent, in that we were originally housed in a building not ideally equipped to culture or handle viruses or the more pathogenic forms of bacteria. Neither did we have access to equipment that would enable quantification of the degradation of chemical weapons simulants. With these limitations in mind, a number of research goals were developed to guide the work:

1) Decide on organisms to be tested.
2) Develop rapid and effective assays for quantification of the biocidal activity.

3) Determine the mechanism of killing, specifically the light-activated killing, assuming that most dark killing would result from the action of the quaternary ammonium moieties only.
4) Ascertain whether the compounds of interest could retain their recognized biocidal capabilities when incorporated into various material substrates.
5) Examine structure/activity relationships and use these to guide future synthetic objectives.

The summative hypothesis then became: "The antimicrobial activity of this family of CPE compounds can be analytically measured, modified and incorporated into various relevant material substrates." Thus, this dissertation developed to encompass the application of a family of functionalized conjugated phenylene ethynylene electrolytes to disinfection of liquids and solid surfaces and the development of techniques and protocols to quantify their activities. Compounds of this type and others with shared characteristics (generally cationic, quaternary ammonium complexes) have been shown to be very effective antimicrobial agents by our group and others.(159, 37, 55, 74, 85, 205) Functionalizing one or both ends of the polymeric chains with appropriate moieties provides a means of attachment to various substrates. This gives the ability to form extended structures such as monolayers and vesicles that are amenable to incorporation in nanotechnological constructs that are specifically intended to intercept and kill pathogens by mechanical damage, chemical toxicity or simple immobilization in the absence of a food source. Mixtures of these compounds, as in layer-by-layer (LbL) coatings of polymers of alternating charge, can generate tertiary structures with other desirable properties. In addition, activation of these complexes by visible light may give rise to

active intermediates that enhance the biocidal effects.(15, 37, 126, 134, 135, 203) These structures also lend themselves to characterization of the photochemical dynamics by various analytical probes, particularly UV/visible and fluorescence spectroscopy. This spectroscopic information may then be used to elucidate the mechanism of biocidal action and help determine the active species most responsible for bacterial membrane disruption and/or chemical toxicity to cell function.

The primary goal of this ongoing research is to examine and quantify the scope of biocidal action of the individual polymers and extended systems under dark and light-exposed conditions. This will promote understanding of how chemical and configurational modification can modulate these properties so that their efficacy can be increased through design and assembly at a molecular level.

Chapter 2

Experimental Methodology for Investigating Biocidal Activity

Bacterial Simulants

Selection and Characteristics

In selecting bacterial species for investigation in this study of the antimicrobial effects of the CPE compounds, a number of factors had to be considered. The bacteria needed to be readily available, robust enough to be grown in our laboratory without requiring specialized equipment (beyond the technology of a chemostat) and non-virulent, to meet the facility standards for hazardous substances. Due to these considerations, the bacterial strains used most frequently were *Cobetia marina*, a marine bacterium (Chapters 3, 4 and 5), *Pseudomonas aeruginosa*, a soil bacterium and opportunistic pathogen (Chapters 3, 4 and 5) and *Bacillus atrophaeus,* a simulant for anthrax (Chapters 5, 6 and 7). Both *Cobetia marina* and *Pseudomonas aeruginosa,* strain PAO1are Gram negative bacteria that can be good simulants for Gram negative pathogenic bacteria such as *Yersinia pestis* and *Vibrio cholerae.* The complex outer membrane and lipoprotein/peptidoglycan layers play a role in shielding these bacteria from potentially harmful reagents such as singlet oxygen.(133)

The Gram-negative (see Scheme 1-2) obligately aerobic halophile *Cobetia marina* (basonym, *Halomonas marina*) was selected for its robustness and, because it is cultured in a strongly saline solution, a low likelihood of contamination from common airborne bacteria. It is of interest for its role in biofouling of marine vessels.

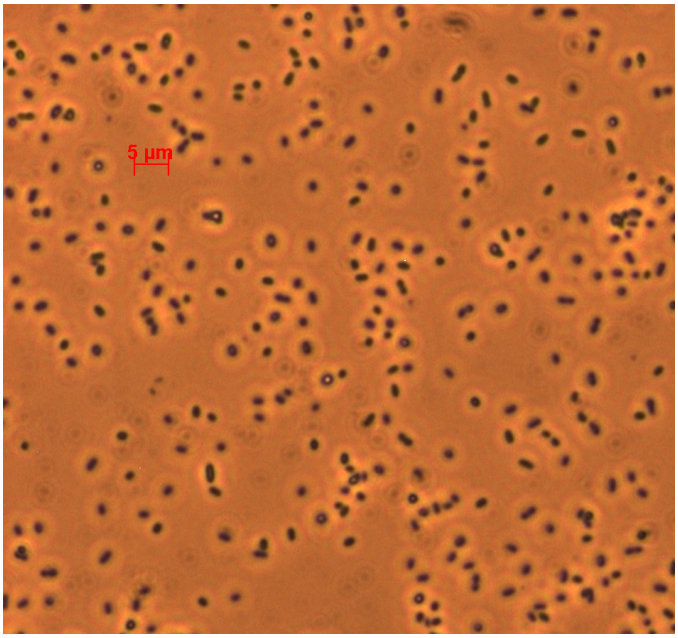

Figure 2-1. Phase contrast image (20x) of *Cobetia marina* grown in our laboratory.

The second bacterium selected was *Pseudomonas aeruginosa*. This ubiquitous Gram-negative organism is an opportunistic pathogen which has a highly elastic metabolism and exhibits increasing antibiotic resistance of nosocomial strains. Of the two million nosocomial infections each year, 10% are caused by *P. aeruginosa*. This bacterium is the second most common cause of nosocomial pneumonia and the most common cause of intensive care unit (ICU) pneumonia and is notorious for contamination of catheters and other medical equipment. It is able to survive on a diverse range of carbon sources, including soap residue, adhesives and even on some quaternary ammonium compounds used as antiseptics.

The laboratory strain PAO1 has been used most extensively in common testing, as it lacks the virulence of other *Pseudomonas* strains while retaining the primary properties concerning biofilm growth and susceptibility to antibiotics (or lack thereof). It is also, as might be expected, quite easily grown in laboratory cultures.

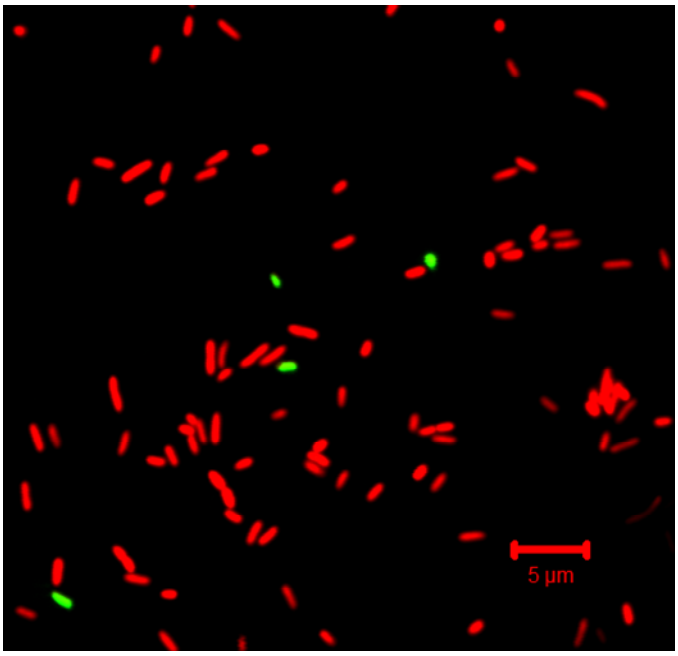

Figure 2-2. *Pseudomonas aeruginosa.* Stained with SYTO 60 (red-live) and SYTOX Green (green-dead).

Although both the Gram negatives *C. marina* and PAO1 show biocidal effects from the polymers, the *Pseudomonas* generally requires longer exposure times to kill.

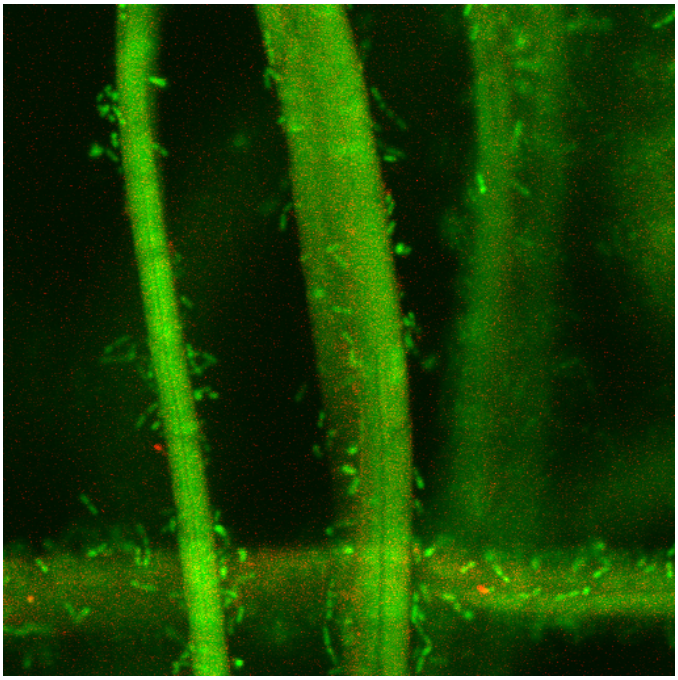

Figure 2-3. CLSM image of *Bacillus atrophaeus* vegetative cells associated with cotton fibers.

Bacillus atrophaeus (also known as *Bacillus subtilis*) has long been used as a simulant for its *Bacillus* relative anthrax, having similar properties in terms of growth, antibiotic susceptibility and sporulation, but lacking in pathogenicity. These are Gram positive organisms, having a single, less complex (but thicker) cell membrane, as illustrated in Scheme 1-2.

Bacterial Growth

General conditions.

The care and feeding of bacterial cultures constituted the main part of a steep learning curve for me concerning general biology and microbiology in particular. Approaching the understanding of biological processes with a chemist's mindset of precise measurement of reagents and close monitoring of conditions proved to be unnecessary and even a bit of a hindrance at times. Despite having been a scientist for the majority of my life, the ubiquity and flexibility of living things, the dynamic nature of bacterial growth, and the complexity underneath it all took me somewhat by surprise. The fact is, microbial growth is everywhere. One estimate of their total numbers on the Earth is around 5×10^{30}, with as much carbon mass as all plant life and 10 times the N and P mass of plants.(214)

Bacterial growth has three phases: First is lag phase; slow growth while the cells are adapting to a high-nutrient environment. The cells then accelerate into the logarithmic (log) phase by increasing biosynthesis rates, producing proteins necessary for rapid exponential growth. During this phase, nutrients are metabolized at a high rate until one of the nutrients is depleted and begins to limit growth, transitioning into stationary phase when the majority of the nutrients are depleted. The cells then decrease metabolic

activity and begin to consume non-essential cellular proteins.(174) Experimenters, when examining bacteria out of medium, must keep in mind that these dynamic processes do not stop and metabolic changes may occur over the time scale of an experiment.

Like all other life, bacteria grow best given the proper conditions; for our test organisms, these come in the form of a rich media broth. These broths, such as Difco's, are optimized for nutrient and beneficial salt (primarily calcium and magnesium) content. The carbon food source in these broths is of a high concentration, to encourage rapid proliferation of the culture. Detrimental ions such as iron and copper are reduced where recommended for clinical applications, bacterial and yeast transformation studies and bacterial molecular genetics applications.

In our experiments, all bacterial work was carried out under sterile conditions (flaming, alcohol rinse). Bacteria for testing were initially obtained from a stock culture stored in 20% glycerol at -70˚C. The thawed stock culture was used to inoculate an agar slant that was then stored at 4°C for up to 2 weeks. Colonies from the slant were used to inoculate flasks (usually 250 mL, with 50 mL broth) to grow "overnight" cultures in the apposite rich media broths. This flask was then sealed with a foam stopper covered by Al foil, in a shaker/incubator held at the appropriate temperature for 16-18 hours, depending somewhat on the particular species. Populations of overnight cultures for all types of bacteria used in these studies frequently exceed 10^9 mL^{-1} when properly prepared with adequate nutrients and sufficient oxygen availability.

The overnight bacteria destined for direct experimentation were used immediately following a washing procedure (see Preparation of bacterial samples below). Alternatively, some of the bacteria from the overnight culture were transferred to a

"minimal" media that consists of a mixture of all necessary salts in appropriate proportions for a given species with a nutrient source that functioned as a limiting factor. These bacteria were then continually grown and harvested from a chemostat, described below.

Once the bacteria from either source had been extracted and washed, they were then counted using a hemocytometer, a specially designed microscope slide with a ruled grid and ridges on either side of the ruled area that insure that the thickness of the liquid layer under the cover slip will be constant (usually 0.1 mm). We could then establish the desired population in solution by dilution with an appropriate buffer solution—either artificial sea water (ASW), phosphate buffer solution (PBS) and/or 0.85% NaCl.

Culture media.

All media and buffers were prepared in filtered, de-ionized water (Barnstead-Thermolyne ROPure/Nanopure system). The final resistivity of the processed water was >18 MΩ cm^{-1}.

Specifically for *C. marina,* Marine Broth 2216 (MB, Difco) was prepared according to the manufacturer's instructions. Marine Agar (MA) was prepared by the addition of 1.5% Bacto agar (Difco) to MB. *C. marina* (ATCC 25374) was revived from the original lyophilate and was stored as frozen stock aliquots in MB +20% glycerol at -70°C. Experimental stock cultures were maintained on MA slants and were stored at 4°C for up to 2 weeks. Prior to experimental use or inoculation into a chemostat, a single colony from a MB slant was inoculated into 50 ml of MB and grown overnight with shaking at 25°C.

Artificial sea water (ASW), used in the preparation of the minimal medium for *C. marina*, contained 400 mM NaCl, 100 mM $MgSO_4$, 20 mM KCl, 10 mM $CaCl_2$.(97) The chemostat solution, modified basic marine medium plus glycerol (MBMMG) (based on Kersters' basal media) contained 0.5× ASW plus 19 mM NH_4Cl, 0.33 mM K_2HPO_4, 0.1 mM $FeSO_4 \cdot 7H_2O$, 5 mM trishydroxyaminomethane hydrochloride pH 7, and 2 mM glycerol.(89, 97) A chemostat culture of *C. marina* was established by inoculating 3 ml of the overnight culture into MBMMG. The chemostat was maintained at a flow rate of 0.8 mL min^{-1} (dilution rate, 0.1 hr^{-1}) with constant stirring. Under these conditions, the concentration of the chemostat *C. marina* culture was ~10^7 cells mL^{-2}.

The *Pseudomonas aeruginosa*, strain PAO1, (a kind gift acquired from Dr Tim Tolker-Nielsen) was stored as frozen stock in Nutrient Broth (NB, Difco) prepared according to the manufacturer's directions +20% glycerol at -70°C. Nutrient agar (NA) was made by the addition of 1.5 % Bacto agar to NB. Experimental stock cultures were maintained on NA slants and were stored at 4°C for up to 2 weeks. Prior to inoculation into a chemostat, a single colony from a NA slant was inoculated into 50 ml of NB and grown overnight (18 hr) with shaking at 25°C.

Chemostatic growth of *Pseudomonas aeruginosa* required minimal citrate medium (PAMCM))(80) containing 2.5% $(NH_4)_2SO_4 \cdot 2H_2O$, 0.6% Na_2HPO_4, 0.3% KH_2PO_4, 0.098% $MgCl_2$, 0.011% $CaCl_2$, 1 mL L^{-1}, *Pseudomonas* trace elements, and 1mM sodium citrate (carbon source). A chemostat culture was established by inoculating 3 ml of the overnight culture into PAMCM. The chemostat was maintained at a flow rate of 1.0 mL min^{-1} (dilution rate, 0.12 hr^{-1}) with constant stirring. The concentration of the chemostat culture was about 10^7 cells mL^{-1}. Chemostatic culturing of *P. aeruginosa* has

been discontinued because of the uncertain biohazard status assigned to this bacterium by the University's Biohazardous Materials oversight committee. This status eventually changed during the course of experiments from BSL1 to BSL2.

The bacterium *B. atrophaeus* was similarly inoculated and grown in overnight cultures using Tryptic Soy Broth (TSB) as the rich medium. Chemostatic cultures used the same minimal citrate medium as the *P. aeruginosa*. The spore form of *B. atrophaeus* was generated using low nutrient agar plating of stock from an overnight culture inoculated with a solution high in Ca^{2+} and Mg^{2+} and allowed to dry at 4 ˚C for 6-7 days. These plates were then rinsed with 0.85% NaCl buffer and prepared for experiments in the same manner as vegetative cells. Spores prepared in this fashion can be stored for up to 2 weeks with no apparent degradation.

Chemostat setup

Chemostatic growth of bacteria is a process developed in early work (1942) by Monod and is based on empirical observation of the relationship between growth rate and substrate concentration.(155, 156, 84) It is a powerful technique for long-term experimental studies owing to the advantages offered in control of environment (for both the bacteria and the laboratory), reproducibility and modeling. A chemostat is essentially a continuous culture system, where a pump regulates medium flow rate into the static working volume of a chemostat vessel, establishing the dilution rate and hence the specific growth rate of the culture (most often represented as μ). One of the systems used in these experiments is shown in Figure 2-4.

Although Monod's design remains the most widely used, some operational problems remain, including foaming, cell damage during agitation, and inhomogeneous

mixing. Dripping the media into the chamber from a point well above the suspension is done to prevent bacteria from reaching the reservoir of sterile medium, but can be problematic, creating small pulses of nutrients and thus oscillations in concentrations, upsetting the static property of the chemostat. A related and potentially more significant effect is cell growth (and migration) on walls and plumbing, due to splashing caused by the drops of falling media.

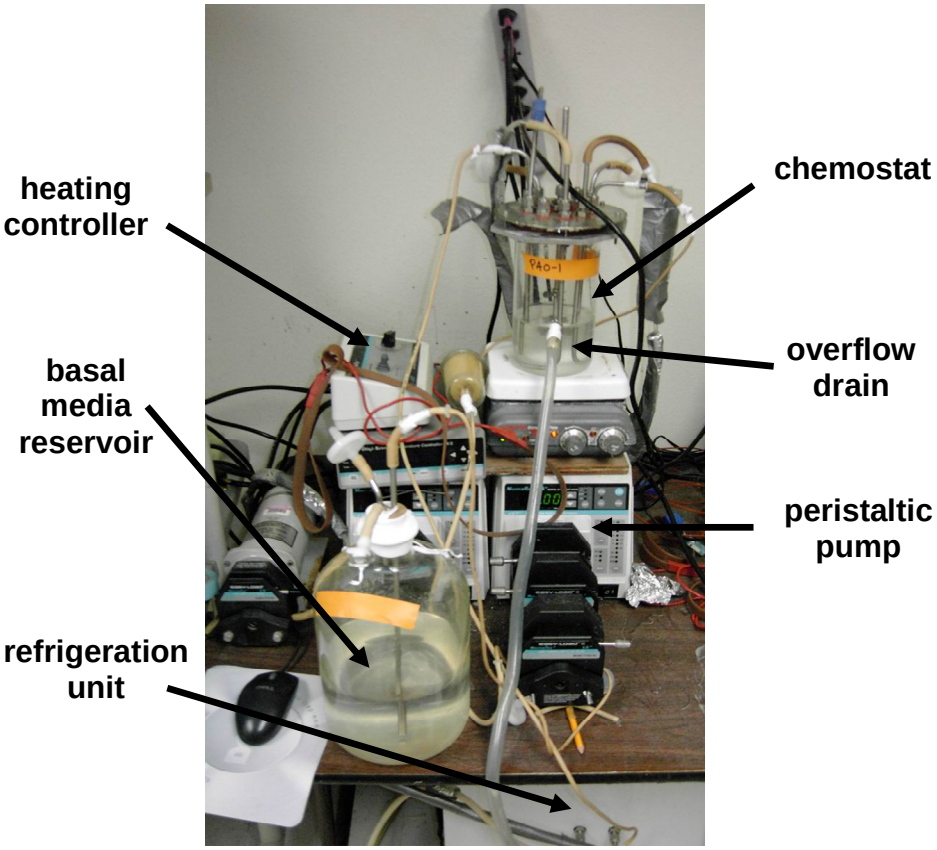

Figure 2-4. Photograph of a chemostat set up for *P. aeruginosa* culture growth. The arrows indicate the various components, some of which (heating and refrigeration) are not required for simple operation. This chemostat has a working volume of 600 mL, which is maintained at this level by peristaltic pumping of basal media from a 4 L glass reservoir.

A metered influx of sterile medium from a reservoir is balanced by the efflux of spent medium, living cells and cell debris, allowing growth of microorganisms to occur at an equilibrium, with growth of new cells being balanced by those washed out. In this

steady state system, new bacterial growth is equal to the rate at which the culture is being diluted. The relationship between rate of flow of the growth medium into the chemostat and the chemostat volume is defined by the dilution rate, D:

$$D = F/V \quad (1)$$

where F is the flow rate, and V is the culture volume. Recalling that μ is the growth rate of the culture, the change in the concentration of biomass (x) over time during steady-state growth can be expressed as

$$dx/dt = \mu x - Dx \quad (2)$$

and since under steady state conditions the biomass concentration is constant:

$$dx/dt = 0, \text{ thus } \mu x - Dx = 0 \text{ or } \mu = D \quad (3)$$

Therefore, in steady state, the growth rate can be manipulated as a function of the dilution rate, provided that the dilution rate is below the maximum specific growth rate (μ_{max}) of the organism under the given conditions. In other words, if the flow is increased (or the volume is reduced), to the point where the system is driven past the critical dilution rate (D_c) (the rate at which the steady-state biomass concentration is zero), the culture washes out of the chemostat.

Since the growth of microorganisms in continuous culture is governed by D, the limiting factor is the rate of supply of a growth-limiting nutrient. To relate the biomass of a steady-state culture to the residual limiting substrate concentration (the limiting nutrient in the feed reservoir) and the dilution rate, Monod used the following equation:

$$\mu = \mu_{max} S / (K_s + S) \quad (4)$$

where S is the residual substrate concentration and K_s is the half rate saturation constant, which is equal to S when the growth rate is 0.5 μ_{max}. Therefore, when applied to continuous culture,

$$D = D_c S / (K_s + S) \quad (5)$$

implying that the growth cycle of an organism is not an inherent property of the organism but a result of its interaction with the physico-chemical environment in which it is growing.

Therefore, using a chemostatic system, lag, log and stationary phases of microbial growth may be accessed. This application of continuous culture systems to modulate growth and avoid the transient conditions encountered in batch culture offers significant advantages to experimenters. Bacteria grown under chemostatic conditions tend to have more uniform characteristics and thus are better suited for experimentation over longer periods of time. In our experiments, cultures of *C. marina* and *P. aeruginosa* were successfully maintained for up to two months before it became necessary to dismantle the chemostats for cleaning.

Substrate Preparation

Microspheres

A detailed study was recently carried out by our group that focused on the preparation and characterization of SiO_2 particles that contain a surface-grafted layer of an anionic conjugated polyelectrolyte.(167) Uniformly sized silica microspheres were purchased from Bangs Lab or from Duke Scientific as a dry powder. A small amount (50-60 mg) was suspended in purified water and the beads were then counted using a

hemocytometer. This weight of 5 µm beads would normally give a population of approximately 1-5 x 10^8 beads/mL.

This approach was used to prepare 5 µm and 30 µm particles with covalently grafted layers of **1a** or **1b** (**SCGP-1a** and **SGCP-1b**). Briefly, the SiO_2 surface of the particles is initially functionalized by reaction with an aryl iodide functionalized organosilane. Then a palladium-catalyzed (Sonogashira) polymerization reaction is carried out in a solution containing a suspension of the aryl iodide functionalized particles. During the step-growth polymerization process, a fraction of the growing chains are captured by cross-coupling with the aryl iodide unit on the particle surface, which leads to covalent grafting of the polymer chain to the surface. Following the grafting procedure, the particles were washed extensively to remove material that is not covalently bound to the surface. Thermal gravimetric analysis was carried out in a previous study of SGCP particles prepared by the same approach, and the materials typically consist of *ca* 10 wt% polymer.(167) In addition, on the basis of the TGA and transmission electron microscope images, the thickness of the surface-grafted polymer layer is estimated to be 12 nm on average.(167)

Microspheres with physisorbed polymer were also prepared: A certain amount of polymer was weighed and dissolved in deionized water (**1** or **4**), or taken from the stock solution (**2**) and the absorption spectrum was obtained by using a spectrophotometer (Spectramax M5). The concentration of the polymer (**1a**, **1b, 2** or **4**) in solution was calculated using the Beer-Lambert law, using the corresponding extinction coefficients. The cationic PPEs have an approximate surface area of 280 square angstroms per polymer repeat unit (PRU).(219)

Calculations of surface area were done using the given bead diameters and assuming a smooth spherical shape to determine the quantity of polymer necessary to provide monolayer coverage plus a 20% excess for a given amount of beads. After the addition of the polymer solution to the beads, they were vortexed for 30 min and washed 5 times in PBS buffer (20 mM PBS + 150 mM NaCl) until the supernatant was no longer fluorescent. The beads were finally suspended in 1 mL of PBS buffer, either PBS, ASW or 0.85% NaCl, depending on the subsequent treatment, and stored at and stored at 4 °C (**1** and **2**) or at room temperature (**4**) until further use.

These physisorbed microspheres were not employed extensively for antimicrobial testing because of a number of perceived inconsistencies in their performance. It was speculated that, despite the extensive washings, these beads were losing some of the polymer coating to solution, possibly due to the ionic strength effects of the buffers used for the bacterial samples. This phenomenon was not investigated further, due to the ready availability of the chemically grafted beads.

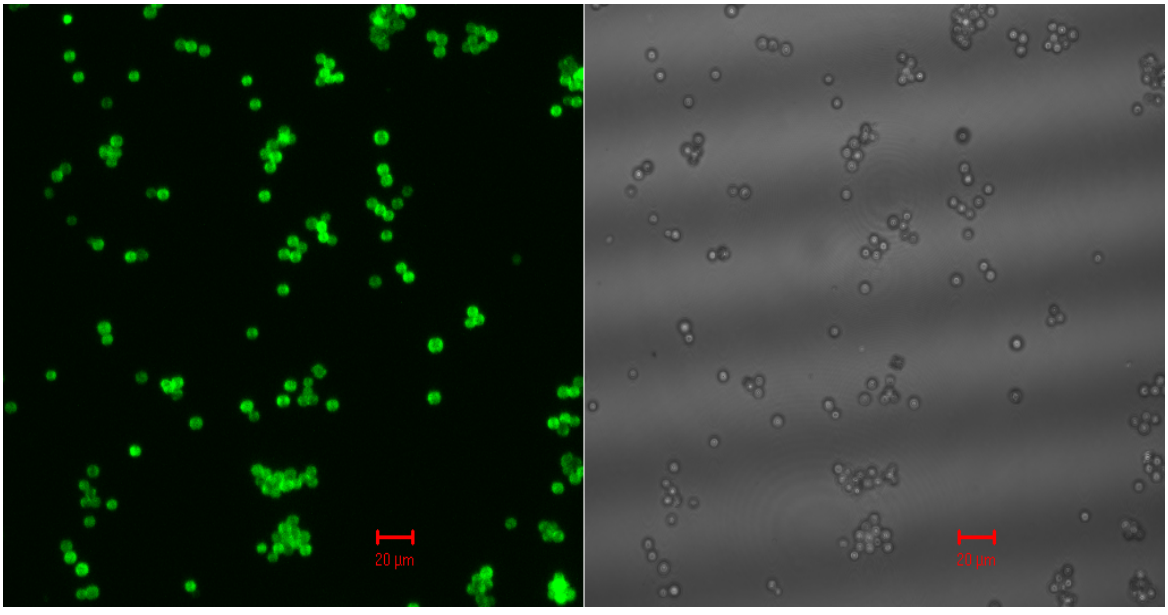

Figure 2-5. Microscopy images (fluorescence, left, and bright field, right) of 5 µm SiO_2 microspheres with polymer **2** grafted on the surface.

Polyelectrolyte Multilayers (PEMs)

A number of more recent experiments have been done using a substrate composed of conjugated polyelectrolyte multilayer capsules (PEMs), fondly referred to within the group as micro"Roach Motels" (μRM). These multilayer constructs of polyelectrolytes of alternating charge (compounds **2** and **3)** are formed around a spherical template of manganese carbonate that is later dissolved, leaving a hollow polymeric shell. The synthesis of these capsules and their use in biocidal experiments are covered in Chapter 5.

Biocidal studies

Preparation of bacterial samples

The bacterial suspension harvested from the chemostat typically contained around 10^7 cells mL^{-1} and, depending on the number of samples needed, 5-50 mL was extracted for washing. The population per unit volume from overnight batch cultures was usually at least an order of magnitude higher and a sufficient quantity for experimentation could consequently be obtained from just a few milliliters.

Once the culture suspensions were extracted, they were then prepared by centrifugation at 10 K rpm in an Eppendorf 5415C centrifuge and the supernatant removed and discarded. The remaining pellet was resuspended in 1 mL of buffer solution and recentrifuged. This cycle was repeated for a total of 3 washes and counting was carried out in a hemocytometer in order to normalize bacterial concentrations. The bacteria were used immediately after preparation to preserve live population and minimize metabolic fluctuations (growth phase changes, sporulation). *C. marina* prepared in this fashion typically remained viable for 2-3 hours and *P. aeruginosa* and *B. atrophaeus* for more than 6 hours. Under low nutrient conditions, the *B. atrophaeus*

would begin to show some signs of sporulation at the longer times (>4 hrs). This phenomenon, which can lead to significant changes in membrane structure and cell metabolism, was noted early and the data gathered under such circumstances was not consolidated with that gathered on the standard vegetative cells.

Staining

Much initial effort was spent in finding a method for quantifying biocidal activity of the various CPE complexes and their substrate-dependent formats. Early experiments indicated that the surface grafted conjugated polyelectrolytes (SGCP) on silica substrates were highly effective both at capturing bacteria and killing them upon irradiation with visible light. After several trials with culturing and examining both the beads and the bacteria in microfluidics channels, it was decided that we would try staining in order to achieve unambiguous discrimination between live and dead bacteria.

In order to assess the effects of the potential antimicrobial compounds, it is often expedient to employ fluorescent dyes which stain cells with certain properties. There are two main mechanisms of selective staining of different cellular components by these dyes. The first involves the contrast development due to differences in concentration of dye in different areas of the cell arising from differences in the affinities of various cellular constituents for the dye. For instance, basic dyes tend to bind in higher concentrations to acidic materials such as nucleic acids, while dyes with high lipid solubility stain membranes.

The second mechanism of staining is environmental enhancement, where association with a particular substance or region of the cell leads to an increase of the quantum efficiency of a fluorescent dye. This implies that the utility of fluorescent dyes

can be affected by ionic strength, pH, polar or non-polar conditions, and transitions between differing environments in the cell.(116, 144, 176, 19) These properties can be used to our advantage; for example, derivatives of fluorescein are routinely used for pH measurement within cells.(177) Reactions of the stains with other chemicals or with themselves (e.g. dimerization, polymerization) can also induce shifts in the absorption and fluorescence emissions.(186, 48)

For our application, we require stains that will differentiate between bacterial cells that have been damaged or killed by the CPEs and those that have not (so-called "vital" staining). This is not as straightforward as the description "live/dead assay" would imply. Bacteria are resilient organisms that, when damaged, may retain some semblance of structure and function, even if unable to reproduce. Bacteria in this state are referred to as "sublethally injured" and may still be pathogenic. Some bacteria can enter a dormant state, not taking up stains, yet having the potential to become active in the right environment. Then there are others that do stain, but are called "ghosts," bacteria that cease to function or respond to stimuli and whose cell walls remain more or less intact. To complicate matters a bit further, some bacteria do not grow well on plates, yet can be metabolically active and able to reproduce in situ.(22, 158, 25)

Therefore, when it comes down to a working definition of viability, there is still some debate; however, most researchers will agree that bacteria which are unable to reproduce and show no signs of cell metabolism are truly dead. Unfortunately, there is no current dye or staining technique that will definitively determine reproductive potential of a bacterium. The criterion we chose for gauging the viability of the cells is the retention of membrane integrity as measured by the lack of infiltration of a given cell

impermeant fluorescent stain.

Impermeant dye molecules are generally barred from transport across membranes by either size or charge or a combination of the two. For example, acid dyes such as fluorescein do not cross cell membranes, but their neutral esters do. Alterations in cell physiology due to membrane disruption may allow penetration of stains that would normally be excluded. Again, there are caveats: some antibiotics, especially at low doses, cause transient permeabilization that will allow cells to take up normally impermeant dyes such as propidium iodide (PI) without killing the cells; the dyes themselves may also be toxic to cells, and; other harm to the cell may occur due to photosensitization when stained cells are exposed to high-intensity laser light. The stains themselves sometimes contain quaternary ammonium and may show a low level of cytotoxicity, but this is usually negligible.(13)

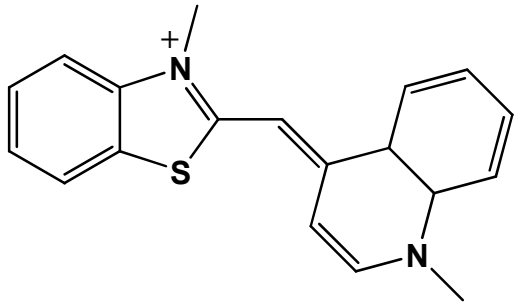

Figure 2-6. Molecular structure of thiazole orange. This molecule has been substituted in various ways to develop a large family of fluorescent dyes, including the SYTO and SYTOX series.(154)

Fortunately, many of these factors have been considered in the design and synthesis of the numerous families of staining compounds. Molecular Probes' SYTO series of dyes based on the structure of thiazole orange (Figure 2-6) and are cell permeant to virtually all cell membranes, staining both DNA and RNA (and sometimes other cellular structures such as mitochondria) in mammalian cells and bacteria. They have a

high molar absorptivity, with extinction coefficients >50,000 $cm^{-1}M^{-1}$ at visible absorption maxima and extremely low intrinsic fluorescence, with quantum yields typically <0.01 when not bound and >0.4 when bound to nucleic acids.(154) The corresponding SYTOX dyes are widely used as viability indicators and are reported to be very impermeant,(186) possibly due to an increased positive charge on the molecules, for which structures have not been published.

Table 2-1. Spectral characteristics of live/dead stains used in these studies.(154)

permeant stains	**absorption maximum (nm)**	**emission maximum (nm)**
SYTO 9	485	498
SYTO 11	508	527
SYTO 21	494	517
SYTO 24	490	515
SYTO 60	652	678
impermeant stains	**absorption maximum (nm)**	**emission maximum (nm)**
SYTOX Green	488	520
propidium iodide	536	617

In order to select stains for the live/dead assays, a number of the SYTO and SYTOX stains from Molecular Probes were screened. The cell permeant (live) stains were tested at the manufacturer's recommended concentrations and at up to three times that strength in some cases to establish a protocol for our system; in each case, the recommended levels were sufficient. The stains were tested in groups using bacteria from the same culture to compare fluorescence intensity, cell specificity (vs. background) and clarity using a Zeiss Axioskop fluorescence microscope. The differing responses between species and even between individual organisms of the same species following exposure make it virtually impossible to develop a single comprehensive fluorescent stain

based test for the effects of antimicrobial compounds.(185) The most reliable way to quantify the effects is to compare bacterial counts over time in treated and control cultures, and no particular set of stains seems superior to another for evaluating biocidal effects and/or viability in all types of bacteria. All of the stains shown in Table 2-1 have been used in our experiments at some point, but the following stain sets were utilized for the majority of the work:

Dye-set-1 (red = live, green = dead): This stain set for live/dead assays consisted of SYTO 60 and SYTOX Green stains obtained from Molecular Probes (www.invitrogen.com). These DNA stains produce red (~678 nm) and green (~520 nm) emission for live and dead bacteria, respectively. Upon completion of experimental treatment, the dyes were added as a 1:1 mixture to the bacterial samples (2 μL mixed dye per mL suspension) and incubated for 15 minutes. Cells were then examined under a 40x oil objective on a Zeiss LSM 510 Meta confocal laser scanning microscope and the number of live cells (*e.g.,* those fluorescing red only) and dead cells (*i.e.* those fluorescing both red and green) compared. *Dye-set-1* was employed extensively for the experiments with *C. marina* and *P. aeruginosa* and can be seen in Figure 2-8, where fresh *C. marina* from an overnight preparation show extensive red fluorescence with very little green, indicating the very low permeability expected from healthy live cells.

Dye-set-2 (red = dead, green = live): This is the commercial LIVE/DEAD® BacLight assay manufactured by Molecular Probes (www.invitrogen.com). These bacterial viability kits contain the dyes SYTO 9 and propidium iodide. With these dyes, red fluorescence from PI indicates dead bacteria or bacterial debris, while green fluorescence is observed for live bacteria due to SYTO 9.(17) This stain set was used

with *C. marina* and *E. coli*. The double positive charge on propidium (Figure 2-7) renders it impermeant to an intact cell membrane and gives it a higher binding affinity for double-stranded nucleic acid.(164)

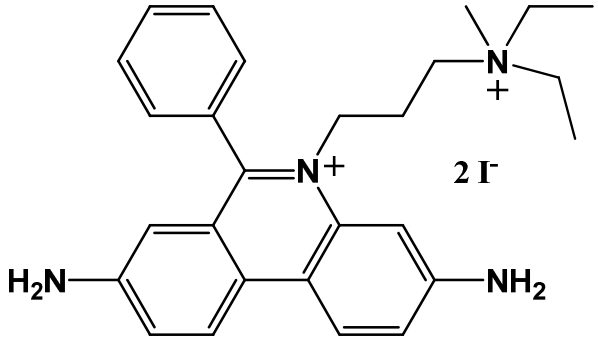

Figure 2-7. Molecular structure of propidium iodide (PI).

A number of other SYTO stains were also successfully paired with PI in experiments with *P. aeruginosa* (SYTO 21), *B. atrophaeus* (vegetative-SYTO 11, 24; spores-SYTO 21), and *S. aureus* (SYTO 21). The fluorescence characteristics of these combinations give a highly reliable live/dead assay where live bacteria only fluoresce green, while killed bacteria may exhibit both green and red fluorescence, with the red gradually coming to dominate in intensity as cell membrane integrity diminishes.

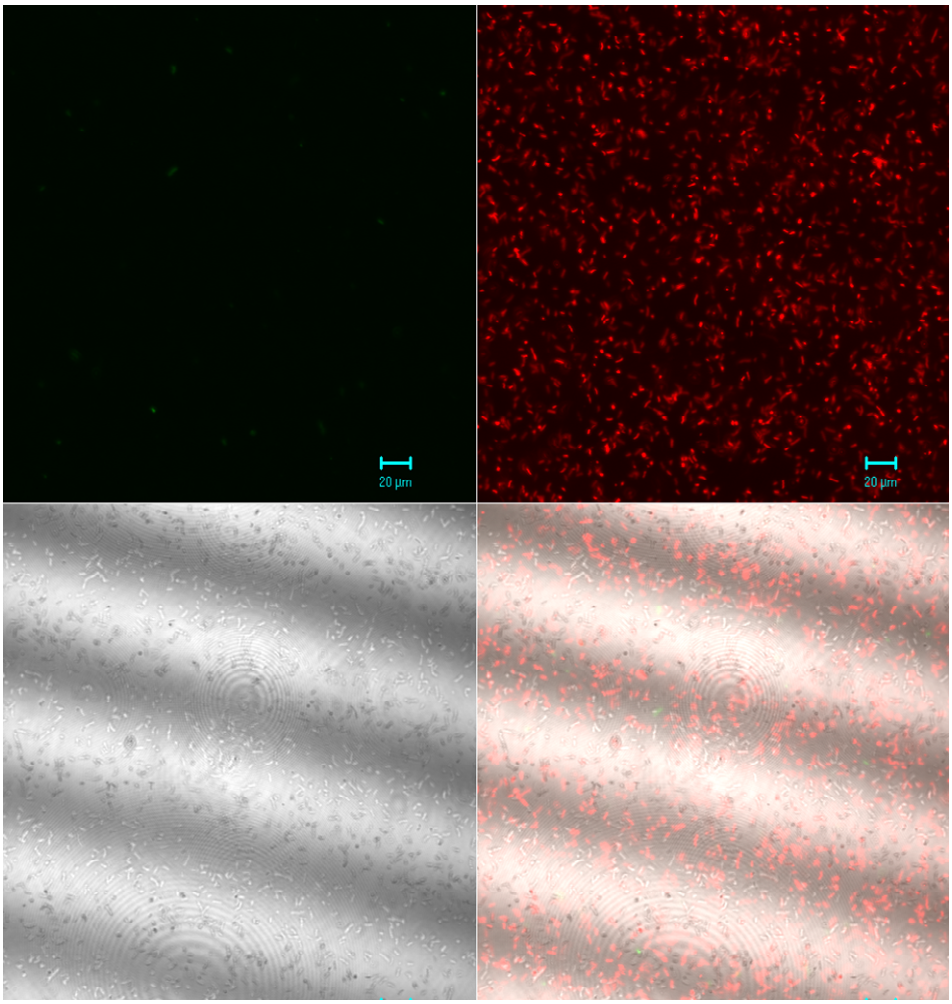

Figure 2-8. CLSM images of the effect of SYTO 60/SYTOX Green staining on an overnight culture of *C. marina* (>10^9 mL^{-1}). The upper left hand (green) channel shows little apparent fluorescence, indicating very few dead *C. marina*; image upper right with red fluorescence indicates live *C. marina*; lower images are lower left phase contrast bright field and right composite.

Experimental Parameters

Once the staining protocols were developed, we carried out studies of bacterial viability under a variety of conditions. Bacteria were mixed with free polymer in solution, suspensions with SGCP-coated beads in the presence and absence of oxygen and light and µRMs in the presence and absence of light.

Up to seven types of samples produced under and/or treated in ambient, oxygenated and deoxygenated conditions were analyzed by confocal fluorescence microscopy and/or flow cytometry:

1. dead control ((killed with 20 min exposure to 50% isopropanol, then stained)
2. live control (stained and unstained)
3. test sample (ambient conditions) with substrate (CPE in solution or coated onto microspheres, fabrics, or fibers) added, then exposed to the light source for the prescribed time, followed by staining (15 minutes for vegetative bacteria, 45 minutes for spores)
4. live oxygenated control (oxygen bubbled for 15 minutes, then stained)
5. live deoxygenated control (bubbled with Ar for 15 minutes, then stained)
6. same as 5, but oxygenated for 15 minutes before adding beads
7. same as 5, deoxygenated for 15 minutes before adding beads

Ensuing experiments with the coated microspheres (Chapter 3) showed that suspensions of *C. marina* could survive deaeration by nitrogen or argon for periods of up to 2 hours; however longer deprivation of oxygen did result in significant bacterial attrition as revealed by the live/dead assay.

Bacteria were added to SGCP modified particles and μRMs such that there were ~10-50 bacteria per particle, depending on experiment. All of these sample preparations were completed by staining for 15 minutes with the selected stain set. Live cells were incubated with 50 μL (1.8×10^8 particles/mL) of SGCP modified particles and then exposed to the light source for times ranging from 15 to 120 minutes, depending on the experiment. The light source, a Dolan-Jenner Industries Fiber-Lite Model 190 (Fiber-Lite 190) high intensity fiber optic illuminator on "high" setting, is rated at 30 watts by the manufacturer and was measured as producing 1 W/cm^2 at 1 cm from the tip of the

aperture (the standard exposure distance for our samples) at 480 nm wavelength, using a silicon pyranometer. A handheld UV lamp was used for the shorter wavelength excitation (365 nm) required by the oligomers **5** and **6**.

More recently, an enclosed photochamber (ORG Luzchem) with interchangeable excitation sources was acquired for sample exposure. This device has greater sample capacity (16 microcentrifuge tubes or cuvettes) and also has a rotating carousel that provides more uniform exposures.

For example, *C. marina* was obtained from 18 mL aliquots of overnight cultures grown for approximately 16 hrs. These were washed with 0.85% NaCl solution followed by centrifugation at 10 K rpm in an Eppendorf 5415C for four minutes and selective pipetting. The pellet was then resuspended in 1 mL 0.85% NaCl solution and recentrifuged. This wash cycle was repeated three times.

Bacterial concentrations were then normalized using hemocytometer counts. The samples were then diluted to 2mL and separated into 200-500µL aliquots. Samples to be oxygenated or deoxygenated were bubbled with the appropriate gas for 15 minutes. Bacteria were added to polymer-coated particles in aliquots of 200-500 µL, depending on concentration, so that a ratio of 10-50 (depending on experimental parameters) bacteria per bead was achieved. The live control consisted of bacterial cells suspended at similar concentrations, but without beads. Dead controls were observed to be uniformly dead, with no fluorescence detected in the red using *Dye-set-1*. Live controls usually showed a few bacteria with compromised membranes, as shown in Figure 2-8. This is expected to occur during handling procedures and the passage of time in getting the samples washed, stained and mounted for analysis.

Polymer-coated microsphere/bacteria samples and live controls which required exposure to white light were placed at 1 cm from the source aperture of the Fiber Lite 190 for 15-120 minutes. All samples were then gently shaken on the lowest setting of a Vortex Genie 2 during this exposure period. A separate control set was kept dark by covering with Al foil. Coated beads were added in the desired ratio and the samples requiring light exposure. Samples requiring dark conditions were covered with Al foil and shaken during the same interval.

All samples were treated approximately 15 minutes before microscopy with a 1:1 mixture of the selected permeant and impermeant stains (2 µL/mL). Samples were mounted on slides with cover slips and examined. Some slides, especially those that had been oxygenated or deoxygenated, were sealed at the edges with immersion oil in order to minimize evaporation and oxygen exposure.

Counting

Upon addition of the appropriate staining compounds described above, samples were incubated for 15 minutes in the dark. Bacteria were then examined under a 40x oil objective on a Zeiss LSM 510 Meta confocal laser scanning microscope and the number of live cells (i.e., for *Dye-set-1*, those fluorescing red only) and dead cells (i.e., for *Dye-set-1*, those fluorescing both red and green and those that were primarily red) compared.

Initially, evaluations of the live/dead assays were carried out by direct visual assessment of confocal microscopy images obtained using a Zeiss Axioskop LSM 510 Meta confocal microscope. These images enable the subjective identification of live and dead bacteria according to staining, fluorescence intensity and size. Enumeration of those bacteria provided a live/dead ratio indicating survival rates under experimental

conditions. Careful visual analysis was required in order to determine bacterial fate based on staining, relative fluorescence intensities and morphology of end products, whether agglomerated or dispersed. For larger sets of images, this process usually required spending several hours in the dark with a large monitor.

Frequently, the bacteria agglomerated around the polymer-coated substrates and in solution, making it difficult to obtain an accurate count. Taking a z-stack (a set of "slices") of the agglomerate enabled more accurate enumeration, but was not always practical, as this process increases light exposure and experiment times, potentially leading to an inaccurate evaluation of polymer-induced bacterial death.

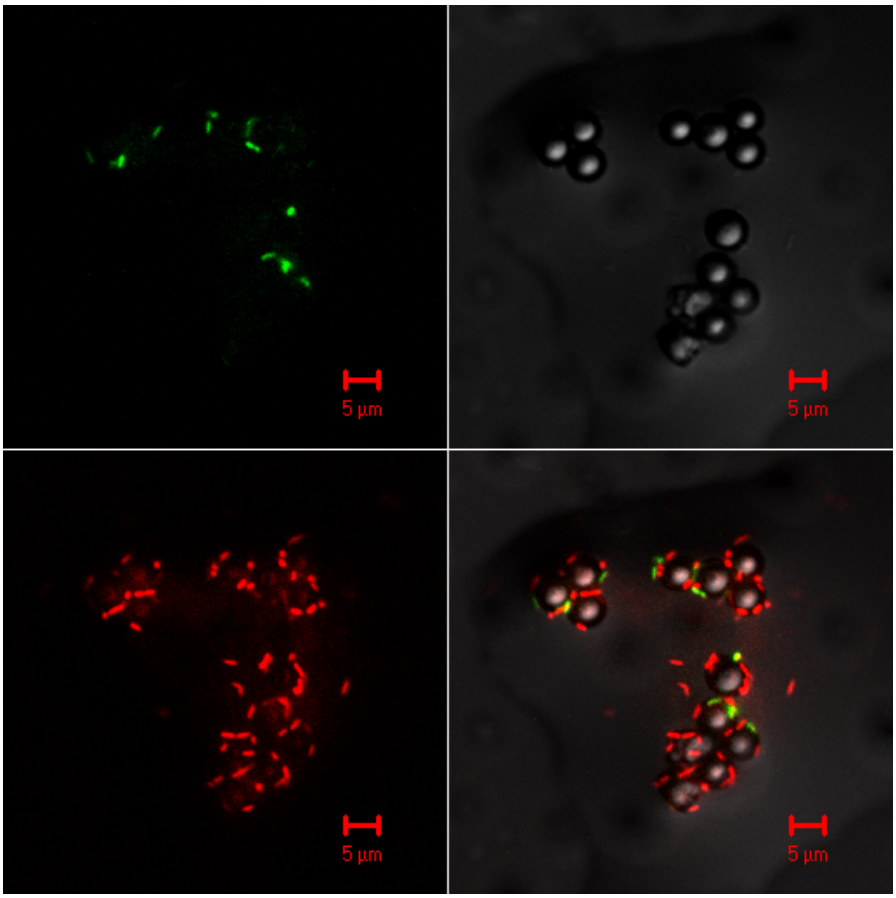

Figure 2-9. Agglomeration of particles accompanied by cell death. These are *P. aeruginosa* with surface-grafted DABCO on SiO_2, exposed to light for 15 min. and stained with *Dye-set-1*. Upper left image is green

fluorescence (dead); upper right-bright field; lower left-red fluorescence; lower right-composite.

Some of the difficulties in CLSM data acquisition and analysis included:

1) For samples in general:
    a. Photobleaching of the stains, especially differential photobleaching, where one stain photobleached faster than another.
    b. Difficulty in re-locating given features after moving the microscope stage.
    c. Drying of the sample.
    d. Fluid flow within the sample (frequently exacerbated by c, above) would occasionally disrupt the acquisition of an image. This was ameliorated somewhat by careful sample preparation and by the serendipitously discovered technique of sealing the edges of the cover slips with immersion oil. This technique was originally employed to decrease air exposure of the samples during oxygenation/deoxygenation experiments.
    e. Aggregation of particles (both in samples with and without beads) post-exposure often gave rise to inhomogeneous distributions of clustered particles with varying sizes and fluorescence properties, as in Figure 2-9. This phenomenon also seemed dependent on bacterial type, although this was not strictly quantified in these experiments.

2) For samples with beads as substrate:
    a. Because of manufacturing methods, the bead sizes may vary somewhat, usually around 10% (i.e. 5 µm ± 0.5 µm).
    b. Some debris is occasionally present, also from the manufacture and/or packaging of the beads, as shown in Figure 2-10. This is generally quite a bit smaller than the average size of the beads, with much of it being in the size range of the bacteria (1-2 µm), but typically more irregular in shape.
    c. Aggregation of the beads sometimes occurs prior to exposure to the bacteria. To ameliorate this, coated beads were typically sonicated for ~5 s prior to exposure. This was generally effective in redistributing the

beads, but may have also introduced unintentional surface damage and/or additional debris.

These factors occasionally led to difficulties in evaluating populations for both substrate particles and bacterial adherents and in assessing the latter for their survivability according to the stains employed.

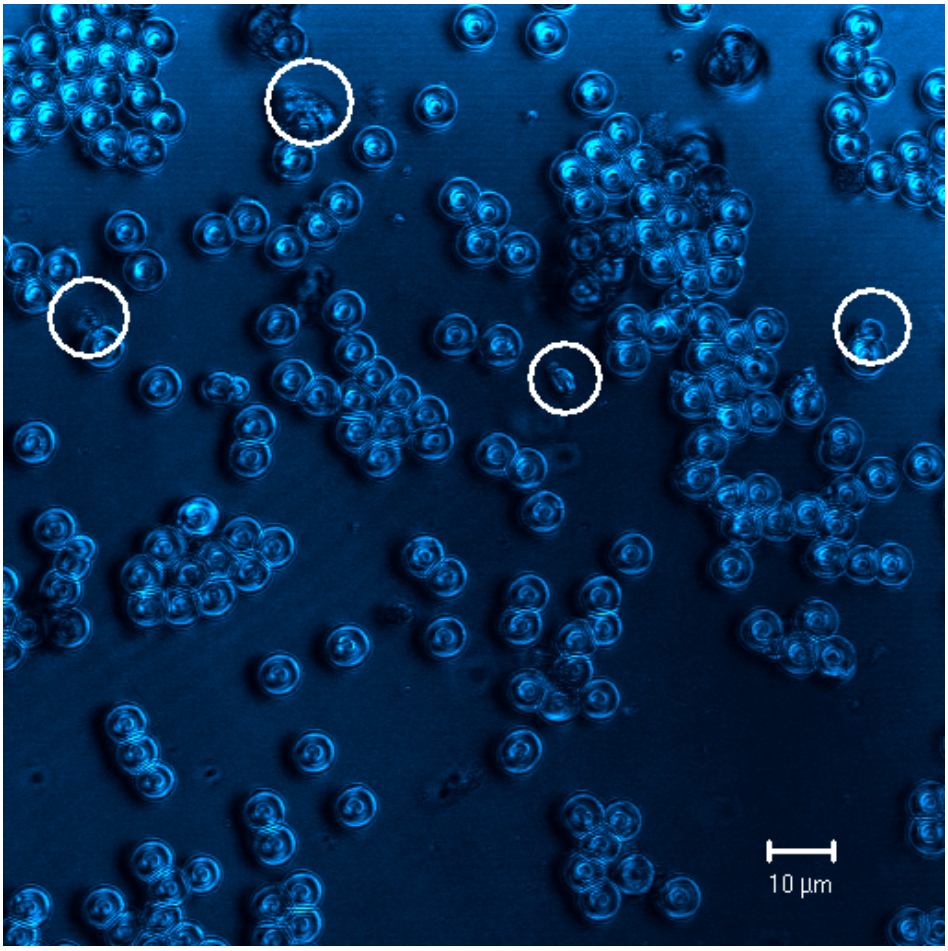

Figure 2-10. Image of PPE-SO_3 (**3**) coated 5 µm SiO_2 beads excited at 483 nm on the Confocal Laser Scanning Microscope (CLSM). Nominal bead sizes can be seen to vary over this population and some debris, believed to be bead-based, is indicated by the circles.

The use of a software-assisted counting method using Image J (a product of NIH) was attempted in order to improve the speed and reproducibility of counting. This software counting method uses grayscale contrast differences and can accelerate the

evaluation of image data in cases where the particle/bacterial population is not too high. However, this technique was not widely employed in these experiments because it does not discriminate individual components of aggregates based on shape. If there is particle clustering or overlap (as was most often the case), the aggregate is counted as one unit and visual evaluation is more accurate. Frequently, fluorescence of both stains was collocated, further complicating evaluation.

Size discrimination was possible, but this would lead to an undesired exclusion of the aforementioned clusters (that mostly contained dead and dying bacteria) and thus skew the data toward a higher live count. The difficulty of developing algorithms to find cells is evident from Figure 2-9. Among the cells present in the image shown, there are substantial differences in size and shape, and there are marked inhomogeneities in staining intensity within cells. Humans are actually much better at finding cells and at discriminating cells from debris or non-cells, even when cell size, shape, and texture vary; we just happen to be much slower.

Table 2-2. shows a typical set of counting data resulting from visual evaluation of the CLSM images. A number of observables were tracked, including cluster sizes, if present, and both the live/dead and dead/live ratios were calculated.

Table 2-2. Example of counting data produced from visual analysis of CLSM images in a *C. marina*/microsphere experiment.

		conditions		biocide			elapsed time	counts					statistics	
file name	bacteria	light/dark	oxy/ded	type	substrate	time	before image	live	dead	# beads	cluster	notes	live/dead	dead/live
CmDcluste	C. marina	dark	amb	OR11	5μm SiO2	15	2	70	29	0			2.41	0.41
CmD2	C. marina	dark	amb	OR11	5μm SiO2	15	4	20	14	10	4		1.43	0.70
CmD2b	C. marina	dark	amb	OR11	5μm SiO2	15	6	15	11	4	4		1.36	0.73
CmD2c	C. marina	dark	amb	OR11	5μm SiO2	15	8	26	22	8	6		1.18	0.85
CmD2d	C. marina	dark	amb	OR11	5μm SiO2	15	10	35	21	4	2		1.67	0.60
CmD3	C. marina	dark	amb	OR11	5μm SiO2	15	12	45	36	0		lower right	1.25	0.80
CmD3	C. marina	dark	amb	OR11	5μm SiO2	15	12	76	59	0		wide field	1.29	0.78
CmD3a	C. marina	dark	amb	OR11	5μm SiO2	15	15	43	37	1	1		1.16	0.86
CmD4	C. marina	dark	amb	OR11	5μm SiO2	15	18	127	102	7	3		1.25	0.80
CmDO1a	C. marina	dark	oxy	OR11	5μm SiO2	15	27	12	12	14	14		1.00	1.00
CmDO2	C. marina	dark	oxy	OR11	5μm SiO2	15	30	55	46	17	15	med field	1.20	0.84
CmDO2a	C. marina	dark	oxy	OR11	5μm SiO2	15	32	13	13	15	15		1.00	1.00
CmDO3a	C. marina	dark	oxy	OR11	5μm SiO2	15	37	18	21	21	12		0.86	1.17
CmDO4	C. marina	dark	oxy	OR11	5μm SiO2	15	40	59	63	41	16	wide field	0.94	1.07
Cm+2hr 2	C. marina	amb	amb	OR11	5μm SiO2	15	120	47	44	0			1.07	0.94
CmL1a	C. marina	light	amb	OR11	5μm SiO2	15	3	13	17	9	7		0.76	1.31
CmL1b	C. marina	light	amb	OR11	5μm SiO2	15	4	13	9	5	5		1.44	0.69
CmL2	C. marina	light	amb	OR11	5μm SiO2	15	6	109	78	23	1	wide field	1.40	0.72
CmL2a	C. marina	light	amb	OR11	5μm SiO2	15	7	8	5	1	1		1.60	0.63
CmL3a	C. marina	light	amb	OR11	5μm SiO2	15	9	17	14	5	3		1.21	0.82
CmL4a	C. marina	light	amb	OR11	5μm SiO2	15	11	34	35	24	19		0.97	1.03
CmL5-2	C. marina	light	amb	OR11	5μm SiO2	15	14	105	121	30	6	wide field	0.87	1.15
CmL6a	C. marina	light	amb	OR11	5μm SiO2	15	16	86	90	20			0.96	1.05
CmL6b	C. marina	light	amb	OR11	5μm SiO2	15	17	34	46	18	7		0.74	1.35

Later in the project, flow cytometry procedures were developed for rapidly assessing populations of bacteria, also based on their staining characteristics. This is covered in detail in Chapter 6.

Chapter 3

Biocidal Activity of Two Phenylene Ethynylene Polymers

Introduction

As mentioned in Chapter 1, polymeric biocides containing pendant cationic groups, especially quaternary ammonium salts, are among the most promising candidates for effective antimicrobials.(111, 199, 100) Tiller *et al*. have described methods for modifying surfaces such as glass, high-density polyethylene, low-density density polyethylene, and nylon with pendant quaternary ammonium salts.(200) Biocidal activity is thought to be the result of cationic groups penetrating the cell membrane and the relationship between structure and reactivity has been explored.(113, 100, 178, 91) Ion exchange, releasing inorganic ions associated with the bacterial membrane and the consequent weakening of the membrane, appears to play a key role.(91, 16, 104) Previous research in our group found that cationic conjugated polyelectrolytes (CPEs) having the general structure **1** can kill bacteria such as *E. coli* or *B. anthracis* when solutions of CPEs are mixed with suspensions of the bacteria and irradiated with visible light.(126)

Light inducible biocides represent potential controlled dose antimicrobial agents. Compounds used for photodynamic therapy exhibit appreciable antibacterial activity; however these and other external singlet oxygen sensitizers are not broad spectrum, exhibiting greater activity against Gram positive than Gram negative organisms.(138, 136, 133, 148) This difference in activity may be related to quenching or consumption of singlet oxygen in the latter, which contain a more complex cell envelope, a property

which contributes both to their increased pathogenicity and resistance to generalized immune response.

The fundamental light-induced reactivity of oxygen with bacteria, viruses and cells is not well understood. It is fairly well-established that irradiation of potential sensitizers of singlet oxygen can result in damage or death of microorganisms, and in several cases, the site of damage produced by the reactive oxygen species (ROS) can be determined or inferred.(109, 204) However, in many cases it is not clear as to what the ROS is or how and where it is generated. In contrast, the reactivity of singlet oxygen with organic molecules in organic solvents is very well understood and is, for the most part, limited to electron-rich alkenes, 1,3-dienes, aromatics and sulfur-containing compounds. The products of these reactions (usually peroxides) are often themselves reactive and some have been shown to undergo secondary reactions with DNA and other biological molecules. It seems probable that in many cases involving light-induced activation of oxygen in microbial systems there is an initial generation of singlet oxygen followed by its reaction with some component of the cell to generate other species that are potentially more reactive and longer lived than singlet oxygen and that these are the likely source of cell killing.

Lu et al.(126) have previously shown that a fluorescent-conjugated polyelectrolyte polyphenylene ethynylene (PPE), with pendant quaternary ammonium groups is an effective light activated biocide that inhibits the growth of Gram negative bacteria such as *Escherichia coli* and Gram-positive bacterial spores. In these experiments we demonstrate biocidal activity of similar cationic conjugated polyelectrolytes (CPE) **1** and **2** and surface grafted conjugated polymer (SGCP) beads

with the same repeat unit as **1,** both in solution and immobilized onto non-porous borosilicate microspheres. The biocidal effects of these CPEs were tested against two Gram negative bacteria: *Cobetia marina,* a marine bacterium studied for its role in biofouling and *Pseudomonas aeruginosa* strain PAO1, a model pathogen. *P. aeruginosa* is emerging in a number of epidemic strains and the matter of its resistance or susceptibility to biocides is becoming a popular topic for systematic studies. Current clinical practices for disinfection are inadequate for eliminating these "superbugs" in all situations.(35, 57, 62, 108, 112, 132, 179)

We investigated the role of oxygen in the light induced bacterial killing and propose a mechanism for the biocidal activity of the CPEs. In addition to interrogating the biocidal nature of the CPEs, their synthesis, photophysical properties and singlet oxygen production were also evaluated.

Experimental methods

Polymer synthesis

Synthesis and characterization of the polymers **1** and **2** were carried out at the University of Florida by our collaborators, Katsu Ogawa and Eunkyung Ji. The synthetic procedures may be found in Appendix B, while a description of photophysical analysis for singlet oxygen production appears in Appendix B.

Live/dead assays

Bacterial samples were prepared according to procedures described in Chapter 2. The two different dead/live assays were used in this particular study were *Dye-set-1*— SYTO 60 (red = live), and SYTOX Green (green = dead) and *Dye-set-2* (LIVE/DEAD® BacLight assay) with propidium iodide (red = dead) and Syto 9 (green = live). *Dye-set-1*

was used in data shown in Figure 3-3, Figure 3-4, and Figure 3-5. *Dye-set-2* was used in data shown in Figure 3-6.

For both controls and, after light exposure, samples treated with CPEs, the dyes were added as a 1:1 mixture to the bacterial samples (2 μL mixed dye per mL suspension) and incubated for 15 minutes. Cells were then examined under a 40x oil objective on a Zeiss LSM 510 Meta confocal laser scanning microscope and the number of live and dead cells compared.

Microchannel studies

The polymer supported particles (average diameter 30 μm) were prepared according to the procedure described in Chapter 2. Microchannels were fabricated using a protocol described by Zeineldin *et al*.(220) Aliquots of polymer supported particles suspension were injected into the microchannels and moved through the channels by vacuum. Particle packed channels were kept hydrated with PBS with 150 mM NaCl until ready for use. A particle-packed microchannel was mounted onto a sample holder of the confocal microscope. The inlet of the column was connected to a buffer reservoir, while the outlet was connected to a vacuum source. Several microliters of PBS buffer were passed through the microchannel before the injection of a bacterial suspension.

While applying a vacuum at the outlet, a bacterial suspension aliquot was injected directly into the column through the inlet silicone tubing using a well calibrated micropipette. As soon as the bacteria reached the “dam” of the microchannel, the vacuum was turned off and the silicone inlet and outlet tubes were sealed to prevent evaporation of the solvent from the channels. The microchannel was removed from the microscope stage and placed under the Fiber-Lite 190 lamp and irradiated for 15 minutes.

The microchannel was remounted onto the confocal microscope sample holder and a vacuum applied. An aliquot of the mixed dead/live dyes was injected and the vacuum turned off. The inlet and the outlet were again sealed as before and the dyes allowed to stain the bacteria for 15 minutes. Confocal images were then acquired.

Results and Discussion

Materials and synthesis

As described in detail in Appendix B, polymers **1a**, **1b**, and **2** were synthesized according to a procedure that is similar to the one reported for preparation of other PPE-type CPEs.(167) All of the polymers used in this study are soluble in water, methanol, DMF and DMSO. After preparation and purification, polymers **1a** and **1b** were completely desiccated to afford a dry powder for storage; the polymers were re-dissolved without difficulty for use in spectroscopic or biocide experiments. However, samples of polymer **2** were stored as aqueous solutions because it was found that after desiccation most of the dry material would not re-dissolve, apparently due to the formation of physical crosslinks in the dry polymer.

Microsphere properties

The method described in Chapter 2-Substrate Preparation-Microspheres was used here to prepare 5 µm particles that feature covalently grafted layers of **1a** or **1b** (**SCGP-1a** and **SGCP-1b**). The SGCP particles were imaged by using scanning electron microcopy (SEM) to confirm the presence of a grafted layer of the polymer on the surface. The SEM image of unmodified silica particles reveals a very smooth surface (Figure 3-1a), whereas the particles that are modified with **1b** (**SGCP-1b)** exhibit a relatively rough, “cotton ball” like texture (Figure 3-1b and c). The cotton ball texture

suggests that the surface of the particles has been successfully modified with polymer **1b**. Although the polymer appears to cover the entire surface of the particles, the coverage is not uniform (Figure 3-1b and c). In particular, there seem to be regions of the surface where "islands" of material are present. This may be due to the presence of aggregates of **1b** which have been covalently attached to the particle surface. While the source of the aggregates is not known with certainty, we suspect that the aggregates are produced in solution during the polymerization; the aggregates then become chemisorbed to the surface by crosslinking with the reactive surface groups. Confocal microscopy (Figure 3-1d and f) shows that the particles exhibit bright fluorescence consistent with the presence of the surface-graft layer of **1b** on the surface. Although the fluorescence is observed from the entire surface of the particles, there appears to be some "clustering" of the fluorescent material on the surface. This finding is consistent with the results observed in SEM images, which suggest that at least part of the polymer on the surface of the particles exists in an aggregated state.

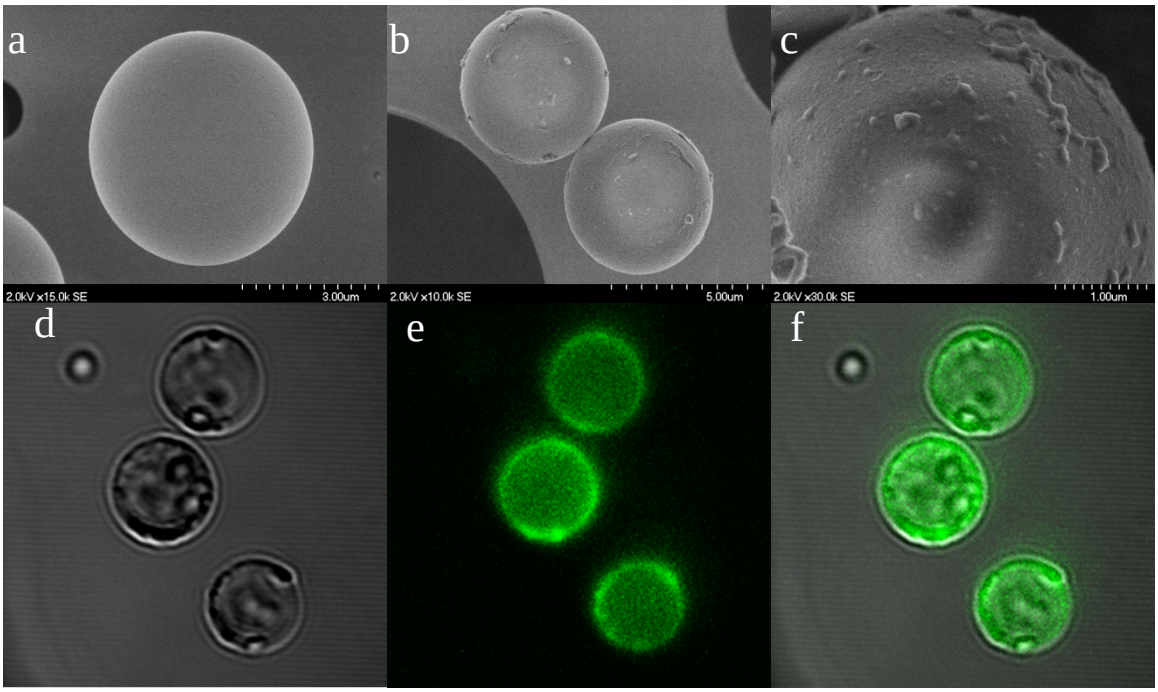

Figure 3-1. Scanning electron microscopy (SEM) images and confocal fluorescence microscopy (CFM) images of 5 µm silica particles. a) unmodified particles (SEM), b) particles with surface grafted **1b** (SEM), c) expanded view of particles with surface grafted **1b** (SEM), d) phase contrast image (CFM), e) fluorescence image (CFM), and f) overlay view (CFM).

Photophysical Characterization.

We have previously studied the photophysical properties of a number of poly(phenylene ethynylene) (PPE)-type conjugated polyelectrolytes.(196, 170, 195, 221, 167) These polymers typically absorb strongly in the violet region ($\lambda \sim 400 - 450$ nm) and fluoresce strongly in the blue or green region ($\lambda \sim 450 - 550$ nm)**.** As shown below, the cationic CPE **1a** exhibits similar photophysical behavior. In particular, the polymer exhibits a strongly allowed absorption band with $\lambda_{max} \sim 415$ nm in methanol and in water. The fluorescence emission spectrum of **1a** is solvent dependent. In a good solvent, such as methanol, **1a** exhibits a narrow emission band with $\lambda_{max} \sim 460$ nm with a shoulder at 500 nm. In a poor solvent, such as water, the emission band is red-shifted to $\lambda_{max} \sim 500$

nm and the relative fluorescence quantum efficiency is lower (Figure 3-2). Similar solvent-dependent fluorescence behavior has been observed for other CPEs, and the effects are attributed to aggregation of the chains in water (poor solvent) and consequent domination of the fluorescence by interchain excitons (analogous to excimers).(167)

Due to Mie scattering from the particles, it was not possible to obtain quantitative absorption spectra of the **SGCP-1a** particles. However, fluorescence spectroscopy was possible and these experiments show that the fluorescence of surface-confined polymer **1a** is similar to the fluorescence of the polymer in water (Figure 3-2). The emission band maximum for **SGCP-1a** (suspension in methanol) appears at $\lambda \sim 468$ nm; however, the fluorescence band is considerably broader compared to that of the free polymer, which is consistent with the notion that the polymer exists in a strongly aggregated state on the surface of the particles. The absorption spectrum of **SGCP-1a** is approximated by the fluorescence excitation scan of the suspended particles which reveal a maximum at 405 nm.

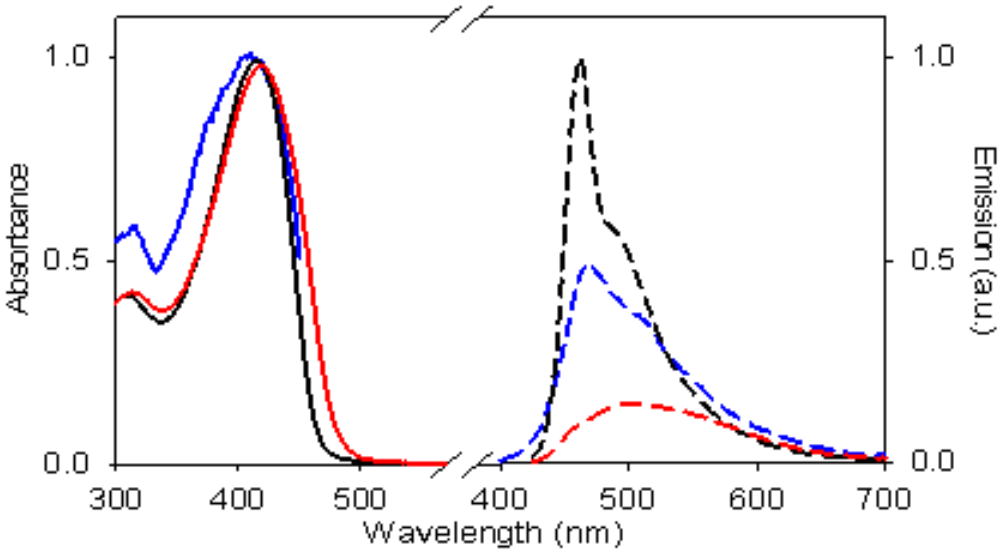

Figure 3-2. Absorption (excitation) and emission spectra of **1a** and **SGCP-1a**. Polymer **1a** in methanol solution shown in black (— absorption, – – emission), polymer **1a** in aqueous solution shown in red (— absorption, – – emission), **SGCP-1a** shown in blue (— excitation, – – emission).

Biocidal activity of CPEs.

For initial investigations suspensions of bacteria were mixed with solutions (5 μM) of cationic CPEs **1b** or **2**, incubated 20 minutes, centrifuged, washed with buffer and resuspended. The bacteria were shown, as previously demonstrated for polymer **1a** with *Escherichia coli* (Gram negative) and *Bacillus anthracis* (Gram positive), to become uniformly coated with the fluorescent CPEs.(126)

Irradiation of the polymer coated bacteria with visible light (Fiber-Lite 190) followed by plating of the bacteria in growth media was shown to result in significant killing. As shown in Table 3-1, the biocidal action of CPEs **1b** and **2** as "coatings" on both bacteria is very efficient; near total (several logs) killing occurs; of the two polymers, **2** appears to be slightly more efficient than **1b** and the killing of *C. marina* is more complete.

Table 3-1. Effect of CPEs **1b** and **2** on *Cobetia marina* and *Pseudomonas aeruginosa*. Legend: (approximate number of cfu/plate): + 100-500, ++ 1000-5000, +++ 10000-50000, ++++ confluent, +/- minimal growth, — no growth.

	C. marina			*P. aeruginosa*		
Dilution	10^0	10^{-1}	10^{-2}	10^0	10^{-1}	10^{-2}
Untreated	++++	++++	++++	++++	++++	++++
Light Only	++++	++++	++++	++++	++++	++++
1b + Light	+++	++	+	+++	+	+/-
2 + Light	++	—	—	++	+	—

One of the major goals of these studies was to determine whether surface coatings of CPEs such as **1** or **2** would be effective at capturing and killing of these bacteria. In the following sections we report studies of the biocidal activity of the cationic CPEs as coatings on silica particles in two specific formats: 1) Polymer **1b** as a covalently attached surface graft layer (**SGCP-1b**); and 2) Polymer **2** as a physisorbed coating. For these studies we used confocal fluorescence microscopy to interrogate suspensions of CPE-coated particles and bacteria and mixtures of DNA-staining dyes were used to perform live-dead assays of bacteria exposed to the coated particles in the light and dark. Examining suspensions of bacteria containing either physisorbed polymer **2** or the **SGCP-1b** particles described above, it was found that *C. marina* are captured by the particles and can form clusters where several (~7-12) bacteria are associated with a single particle (Figure 3-3). The association is reversible to some extent and real time observation of a single particle-bacteria cluster reveals that some bacteria associate briefly and then are released while others appear to be captured irreversibly.

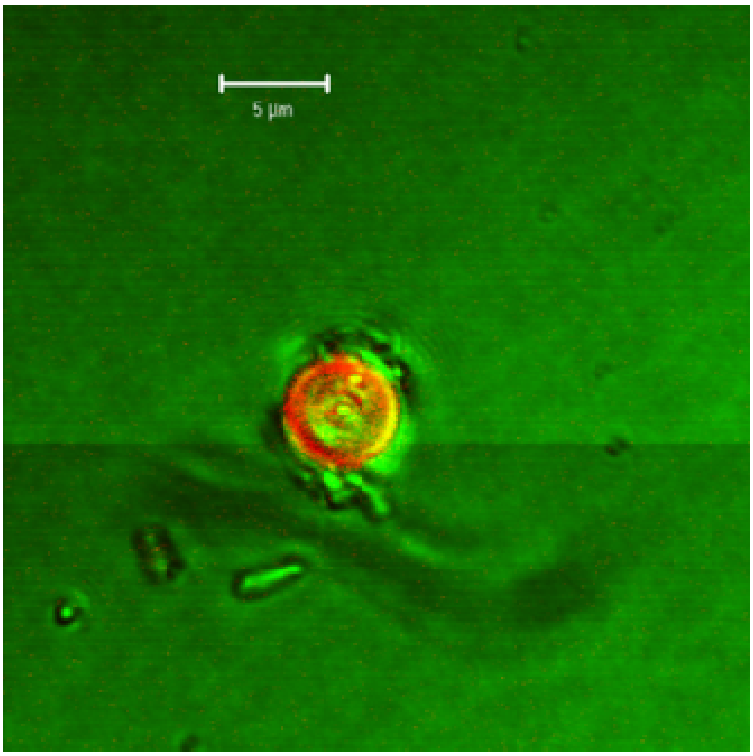

Figure 3-3. Image of single SGCP-particle (red/orange) with captured bacteria (brighter green).

Irradiation of suspensions of *C. marina* with the CPE-coated particles with visible light for short periods (using the Fiber-Lite 190 as described in Chapter 2; typical irradiation times for *C. marina* are 15 minutes) results in effective killing of bacteria that are associated with or in the vicinity of the particles; however, very little killing of bacteria distant from the particles is observed on short term irradiation. Figure 3-4 shows both wide field and close up images of a suspension of *C. marina* and 5 µm **SGCP-1b** particles after irradiation of samples in ambient air. Here the ratio of beads to C. marina is 1:50. Beads and C. marina were mixed together with slight shaking while simultaneously being exposed to the Fiber-Lite 190 on the highest setting for 15 mins. The close up image shows a cluster of particles and bacteria which typically builds up when these suspensions are irradiated. Most of the bacteria in this cluster are dead as

shown by the predominance of green fluorescence from the SYTOX Green nucleic acid stain. While irradiation of suspensions of polymer coated particles and bacteria is not necessarily an efficient way of eliminating the bacteria, it is a useful way to obtain mechanistic information regarding the biocidal activity of the polymers and gauging bacterial response.

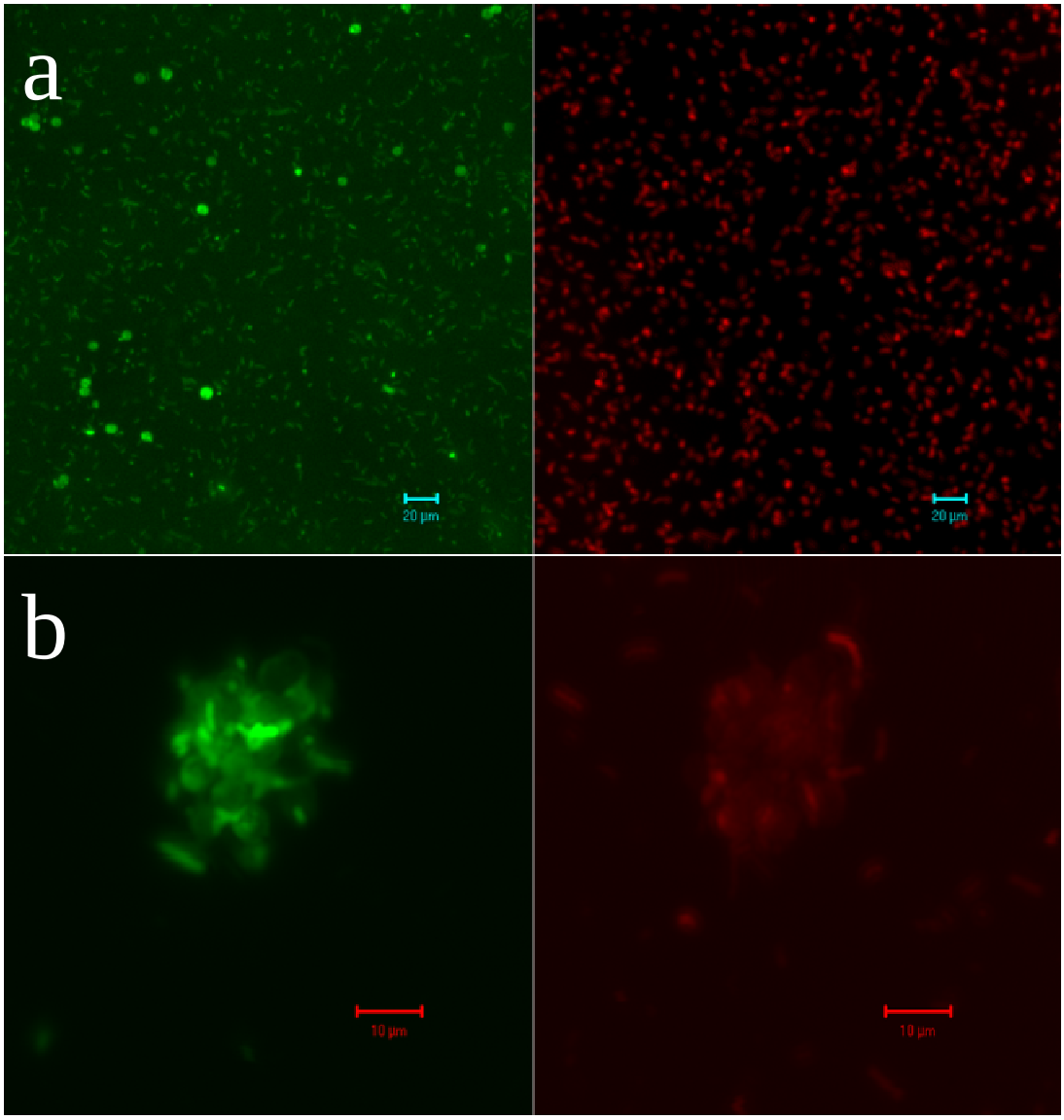

Figure 3-4. Composite images of **SGCP-1b** coated beads with *C. marina* after irradiation in ambient air. a) wide field of view and b) enlarged region with a single cluster. Left panels show green channel corresponding to dead bacteria and polymer emission; right panels show red channel corresponding to live bacteria (*Dye-set-1*).

We examined suspensions of *C. marina* and 5 μm **SGCP-1b** particles kept in the dark and those irradiated with visible light. What is shown quite clearly in Figure 3-5 is that association of *C. marina* with **SGCP-1b** particles occurs in the dark, yet few of the associated bacteria are killed during incubation in the dark (i.e., the bacteria still appear red). In contrast as shown in Figure 3-4, most, if not all of the *C. marina* associated with the SGCP particles are killed (i.e., the bacteria appear green) as a consequence of irradiation. A caveat in these studies is that it is very difficult, if not impossible to keep the "dark" suspensions rigorously dark; indeed during irradiation for confocal fluorescence interrogation with the dead/live stained bacteria it is possible to observe the conversion of individual bacteria near or associated with **SGCP-1b** from red to green fluorescence (i.e., live $\rightarrow$ dead). While there are always a few dead bacteria observed in aerated suspensions of bacteria and particles kept in the dark, the extent of the killing is much less as shown visually in Figure 3-5 and through counts of live and dead bacteria as compiled in Figure 3-8. While we cannot exclude dark biocidal activity as a consequence of bacteria-surface coated polymer contact, the much greater killing of the bacteria in a light-activated process in ambient air is evident.

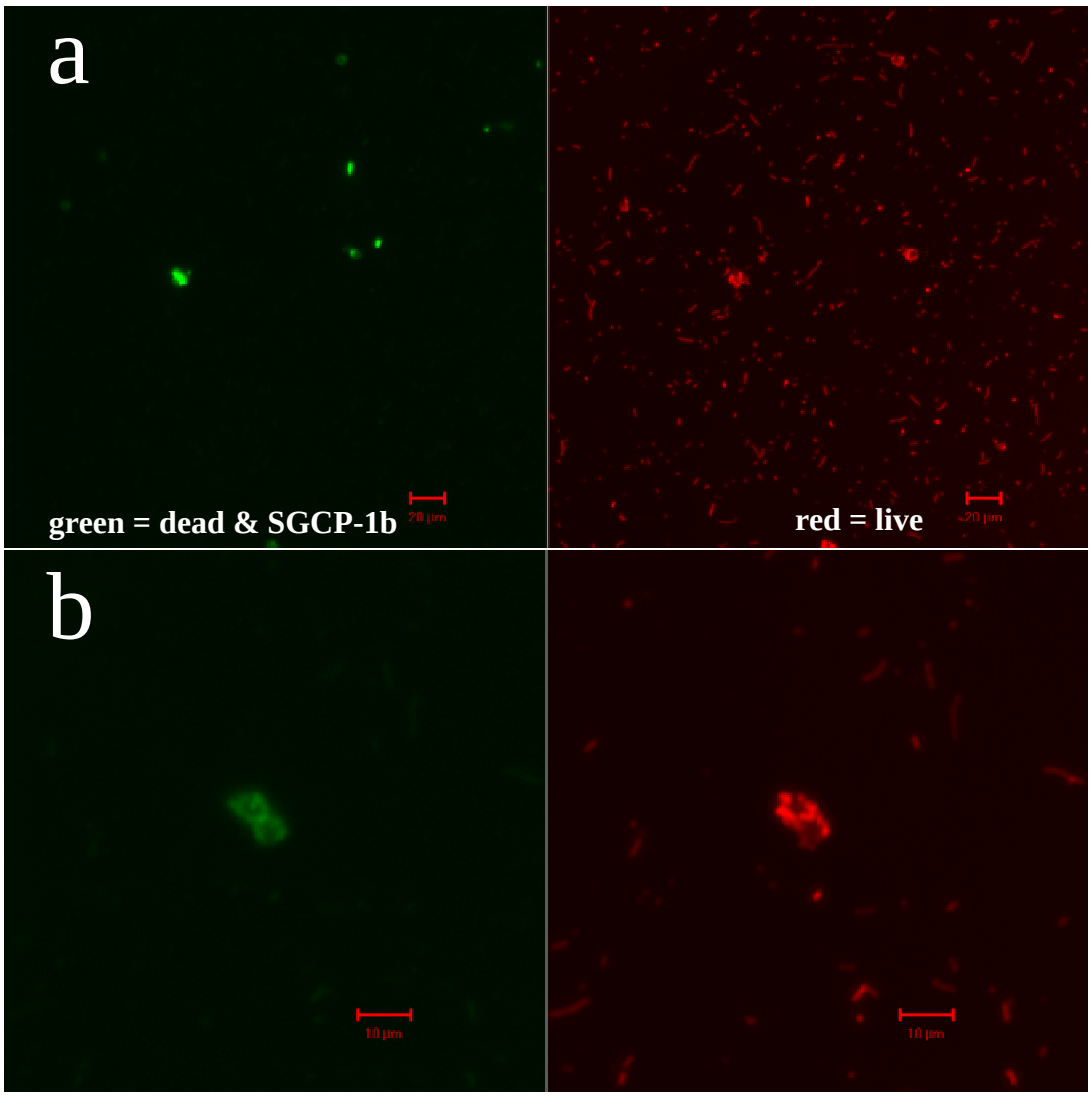

Figure 3-5. Composite images of **SGCP-1b** with *C. marina* without irradiation in the presence of ambient air. a) a large field of view and b) enlarged region with a single cluster. In both pairs of images, the green channel (left) corresponds to dead bacteria (with green fluorescence from **SGCP-1b**) and the red channel (right) corresponds to live bacteria (*Dye-set-1*).

More pronounced evidence of killing of *C. marina* was obtained by using larger (30 micron diameter) silica particles coated with physisorbed polymer **2** in a microfluidics channel. As shown in Figure 3-6a, microchannels can be packed with these larger polymer coated particles such that the much smaller *C. marina* can flow through the channel and undergo frequent and multiple collisions with the particles.

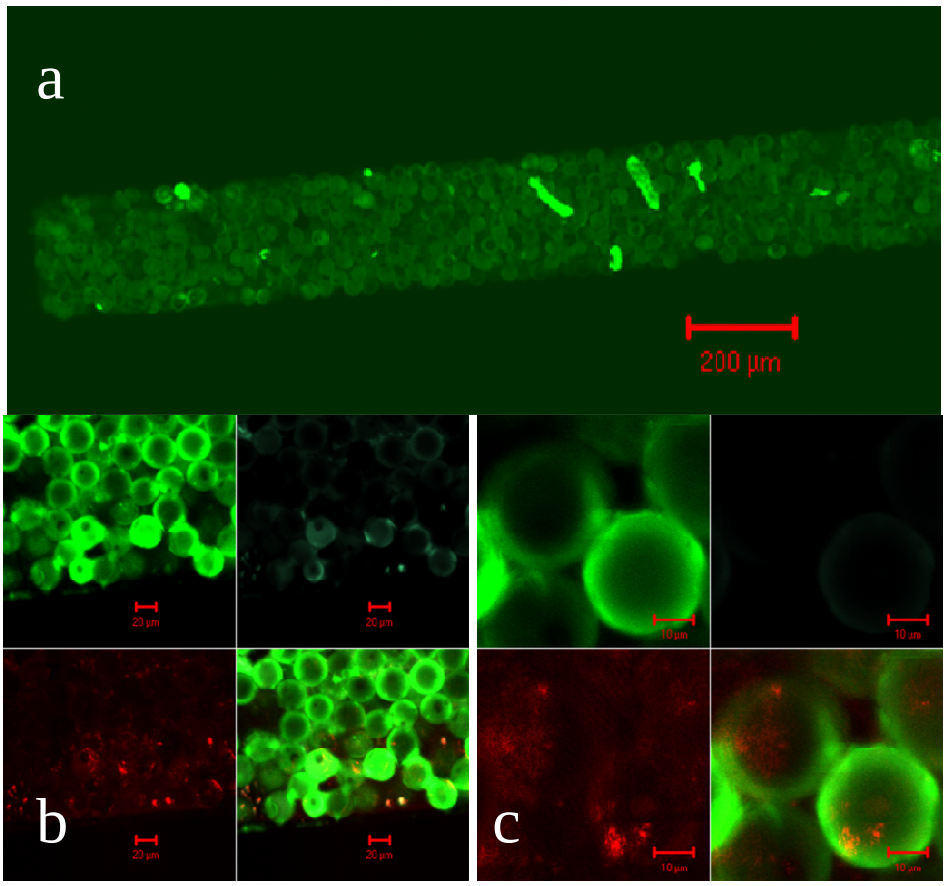

Figure 3-6. Confocal microscope images of a microchannel formed by 30 micron silica particles whose surface is modified with single layer of physisorbed polymer-**2**. a) overview, green channel only b) particles and bacteria after killing in the middle part of the channel; c) particles and bacteria after killing at the edge of the channel. Note that parts b) and c) each contain four different images of the same region, these images correspond to the following: upper left, green channel which highlights fluorescence from polymer-**2** along with green fluorescence of live bacteria; lower left, red channel which highlights fluorescence from dead bacteria and bacterial debris; upper right is a 633 nm illuminated image; lower right is a composite of the green, red and illuminated images (*Dye-set-2*).

When a suspension of *C. marina* was passed through the channels until bacteria reached the "dam" at the end of the channel and the channel subsequently irradiated for 15 minutes, the bacteria remaining in the channel were shown by a live/dead assay using *Dye-set-2* to be almost entirely killed. Interestingly in addition to intact dead bacteria, several "red" features smaller than intact bacteria were observed near the end of the

channel (Figure 3-6c), that may be debris formed during physical destruction of the bacteria. We believe that this bacterial debris may be the same material responsible for the collection of large clusters of bacteria and the 5 µm **SGCP-1b** particles shown in Figure 3-4b and Figure 3-7.

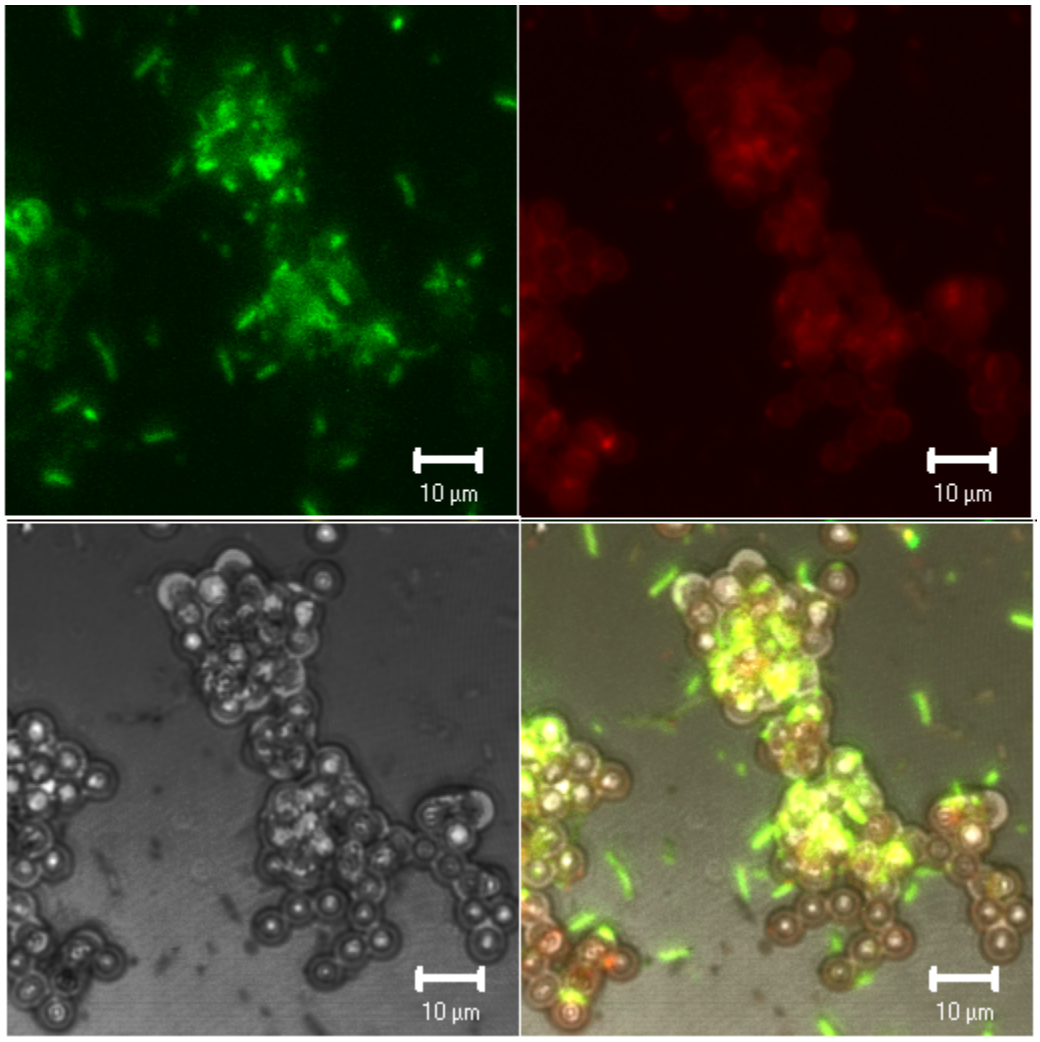

Figure 3-7. Confocal images of dead bacteria/microsphere agglomerates in an oxygenated sample with *Dye-set-1*. Images are: upper left-dead; upper right-live; lower left-633 nm illumination; lower right-composite.

Of major interest is the mechanism for the light-induced bacterial killing. At least two very different initial steps for the biocidal activity appear possible.(138) As previously discussed, polymer **1a** has been shown to be a sensitizer of singlet oxygen in

both methanol and aqueous solutions. Studies with $^1O_2$ trapping by CHDDE demonstrate that **SGCP-1b** is also an effective sensitizer (see Appendix B). Thus, initiation of reaction via sensitization of $^1O_2$ at the bacteria-polymer interface is one possibility. However a reasonable alternate initial step could be photoinduced charge transfer between excited polymer (a polycation) and halide ions associated with the polymer as counterions. This could be thought of as an example of a so-called Type I photosensitized process.(136) Oxidation of a halide ion to a neutral halogen atom followed by escape of the halogen onto the surface of the bacteria could result in strong damage and subsequent disruption through oxidation of the bacterial membrane, lipoproteins and/or peptidoglycans. The former initial step (via $^1O_2$ sensitization) should be catalytic while the latter would lead to destruction of the polymer in prolonged irradiation. While we have observed some slow photobleaching of the polymer during prolonged irradiation of the polymer-bacterial suspensions, it is not possible to differentiate the two mechanisms on this basis. More definitive results have been obtained by studies of ambient air exposed, deaerated and oxygen-purged suspensions.

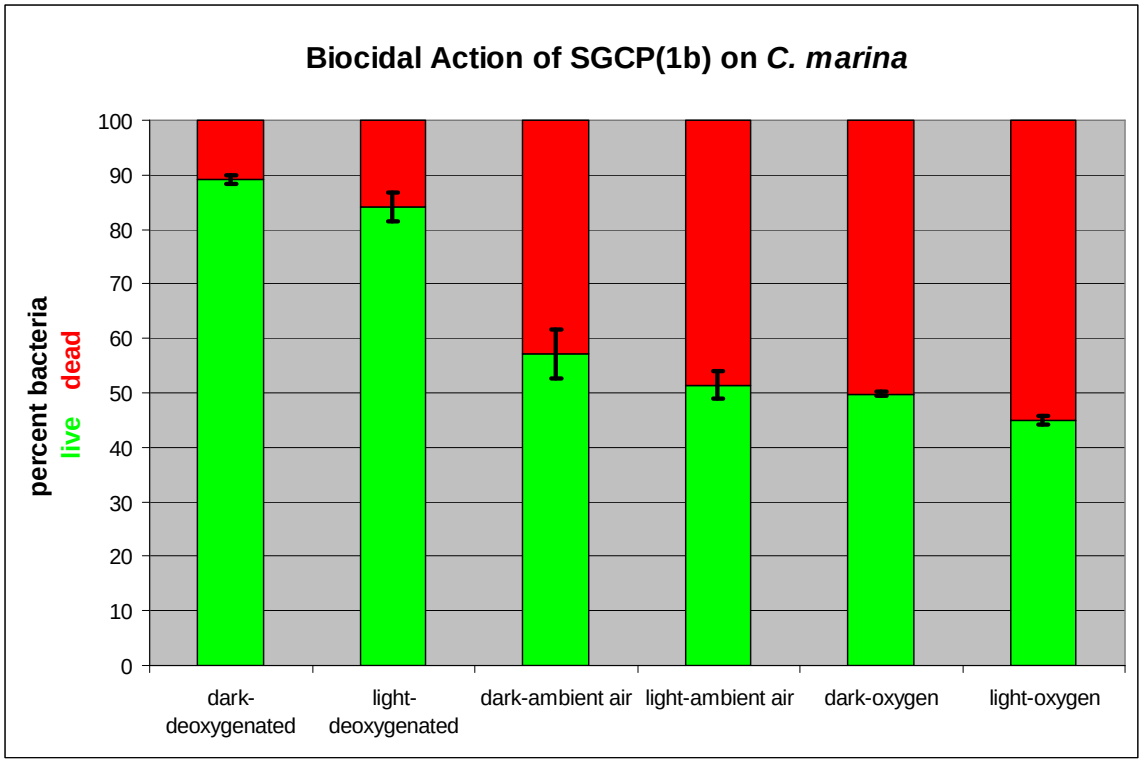

Figure 3-8. Effects of exposures to 5 µm **SGCP-1b** particles on dead to live ratios of *Cobetia marina* under various conditions. (Data compiled from measurements on 142 CLSM images.)

As shown in Figure 3-8, dead/live counting experiments from confocal fluorescence images give reasonable reproducibility for dead/live ratios of bacteria under each condition. For light-exposed solutions (in ambient air) there is a consistent but small increase in the number of dead bacteria as compared to those kept in the dark (recall the caveat discussed above about "dark" samples). Samples purged with oxygen and irradiated with visible light show an increased dead/live ratio. In contrast, argon deaerated samples, dark or irradiated, show very low dead/live ratios, indicating a clear role of oxygen in the antimicrobial activity. Interestingly there is a much more substantial difference in the dead/live ratio for deoxygenated in both dark and irradiated samples; these samples are purged with argon for 15 minutes prior to irradiation for aerated samples and it is expected that little oxygen should enter the suspensions prior to

their interrogation with the microscope. Taken together with the photophysical studies described above, these results point to a likely role of oxygen in the light-activated biocidal effect of the CPEs. Interestingly, the dark oxygenated samples show increased killing compared to the dark deoxygenated samples, but the mechanism for this is not yet understood.

At this point what we can make several statements regarding the mechanism of CPE biocidal activity towards *C. marina*: The surface associated CPE (either grafted or physisorbed) can associate with the bacteria in an adsorptive process, likely driven by hydrophobic and electrostatic interactions, analogous to adsorption of CPEs and other polyelectrolytes to an oppositely charged colloidal particle.(126) This process occurs in the dark or light and does not, in itself, result in short term killing of the bacteria although some physical damage (and longer term killing) of the bacteria may occur. The longer polymer chains with pendant cationic groups may play a key role in this process.(111, 199, 218, 117, 178) Irradiation of bacteria-associated polymer with visible light in the presence of air results in generation of "reactive oxygen intermediate", very likely excited $^1O_2$, which can enter the bacteria ultimately causing severe damage and cell death. As contents of the bacterial cells are released from the dead or dying bacteria, the released debris collects polymer coated particles and bacteria into large aggregates (Figure 3-4b). The extensive degradation of the bacteria (as opposed to simple killing) suggests that the initial generation of singlet oxygen may be followed by generation of more corrosive reactive oxygen intermediates such has been suggested in other investigations.

While the initial results reported above with solution phase polymers **1a** and **2** show that both *Cobetia marina* and *Pseudomonas aeruginosa* are killed effectively following coating by the polymers and irradiation with visible light, preliminary studies with the particle-based CPE coated silica samples show that comparable treatment of suspensions of *P. aeruginosa* results in much less killing than for *C. marina*. Prolonged irradiation of suspensions (~1 hour) does result in significant killing and purging of the samples with oxygen prior to irradiation enhances the killing. The matrix of bacterial species and polymer structure remains an important area for future investigations. The studies with large polymer **2** coated particles (30 μm) in a microchannel suggest one possible application format for light-activated antimicrobial activity in water purification and related filtration processes.(27)

Summary

A series of water soluble, cationic conjugated polyelectrolytes (CPEs) with backbones based on a poly(phenylene ethynylene) repeat unit structure and tetraakylammonium side groups exhibit a profound light-induced biocidal effect. The biocidal activity of the CPEs appears to be correlated with the photophysical properties of the polymers. Biocidal activity was observed both in solution and immobilized, with the polymers either physisorbed or surface grafted on non-porous borosilicate microspheres. The colloidal polymer-bead assemblies tend to entrap and kill bacteria and agglomerate into large aggregates over time.

Scheme 3-1 summarizes what we believe to be the mechanism. First, the colloidal polymer bead assemblies entrap bacteria in a dark process, as shown in Figures 3 and 5 (Scheme 2, i). Next (ii), illumination of the polymer leads to production of

singlet oxygen at the polymer/bacteria interface and this singlet oxygen or some subsequently produced reactive oxygen intermediate interacts with the bacteria resulting in bacterial killing and eventual degradation (iii, iv). Finally, the bacterial debris resulting from the disruption of the bacterial envelope collects and associates with the beads resulting in formation of large aggregates of dead bacteria and colloidal particles (v).

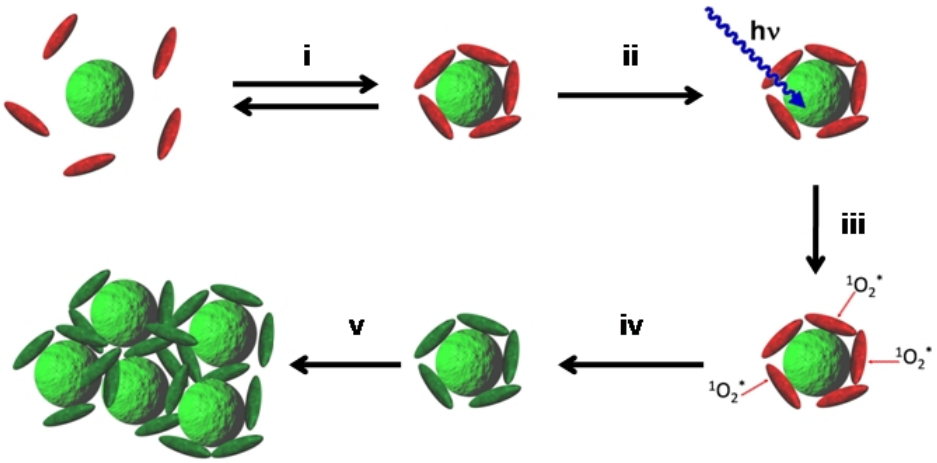

Scheme 3-1. Mechanism of biocidal action (following the color scheme of *Dye-set-1*). i) reversible and irreversible bacterial adhesion to the particle. ii) photoexcitation of CPE. iii) singlet oxygen generation. iv) killing of bacteria by singlet oxygen/other reactive species. v) aggregation of particles.

The effective killing of *Cobetia marina* and *Pseudomonas aeruginosa* in these systems is also correlated with a requirement for oxygen suggesting that interfacial generation of singlet oxygen is the crucial step in the light-induced biocidal activity. Photophysical studies show clearly that direct excitation of the CPEs leads to moderately efficient production of a long-lived triplet excited state, and the triplet is an efficient sensitizer of $^1O_2$. The study shows that suspensions of bacteria plus SGCP beads deaerated with argon show little killing in dark or when irradiated. In contrast, beads

plus bacteria oxygenated and irradiated show significant killing (Figure 3-7, Figure 3-8). We postulate that, in close proximity to the cell membranes, or once associated with the membranes through the interaction of the pendant quaternary ammonium groups, the reactive species generated are able to effect or exacerbate reactions disrupting the cell membranes, leading to bacterial mortality. This provides good evidence for an effective light-induced biocidal activity of colloidal assemblies containing the CPEs as a surface coating.

Chapter 4

An Exception to the Rule: Light and Dark Biocidal Activity of a Cationic Polythiophene-ethynylene

Introduction

At this point in our investigations, we considered it to be a fairly well-established trend that irradiation of the polymers at their relevant absorptive wavelengths would increase their biocidal activity. We expected that trend to hold for a novel cationic poly(arylene ethynylene) conjugated polyelectrolyte compound (**4**, Figure 1-5**)**, for which the singlet oxygen producing capacity had been verified and measured quantitatively (Appendix B). This compound is analogous to compound **1a** with thiophenyl groups in place of the unsubstituted phenyl rings. The objective of the study then undertaken was to compare the behavior of this polymer's light and dark biocidal activity to the cationic PPE polymers **1** and **2** that were previously investigated. Properties of solution phase **2** and **4** and physisorbed suspensions of these polymers on silicon microspheres (Si-**2** and Si-**4**) were observed. The photophysical properties of the polymers were evaluated and used to understand the striking differences in biocidal activity between the compounds.

In chapter 3 we found that cationic conjugated polyelectrolytes **1** and **2** show little biocidal activity in the dark against *Cobetia marina* or *Pseudomonas aeruginosa* strain PAO1 (PAO1) when microspheres with physisorbed or surface grafted conjugated polyelectrolytes are mixed with bacterial suspensions for short periods of time (15 minutes-1 hour).(37) Over prolonged incubation in the dark there is a slow killing of the bacteria. When the same suspensions are irradiated with visible light in the presence of

oxygen, however, there is a relatively rapid light-activated biocidal activity that likely involves interfacial generation of singlet oxygen and perhaps subsequent formation of more corrosive reactive oxygen species. The principal findings are that the thiophene-polymer **4** exhibits somewhat different photophysical behavior from CPEs **1** and **2** and the new behavior results in dramatically reduced light activated biocidal activity. We find however that **4** does show substantial dark biocidal activity against *Pseudomonas aeruginosa* strain PAO1. Here we attempt to account for that difference in behavior and provide insights into the way dark and light-activated biocidal activity may be adjusted.

Experimental methods

Materials

The syntheses of **2**, **4** and CHDDE are covered in Appendix B. Nonporous borosilicate glass microspheres (5 μm diameter) were purchased in dry powder form from Duke Scientific (Palo Alto, CA). 1,2-Dioleoyl-sn- Glycero-3-[Phospho-*rac*-(1-glycerol)] (Sodium Salt) (DOPG) was purchased from Avanti Polar Lipids (Alabaster, AL). Phosphate buffer saline (PBS) was prepared according to a standard procedure and has a pH value of 7.4. Milli-Q water (18.2 MΩ cm-1) was used to prepare all aqueous solutions.

Preparation of PPE-coated silica microspheres

Following the process outlined in Chapter 2, two different cationic CPEs, **2** and **4** were adsorbed onto the surface of borosilicate microspheres. A given quantity of microspheres (50 mg, ca. 3.0×10^8 spheres) were suspended in 1 mL of water first and mixed for a few minutes by using a vortex mixer. Then, the amount of PPE needed to provide 1.2 monolayers of CPE per Si-**4** sphere was calculated using molecular surface

area per repeat unit and then added to the microsphere suspension. The whole system was mixed strongly using a vortex mixer for 30 min. Finally, the suspension was centrifuged, and the supernatant was decanted and discarded. The PPE-coated silica microspheres (Si-**2** and Si-**4**) were resuspended in water and the cycle-centrifuge, decant, discard, and resuspend-was repeated 10 times to insure there was no unbound PPE polymer remaining in the suspension.

Preparation of DOPG liposomes and lipobeads

DOPG liposomes were prepared starting with a 2 mM solution of DOPG in chloroform. The chloroform solution was added to a vial and the chloroform was removed under vacuum overnight. The dried lipids were then resuspended in PBS buffer and mixed for 5 min, and finally extruded to optical clarity by using a mini-extruder (Avanti Polar Lipids, Alabaster, AL) and extruding through an 0.8 μm polycarbonate membrane filter 11 times. Lipobeads were prepared by adding 100 μL of each stock Si-PPE suspension to 1 mL of DOPG liposome (2 mM) and mixing at room temperature using a vortex mixer for 30 min. The resulting lipobeads, Si-**2**-DOPG and Si-**4**-DOPG, were centrifuged and the supernatant containing extra liposome was decanted and discarded. The cycle—resuspend, centrifuge, decant and discard—was repeated four additional times to make sure there was no extra DOPG in the supernatant. At that point the lipobeads were resuspended in 1 mL PBS.

Data collection

Fluorescence spectra of polymers 2 and 4 mixed with either PAO1 bacteria or DOPG liposome and microspheres coated by these polymers were performed on a SpectroMax M-5 microplate reader (Molecular Devices) using a 96-well plate, where 100

μL of each sample containing either 1.3 $\times 10^{-5}$ M PPE polymers solution or 3.0 $\times 10^{6}$ Si-PPE microspheres was analyzed. The excitation wavelengths for polymer 2 and 4 are 394 nm and 427 nm, respectively. The emission spectra were collected from 430 to 650 nm for polymer 2 and from 460 nm to 700 nm for polymer 4.

Results and discussion

Photophysical properties

The structures of CPEs analyzed herein are illustrated in Figure 1-3 and Figure 1-5. Polymers **2** and **4** are poly(phenylene ethynylene) (PPE)-based CPEs that feature quaternary ammonium salts on the side chains. CPEs exist in a "molecularly dissolved" state with minimal aggregation in a good solvent, such as methanol. In poor solvent, on the other hand, they exist as aggregates.(196, 195) Aggregation of polymer chains results in changes in photophysical behavior of the polymers in solution.(221, 170, 167) In general, PPE-based CPEs exhibit red-shift and narrowing of absorption spectrum and red-shift and broadening of fluorescence spectrum upon switching from a good solvent to a poor solvent.

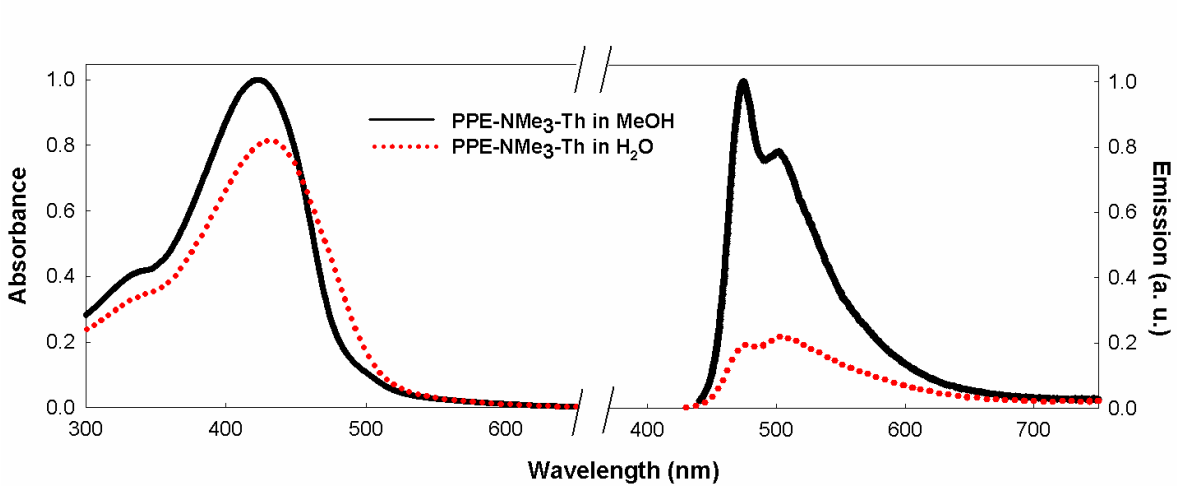

Figure 4-1. Absorption and emission spectra of **4** in methanol and aqueous solution. The spectra are normalized according to absorption coefficients (absorption) and relative emission quantum yields (emission).

As seen in Figure 4-1, a methanol solution of polymer **4** exhibits a broad absorption band with λ_{max} at 422 nm. In aqueous solution, the absorption maximum red-shifts to 432 nm and also the absorption coefficient decreases. Here, the emission properties are more dependent on the nature of the solvent. In methanol solution, polymer **4** exhibits a narrow emission band at λ_{max} = 475 nm with a vibronic band at λ_{max} = 502 nm. In aqueous solution, the emission band becomes broader and the fluorescence quantum yield (Φ_{fl} = 0.016) is lower than that in methanol (Φ_{fl} = 0.045). Interestingly, the emission maximum is at the same position as in methanol (475 nm) with a shoulder at 502 nm. Such behavior is different from other PPE-based CPEs, which exhibit large red-shifts of emission band in a poor solvent. The lack of a spectral shift for **4** is likely due to the fact that the aggregated state of the polymer has a much lower quantum yield, and therefore its contribution to the total emission spectrum is small. The photophysical properties of **2** were previously studied and reported in the literature.(221) The photophysical data of polymer **2** and **4** are summarized in Table 4-1.

Table 4-1. Photophysical properties of **2** and **4**.

polymer	solvent	λ_{max}^{abs}/ nm	λ_{max}^{fl} / nm	Φ_{fl}	Φ_{Δ}[e]
2[c]	MeOH	422	441	0.15 (± 0.02)[d]	0.122 (± 0.012)[b]
	H_2O	394	436	0.047 (± 0.005)[d]	0.32 (± 0.039)[b]
4	MeOH	422	475, 502	0.045 (± 0.005)[a]	0.112 (± 0.008)[b]
	H_2O	432	475, 502	0.016 (± 0.002)[a]	0.037 (± 0.001)[b]

[a] Coumarin 30 in MeOH as standard, Φ_{fl} = 0.307 (ref. (183)), λ_{ex} = 425 (MeOH), λ_{ex} = 419 (H_2O). [b] Oxygen saturated solution. [c] From ref. (221) [d] Coumarin 1 in EtOH as standard, Φ_{fl} = 0.73 (ref. (92)), λ_{ex} = 370 nm. [e] Quantum yield of singlet oxygen.

Transient absorption spectroscopy of **4** also indicates lower intensity of the transient absorption in water suggesting that the triplet yield is lower in comparison to methanol solution.(46) This lower triplet yield in water can be explained by aggregation of the polymer, which quenches the singlet excited state of the polymer. This is consistent with the reduced fluorescence intensity of the polymer in water compared to in methanol.

Biocidal studies

Microsphere-based

A series of experiments to test for biocidal activity were carried out using **4** as a physisorbed coating on 5 µm SiO_2 microspheres. These microspheres were exposed to PAO1 and observed for association and biocidal activity using confocal microscopy. The bacteria attach to the surface-associated polymers in an adsorptive process, likely driven by hydrophobic and electrostatic interactions, analogous to adsorption of polyelectrolytes to an oppositely charged colloidal particle.(126) This process occurs in the dark or light and does not, in itself, result in short term killing of the bacteria although some physical damage (and longer term killing) of the bacteria may occur. This association is reversible to some extent and real time observation of a single particle-bacteria cluster reveals that

some bacteria associate briefly and then are released while others appear to be captured irreversibly.

As previously observed,(47, 37) and as shown in Figure 4-2, clusters of microspheres along with bacteria begin to agglomerate as bacteria are killed, presumably due to the release of microbial agglutinants as the cell membranes are compromised. In solution, these agglomerates tend to be a rough indicator of the antimicrobial activity over time, with samples starting out with fairly monodisperse solutions of coated microspheres to which the bacteria are added. In the samples using **4,** large aggregates with pronounced antimicrobial activity appeared within 15 minutes of introduction of bacteria. Light-exposed samples tended to have less aggregation and actually showed diminished biocidal action, even with bacteria intimately associated with the coated microspheres (Figure 4-2b).

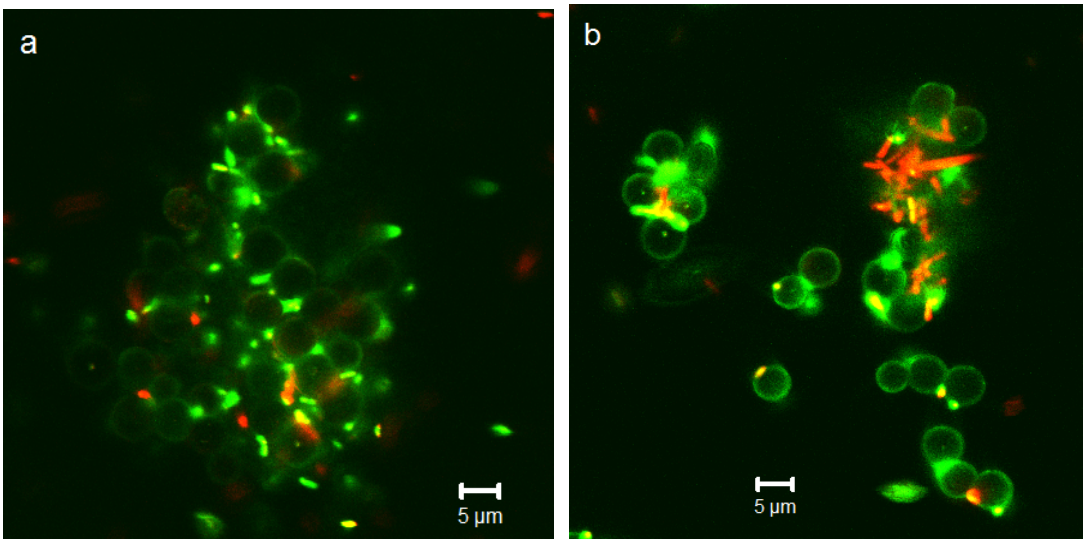

Figure 4-2. Comparison of biocidal activity in the dark (a) and light-exposed (b) solutions of **4** physisorbed onto 5 µm glass microspheres. In the images, the live bacteria are red and the dead bacteria are green. The polymer is observed as a very faint green color on the surface of the glass microspheres.

This is in contrast with the behavior of physisorbed **1** and **2,** suspensions of which show some dark and significant light-activated biocidal activity against PAO1 but less agglomeration.(37) Microspheres with physisorbed **1** and **2** also show much stronger fluorescence than physisorbed **4** even when coated at the same density. Interestingly, when microspheres of physisorbed **4** are overcoated with a phospholipid bilayer the fluorescence levels are much stronger.(38) It should be noted that it is very difficult to keep dark suspensions rigorously dark and some irradiation does occur during subsequent confocal fluorescence imaging. Unexposed PAO1 typically remained viable for more than six hours, longer than the total experimental time. For microspheres with physisorbed **4** incubation with PAO1 in the dark for 2 hours results in greater than 95 percent killing of the bacteria.

Solution activity

Addition of polymer solutions to suspensions of PAO1 also results in dark biocidal activity for both **2** and **4**; however there are clear differences in the behaviors of the two polymers as shown in Figure 4-3. Treatment of PAO1 with **4** results in clustering of the bacteria and rapid killing, as shown in Figure 4-3a. In contrast, treatment of PAO1 with **2** results in very little agglomeration of the bacteria (Figure 4-3b). As will be discussed below we believe this behavior can be attributed to the lipophilic character of polymer **4.**

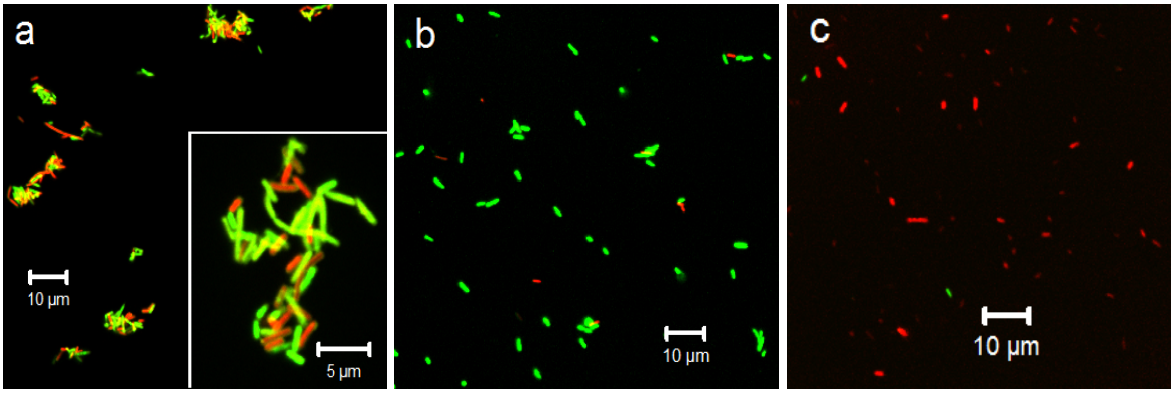

Figure 4-3. Confocal microscopy images of PAO1 added to a solution of **4** (a) and **2** (b) in the dark. We note the formation of large bacterial clusters for **4** (a) with very few individual bacteria as compared to **2** (b) and to the live control (c). *Dye-set-1* (red indicates live bacteria; green indicates dead bacteria.) Live control is bacteria with same concentration but without beads or polymers.

Fluorescence studies

Fluorescence spectra of both polymers **2** and **4** in 0.85% NaCl aqueous solution were measured in the absence and presence of PAO1 bacteria using a plate reader. As the rod-shaped PAO1 we used is *ca.* 2 µm in length and 0.7 µm in diameter, the calculated surface area of per PAO1 is *ca.* 4.7×10^{-12} m^2. According to the literature, the surface area per PPE repeat unit is ca. 2.8×10^{-18} m^2. (195) Therefore, about 1.7×10^6 PPE repeat units can be associated on the surface of each PAO1. A volume of 10 µL of polymer **2** and **4** stock solutions (1.3 mM in PPE repeat unit) was respectively added to 500 µL of PAO1 solution (ca. 2.3×10^8 mL^{-1} PAO1). This provides 20 times the concentration required for full coverage of PPE polymers on PAO1 surface. The fluorescence emission spectra of mixtures of polymers with PAO1 as well as control samples without PAO1 are shown in Figure 4-4. While mixing with PAO1 resulted in a moderate decrease (30%) in the fluorescence intensity of polymer **2,** the fluorescence intensity for polymer **4** decreased dramatically (~80%) under the same conditions. This

result could be attributed to the fact that clusters were formed between PAO1 and polymer **4** and that not many clusters formed between PAO1 with polymer **2**, as shown in Figure 4-3. In the clusters, polymer **4** aggregated around PAO1 and resulted in higher local concentration, which could result in an apparent quenching of the polymer fluorescence. Since the polymer **2** was well distributed in the solution in the presence of PAO1 as shown in confocal data, it is reasonable to observe less fluorescence decrease for polymer **2**. These results once again confirmed that the structure difference between polymers **2** and **4** brings different interaction between CPEs and bacteria, and results in different dark biocidal activity.

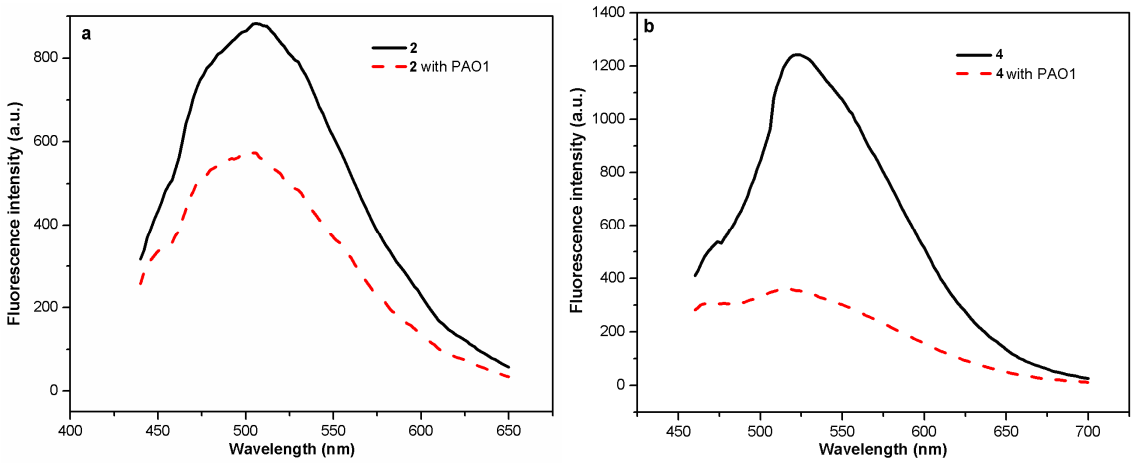

Figure 4-4. Fluorescence spectra of polymer **2** (a, λ_{ex} = 394 nm) and **4** (b, λ_{ex} = 427 nm) with absence and presence of PAO1.

Singlet oxygen production

Previous work demonstrated that cationic PPE-type CPEs sensitize singlet oxygen ($^1O_2$) due to triplet states generated by direct excitation of the CPEs.(37) In the present work singlet oxygen sensitization by **2** and **4** was investigated in CD_3OD by monitoring the emission at 1260 nm. The $^1O_2$ emission intensity at 1260 nm was measured for various concentrations of the polymer in solution. A linear relationship was observed

between the polymer absorbance at 335 nm and the $^1O_2$ emission intensity. The quantum yields of singlet oxygen generation were determined as 0.112 (± 0.008) for **4** and 0.122 (± 0.012) for **2** using 2´-acetonaphthone as an actinometer (Φ_Δ = 0.79).(216) The observation of the strong 1260 nm emission strongly supports the notion that these CPEs sensitize the production of $^1O_2$ in methanol solution.

Since the biocidal experiments were carried out in aqueous conditions, attempts were made to measure the quantum yields of $^1O_2$ emission sensitized by **2** and **4** in D_2O. However, the direct detection of $^1O_2$ emission was not possible in D_2O due to the very low efficiency of $^1O_2$ emission in this solvent.(37) Therefore, an indirect chemical method was utilized via chemical trapping of $^1O_2$ using the water soluble "chemical trapping agent" 1,3-cyclohexadiene-1,4-diethanoate (CHDDE). CHDDE reacts with $^1O_2$ to form stable peroxide (88%) and hydroperoxide (12%) (Scheme 2).(161) The reaction of CHDDE with $^1O_2$ is monitored by UV absorption spectroscopy. The disappearance of CHHDDE is detected as decrease in its absorption band at 270 nm (Figure 4-5). The quantum yield of $^1O_2$ production was determined according to the literature procedure using 5,10,15,20-tetrakis(4-sulfonatophenyl)porphyrin (TPPS) as an actinometer (Φ_Δ = 0.66) to give Φ_Δ = 0.32 for **2** and Φ_Δ = 0.037 for **4**.(37, 163) These results clearly demonstrate that $^1O_2$ can be generated by irradiation of **2** or **4** in water. However, for **4**, the efficiency of $^1O_2$ generation in water is much lower than that in methanol. The decreased efficiency is consistent with the lower triplet yield of **4** in water due to quenching of singlet excited states by aggregation (*vide supra*). On the contrary, **2** generates singlet oxygen more efficiently in water than in methanol. Such a difference is

most likely due to the high solubility of the polymer in water because of its high charge density per polymer repeat unit.

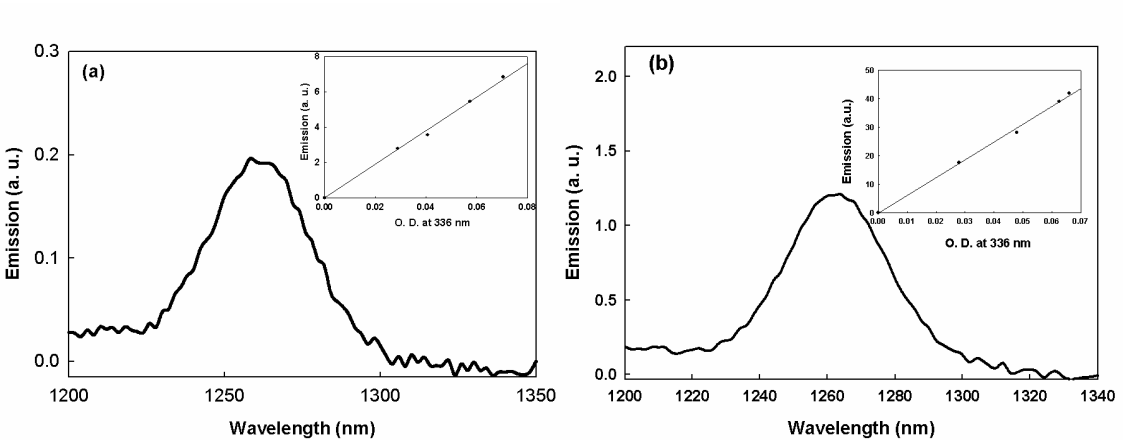

Figure 4-5. Singlet oxygen emission sensitized by 4 (a) and 2 (b) in CD_3OD. Inset: Integrated $^1O_2$ emission intensity versus optical density of the polymer solution.

Influence of negatively charged phospholipids.

A negatively charged phospholipid, DOPG, was chosen to interact with polymer 2 and 4 either in solution or on microspheres. The mixtures of polymer with DOPG liposome were prepared by adding 10 μL of stock PPE solutions to 1 mL of DOPG liposome solution followed by 30 min of vortexing. The resulting ratio between the DOPG liposome and PPE polymer in repeat units is 1: 2000. (The hydrodynamic radius of DOPG liposomes prepared by the method mentioned earlier is ca. 110 nm as determined by dynamic light scattering.(54) This results in a calculated surface area of ca. 1.5×10^{-13} m^2 for each spherical liposome. As the surface area of each DOPG lipid is ca. 55×10^{-20} m^2, there are ca. 2.7×10^5 DOPG lipid in each DOPG liposome. Therefore, 1 mL of 2 mM of DOPG lipid solution can yield 7 nM of DOPG liposome. In 1 mL liposome-polymer mixtures, there are ca. 7×10^{-12} mol of DOPG liposome and ca. 1.3 $\times 10^{-8}$ mol of PPE repeat units, giving a ratio of 1: 2000 between DOPG liposome and

PPE repeat unit.) A control sample of polymer solution without DOPG liposome was also prepared by adding the same amount of polymer into 1 mL of PBS solution. Figure 4-6 depicts the fluorescence spectra of polymers **2** and **4** in the presence and absence of DOPG liposome. Since DOPG was prepared in PBS buffer, the corresponding liposome free samples of polymers were also measured in PBS buffer. For polymer **4**, its fluorescence emission in water was also measured and it was found that the change from water to PBS buffer induced a red shift from 475 nm to 524 nm. This showed the increase in the ionic strength of the solvent makes the environment more hydrophilic and then resulted in more aggregation of polymer **4** and even weaker fluorescence emission. Interestingly, fluorescence enhancement and blue shifts of the emission maximum were found for both polymer **2** and **4** in the presence of DOPG, except that the extent of enhancement is different. In the case of polymer **2**, the emission maximum shifted from 506 nm to 460 nm and fluorescence intensity increased by less than 2 times in the presence of DOPG; on the other hand, in the case of polymer **4**, the emission maximum shifted from 524 nm to 482 nm and the fluorescence intensity increased by almost one order of magnitude. As described elsewhere and investigated in detail,(54) this fluorescence enhancement could be attributed to the interactions between cationic CPEs and negatively charged phospholipids, which induce association and further insertion of PPE CPEs into DOPG liposome and results in some level of deaggregation of polymers and gives rise to increased fluorescence. The dramatic difference in the fluorescence enhancement between polymers **2** and **4** could be due to the difference in their structures, where **4** has shorter and less sterically hindered pendant quaternary ammonium groups than **2**.

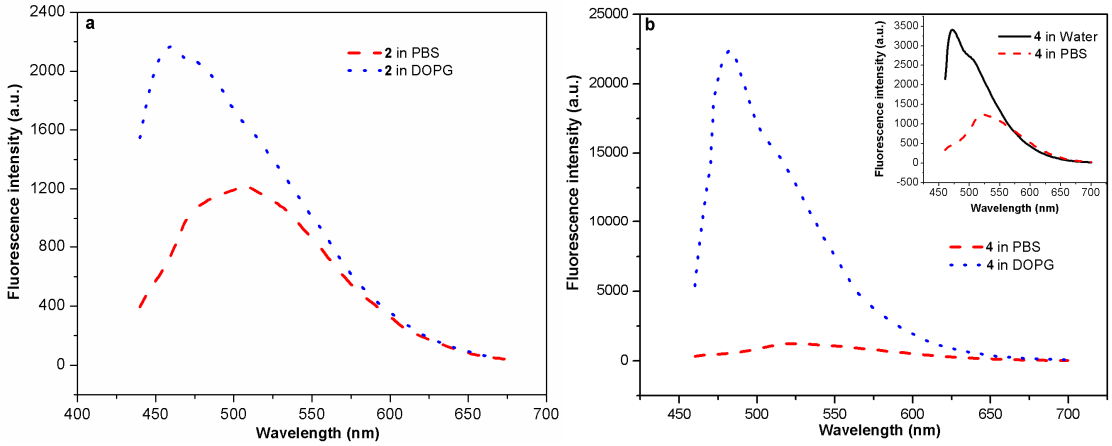

Figure 4-6. Fluorescence spectra of polymers **2** (a, λ_{ex} = 394 nm) and **4** (b, λ_{ex} = 427 nm) in the absence and presence of DOPG liposomes.

Similar results were also found for lipobeads, where a DOPG bilayer is coated on polymer **2** or **4** physisorbed microspheres. Although both blue shifts in the emission maximum and enhancement of fluorescence intensity were found for Si-**2**-DOPG and Si-**4**-DOPG, the fluorescence enhancement for Si-**4**-DOPG is dramatically larger than Si-**2**-DOPG, and there is about 7 times increase for the former, and less than 2 times for the latter. This once again shows polymer **4** is easier to insert into the DOPG bilayer and provides for more efficient deaggregation. Finally, polymer **4** also shows faster and higher extent insertion into negatively charged phospholipid monolayer in the Langmuir trough than polymer **2**.(54) Clearly polymer **4** is much more lipophilic than polymer **2** as indicated by the different interactions with negatively charged phospholipids. The enhanced lipophilicity of **4** is a reasonable source of its comparatively enhanced dark biocidal activity.

Summary

We have found that polymer **4**, although similar in structure and overall photophysical behavior to the PPE polymers **1** and **2**, exhibits remarkable differences in its light activated and dark biocidal activity. The comparison of the photophysical properties of the two cationic CPEs **2** and **4** indicate the effect of solvent on the absorption, fluorescence, transient absorption and singlet oxygen sensitization efficiency. Both of the polymers exhibit strong fluorescence in methanol solution, but the fluorescence is suppressed in aqueous solution (and on microspheres as a physisorbed coating) due to aggregation of the hydrophobic polymers. In the aqueous solutions, the fluorescence of **4** is more strongly quenched, indicating that this polymer has a much greater propensity to aggregate. This aggregation of **4**, also suggested by the rapid accretion of the polymer with bacteria observed by CLSM, thus reduces light activated biocidal activity by suppressing singlet oxygen generation.

The transient absorption studies show that direct excitation of **2** and **4** leads to production of a long lived triplet exciton that exhibits broad triplet-triplet absorption in the mid-visible region. For both CPEs the triplet-triplet absorption is more intense in methanol than in water, suggesting that the triplet yield is reduced in aqueous solution. The suppressed triplet yield likely arises due to quenching of the singlet exciton in the aggregate. Finally, singlet oxygen emission and trapping studies indicate that both **2** and **4** sensitize singlet oxygen.(196) For polymer **4**, the singlet oxygen yield is strongly reduced in aqueous solution compared to methanol, and this reduction in yield correlates with the reduced triplet yield observed for this polymer in water.

Although at first surprising, the decrease in light-activated biocidal activity can be reasonably attributed to the highly aggregated state of the thiophene polymer in aqueous solutions. This results in low triplet yields and a very poor sensitization of singlet oxygen and other reactive oxygen intermediates. The enhanced dark biocidal activity of the thiophene-containing polymers is attributed to their high lipophilicity, which may promote bacterial association, and to the presence of the accessible quaternary ammonium functionality on the pendant ether side chains, which is likely responsible for the immediate cell killing. The differences in behavior among these polymers suggest that the dark and light-activated biocidal activity may be tuned by altering overall lipophilicity, according to the membrane properties of the bacterial target, and by adjusting relative density, chain length and charge for the associated quaternary ammonium groups.

Chapter 5

Polyelectrolyte Multilayer Capsules: Micro-Roach Motels

Introduction

New types of coatings that can capture, entrap and kill pathogens, especially Gram negative bacteria, have been the subject of several recent investigations.(208, 178, 34, 8, 2) Especially interesting and attractive are antimicrobial coatings that can function catalytically and that can be used in a variety of environments. In Chapter 3, we reported the use of cationic conjugated polyelectrolytes (CPEs) supported on colloids as antimicrobials that can entrap Gram negative bacteria such as *Pseudomonas aeruginosa* and *Cobetia marina* in a dark process at the colloid-suspension interface and subsequently kill the bacteria on irradiation with visible light.(36) Here we report the remarkably enhanced light activated biocidal activity of micron-sized polyelectrolyte hollow capsules consisting of alternating layers of a pair of anionic and cationic (phenylene ethynylene)-type CPEs. These novel photoactive polyelectrolyte capsules function in a manner reminiscent of the insect entrapping "Roach Motels^{TM}" with respect to their ability to collect, concentrate and kill bacteria trapped within and on the surface of the capsules. This work has recently been published under the title "Conjugated Polyelectrolyte Capsules: Light-Activated Anti-microbial Micro 'Roach Motels.'"(47)

As discussed extensively in Chapter 1, controlling pathogenic bacteria is a major global concern, from basic household maintenance to intentional release by terrorists. Although standard disinfection protocols work well on cells in suspension, those which are attached to surfaces, which account for the majority of bacteria in the world, are

notoriously resistant to standard disinfection protocols. Some of these bacterial colonies demonstrate a propensity for forming communities, sometimes with several other species, that develop their own protected habitat, referred to as a biofilm. These biofilms can be quite complex in makeup and are generally able to withstand harsher conditions, allow for communication within their structure, share adaptive traits (through the exchange of plasmids) and can confer a robustness to the whole which could not be maintained by the individual component bacteria.(49, 18, 30, 63, 173) The old adage "There's safety in numbers" would seem to apply here. The harboring of organisms in biofilms is also thought to be a potent contributor to the development of antibiotic resistance.(179, 41, 191)

The magnitude of this problem is well illustrated in medical settings in which bacteria attached to medical devices are associated with up to 1.4 million deaths per year.(30, 79, 175) Among the organisms associated with nosocomial infections, the Gram negative opportunistic pathogen *Pseudomonas aeruginosa* is one of the most common, persistent and lethal; the second leading cause of infection in intensive care units, this organism quickly acquires multiple drug resistance and lethality factors when introduced into the hospital setting.(160) The strain *P. aeruginosa* PAO1 has served for many years as a nonpathogenic model for understanding mechanisms of *P. aeruginosa* adhesion, and is therefore also a good model organism for understanding disinfection.(75)

Microcapsules consisting of alternating layers of oppositely charged polyelectrolytes have been studied extensively in recent years.(119, 9, 52, 118) Work in this area has explored the fabrication, structure and function of the polyelectrolyte

capsules, towards their application for compartmentalization and/or release of drugs or other agents under a controlled stimulus.(52, 20) Polyelectrolyte microcapsules are prepared via layer-by-layer (LbL) deposition of oppositely charged polyelectrolytes onto the surface of micron-sized sacrificial template particles. Dissolution of the template particles affords the hollow polyelectrolyte microcapsules. In the present investigation we have adopted literature methods to fabricate novel polyelectrolyte capsules consisting of alternating layers of the (phenylene ethynylene)-type conjugated polycation and polyanion, **2** (Figure 1-3) and **3 (**Figure 1-4**)**, respectively.(223, 10) These CPE microcapsules are prepared via LbL deposition, beginning with the negatively charged polymer **3,** which is expected to strongly bind with the predominantly positive surface of the $MnCO_3$ template particles. Alternating coatings of **2** and **3** are then applied to build a multilayered structure, ending with an outer deposit of **2**. Given the positive charge of the capping polymer **2**, we infer that the exterior of the polyelectrolyte capsule surface has a positive surface potential. The reasoning here was that, for our target bacteria, the cationic complexes have proven to be more effective in terms of their antimicrobial activity than the anionic complex. Following LbL deposition, the $MnCO_3$ template is dissolved by exposure of the particles to a solution of ethylenediamine tetraacetate (EDTA). The resulting polyelectrolyte capsules retain the photoactive properties characteristic of the poly(phenylene ethynylene) units, i.e., they are strongly fluorescent in the mid-visible, and as shown below, they display light activated biocidal activity.

The materials present at various stages of the CPE microcapsule fabrication process were characterized by a variety of techniques, including dynamic light scattering

(DLS), scanning electron microscopy (SEM), epifluorescence microscopy and confocal laser scanning microscopy.

Experimental methods

Synthesis of PEM capsules

$MnCO_3$ microparticles were synthesized by modification of a literature procedure using nanometer sized particles to seed growth of monodisperse, micron-sized particles.(223) In a typical run, $MnCO_3$ particles were prepared having a mean particle size of ~5.0 µm with a standard deviation of ~0.5 µm (DLS). SEM images of the $MnCO_3$ template particles reveal their spherical shape and uniform size distribution. In separate containers aqueous solutions of $MnSO_4$ (1 L, 6 mM) and NH_4HCO_3 (1 L, 60 mM) were heated to 50 °C. A nanoseed solution was prepared by mixing 4 mg of NH_4HCO_3 and 0.1 mg of $MnSO_4$ in 20 mL of DI water and stirring the solution for 10 min. Prior to the addition of the nanoseed solution, 5 mL of isopropanol (IPA) was added to each of the warm salt solutions to give a final concentration of 0.5%. Immediately following the addition of the IPA, a 10 mL aliquot of the nanoseed solution was added to the $MnSO_4$ solution.

The solution was vigorously stirred and the NH_4HCO_3 solution was quickly poured into the $MnSO_4$ solution while stirring. The mixture instantly turned cloudy, and stirring was continued for 2 min, then the solution was allowed to stand for 35 min. Excess aqueous solution was decanted from the precipitated $MnCO_3$ microparticles, which were then isolated by centrifugation, followed by washing 3 times with DI water. Typically this procedure yields $MnCO_3$ particles with a mean particle size between 4.5-5.0 µm with standard deviations of 0.5-0.3 µm between particle batches. The size

distribution of the $MnCO_3$ microparticles was characterized using scanning electron microscopy (SEM) and dynamic light scattering (DLS). SEM images reveal the spherical shape of the particles and uniform size distribution. A typical preparation afforded ~150 mg of $MnCO_3$ microparticles with 5 µm median diameter (Figure 5-1).

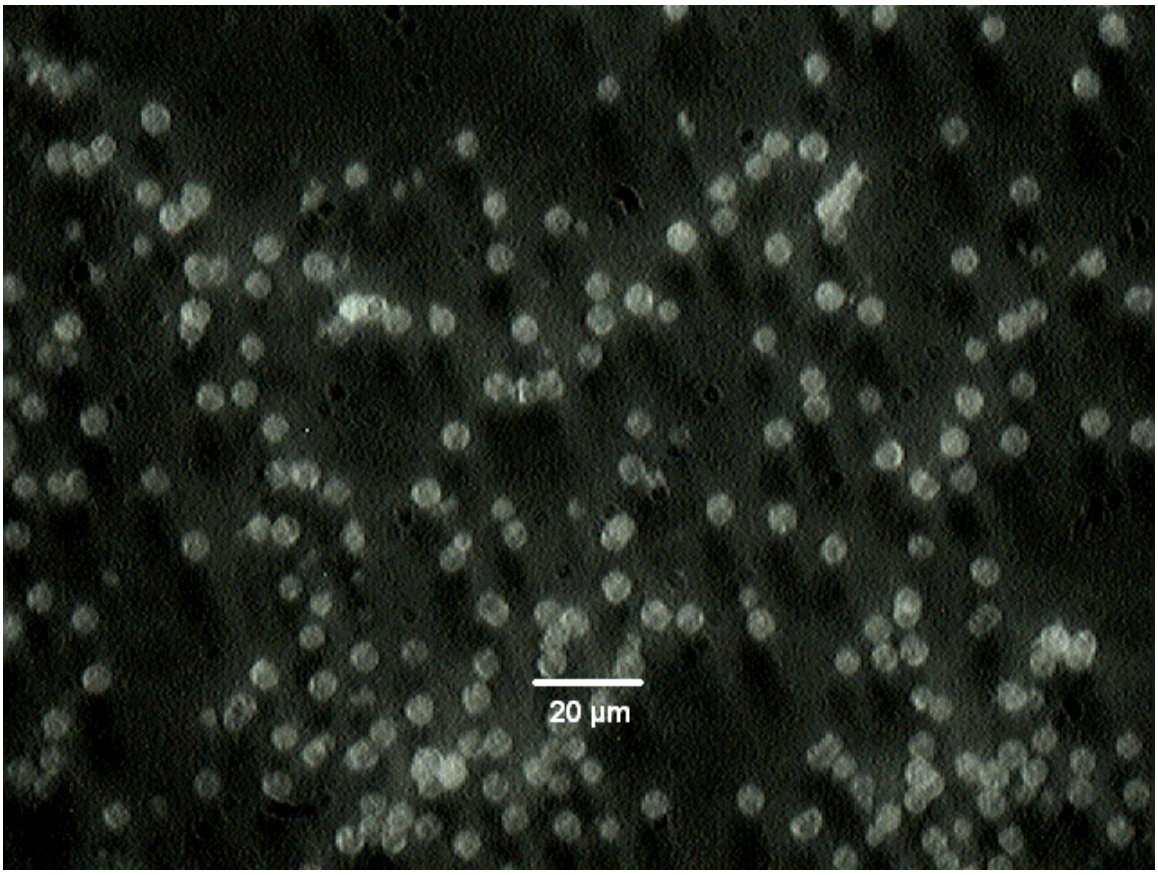

Figure 5-1. Microscopic image of $MnCO_3$ particles with 5 µm median diameter.

The surface of the MnCO3 particle is somewhat rough from the formation of tiny rectangular crystals forming the spherical particle, which is indicated in other literature reports for spherical $MnCO_3$ particles. Data from DLS experiments show a monodisperse sample in the 4-6 µm range comprising of 92-98% of the sample, with a small signal indicating the formation of aggregates at 8-12 µm range. This aggregate is sensitive to concentration and vigorous stirring during the DLS experiment and therefore

can be controlled. Typical DLS data reveals a sample distribution with a mean particle size of 4.568 µm with a standard deviation of 0.387mm representing 98% of the sample, with 2% of the sample as an aggregate. The mean particle size is in agreement with measurements made during SEM imaging.

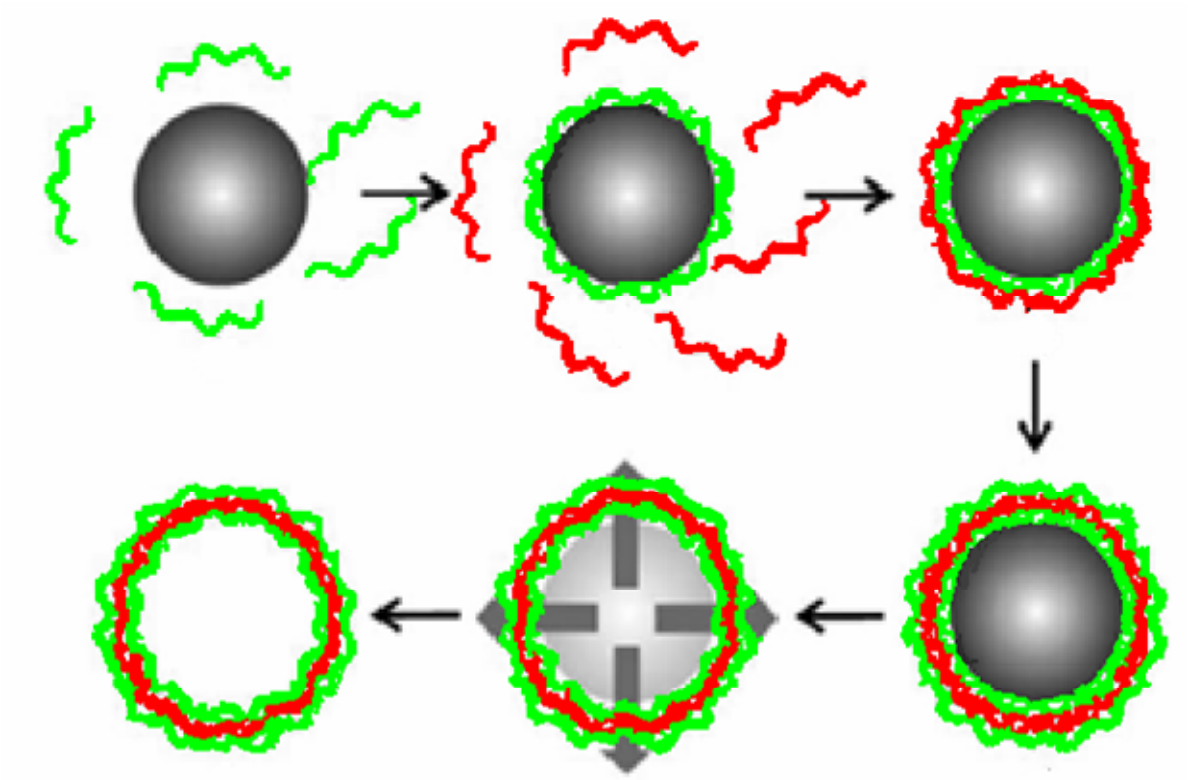

Scheme 5-1. Scheme illustrating CPE polymer coating of $MnCO_3$ microparticles and subsequent etching of the template with EDTA.

The **2**/**3** coated $MnCO_3$ microparticles were prepared by a modified literature procedure.(95, 9, 10, 223, 52) The $MnCO_3$ particles (155 mg) were dispersed in 11.75 mL of DI water assisted by stirring and sonication (~10 s). A 3.25 mL aliquot of a solution of **3** (4.61 mM) and 430 mg of NaCl was added to the $MnCO_3$ particle suspension and the mixture was stirred for 15 min. The **3**-coated particles were collected by centrifugation and washed 3 times with an aqueous NaCl solution (0.2 M). The particles were redispersed in 3.5 mL of DI water assisted by stirring and sonication and

the same procedure was repeated using an 11.5 mL aliquot solution of **2** (1.3 mM). The overall process was repeated three more times to afford particles coated with four bilayers. A simplified version of this process is illustrated in Scheme 5-1.

The resulting CPE-coated particles were inspected using epifluorescence and confocal fluorescence microscopy. As shown in Figure 5-2b, the presence of the **2/3** coating on the surface of the $MnCO_3$ particles is signaled by the bright green fluorescence that is characteristic of the CPEs.(221) Bright field confocal images (DIC mode) of the **2/3** coated particles clearly show the core due to light refraction by the high index $MnCO_3$.

In the final step of the microcapsule preparation, the $MnCO_3$ cores were dissolved using a modified literature procedure.(9, 10) An aqueous suspension of the CPE-coated particles (1.5 mL) was placed into a 3 mL centrifuge tube and 1.5 mL of 0.2 M EDTA solution was added. The mixture was shaken occasionally during a 2 hour period to keep the particles and capsules suspended. The resulting CPE microcapsules were washed twice with DI water and collected via centrifugation at 10,000 G for 15 min.

Analysis of the resulting hollow capsules by using epifluorescence microscopy clearly shows the fluorescence from the conjugated polyelectrolyte layers (Figure 5-2c). Interestingly, the polyelectrolyte capsules appear to be flexible, as indicated by the creases in the capsule walls. In Figure 5-2d, SEM images of dried **2/3** capsules reveal flat pancake-like structures confirming that complete dissolution of the $MnCO_3$ template has occurred. Characterization of the capsules by confocal microscopy also confirms the absence of the $MnCO_3$ templates.

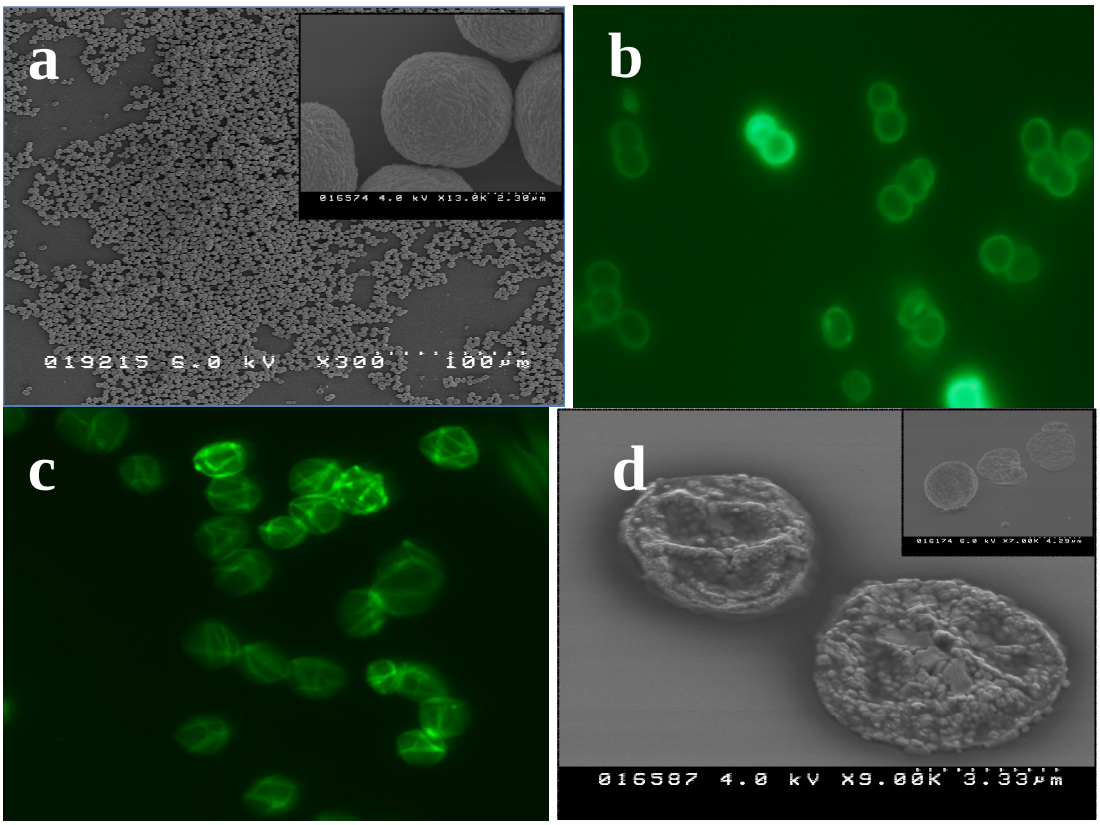

Figure 5-2. a) SEM images of $MnCO_3$ microparticles (inset: expanded view). b) Fluorescence microscope image of microparticles coated with 4 bilayers of CPEs. c) Fluorescence microscope image of polyelectrolyte capsules. d) SEM images of polyelectrolyte capsules.

Parameters for biocidal testing

The bacteria used in this study, *Cobetia marina* and *Pseudomonas aeruginosa* strain PAO1, were grown in chemostat as described in Chapter 2.(36) The preparation of bacteria and conditions for sample preparation with the CPE colloids has also been described in Chapter 2. Cells were examined under a 40x oil objective on a Zeiss LSM 510 Meta confocal laser scanning microscope and the number of live cells (*i.e.*, those fluorescing red only) and dead cells (*i.e.* those fluorescing green) compared.

Interactions between *P. aeruginosa* and the hollow CPE capsules [hereafter referred to as micro "Roach Motels", (µRM)] were monitored by confocal fluorescence microscopy. Bacterial viability was determined upon completion of experimental

treatment by staining the bacteria with a 1:1 mixture of SYTO 60 and SYTOX Green stains (2 μL mixed dye per mL suspension), then incubating for 15 minutes. These DNA stains penetrate the cells and produce red (~650 nm) and green (~530 nm) emission for live and dead bacteria, respectively. As noted above, the μRM also exhibit green fluorescence when irradiated with 400-450 nm light (Figure 5-2b and c).

Results and discussion

We have previously shown that 5 micron solid particles coated with the cationic conjugated polyelectrolyte **2** by physisorption can capture several bacteria on their surface; capture of the bacteria by these particles is at least initially a reversible process.(36) In the same experiments, we observed slightly more efficient capture (and killing) of *P. aeruginosa* occurs when a cationic polymer having similar polymer repeat unit structure is grown covalently from the surface of 5 micron silica beads. Studies with electron microscopy indicate that the covalently grown polymer provides a rougher surface that may be better suited for trapping bacteria irreversibly.

The surfaces of the μRM capsules formed from the combination of **2** and **3** appear much more corrugated than those studied previously (Figure 5-2) and we suspected that the μRM surfaces might be more effective at capturing bacteria than the solid colloids. We also felt that the open interior of the μRM might afford an irreversible capture of bacteria and much more efficient biocidal activity.

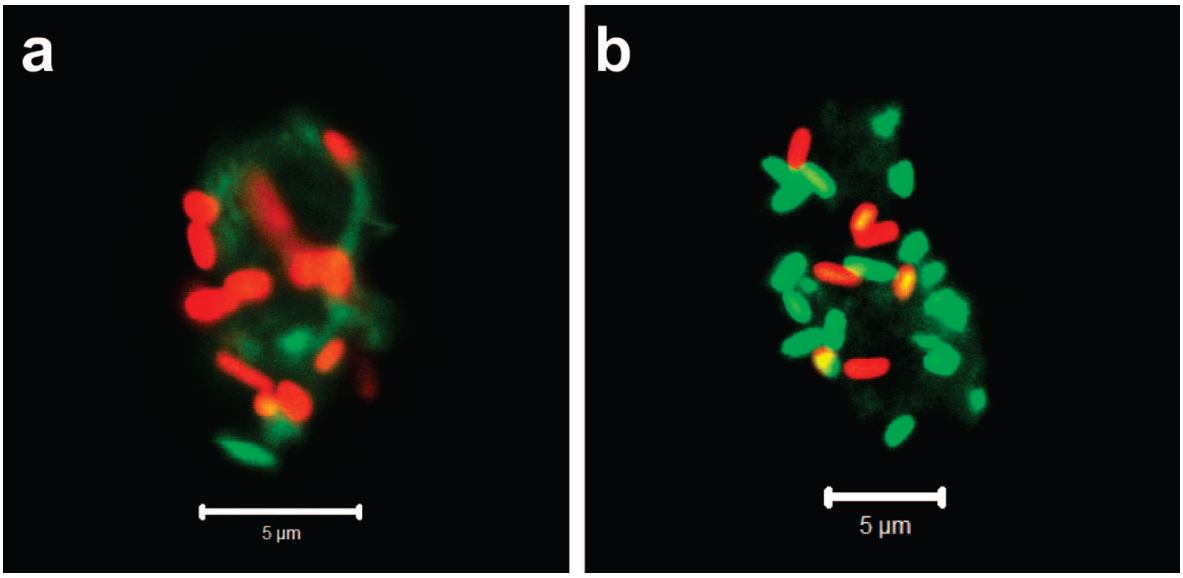

Figure 5-3. Composite confocal microscope images of µRM s with trapped *P. aeruginosa* (a) before and (b) after 15 min. irradiation with the Fiber-Lite 190 lamp. Approximate live:dead ratios are (a) 7.0 and (b) 0.33. These samples of CPE were taken around 25 minutes after their respective treatments, with the bacteria appearing mainly on the outside of the particles.

As shown in Figure 5-3, mixing a suspension of *P. aeruginosa* with the µRM clearly results in effective capture of the bacteria before the capsules are irradiated. In Figure 5-3a the live bacteria show an intense red fluorescence, while the single µRM exhibits a dull green fluorescence; at least 14 live (and 1-2 dead) bacteria are associated both on the surface of the µRM and within the interior.

In our study in Chapter 3 with microspheres containing physisorbed **2** we found that the colloids entrap *C. marina* fairly effectively, and the entrapped bacteria are largely killed by 15 minute exposure to visible light with a fiber optic lamp (Fiber-Lite 190).(36) For *P. aeruginosa* with the same microspheres there is some entrapment but light-induced killing requires much longer exposures (up to 1 hour) and even under these conditions there is only moderate killing. The surface grafted conjugated polymer beads are somewhat more effective towards *P. aeruginosa* but there is still much less killing

than for *C. marina*. In the present study we find that the µRM are much more effective at killing and capturing both *C. marina* and *P. aeruginosa*. In Figure 5-3b is shown a fused cluster of µRM that has been irradiated with the Fiber-Lite 190 lamp for 15 min in a suspension containing *P. aeruginosa*. Under these conditions there has been considerable photobleaching of the µRM and their fluorescence is very weak. Significantly, most of the bacteria associated with the µRM exhibit green fluorescence indicating that they have been killed by visible irradiation. (Under these conditions irradiation of similar concentrations of physisorbed or covalently grafted polymer on solid colloids results in relatively little killing of *P. aeruginosa*.) Similar results were obtained when suspensions of µRM and *C. marina* are irradiated. Even more effective bacterial trapping and light-induced biocidal activity is observed for larger clusters of µRM as shown in Figure 5-4.

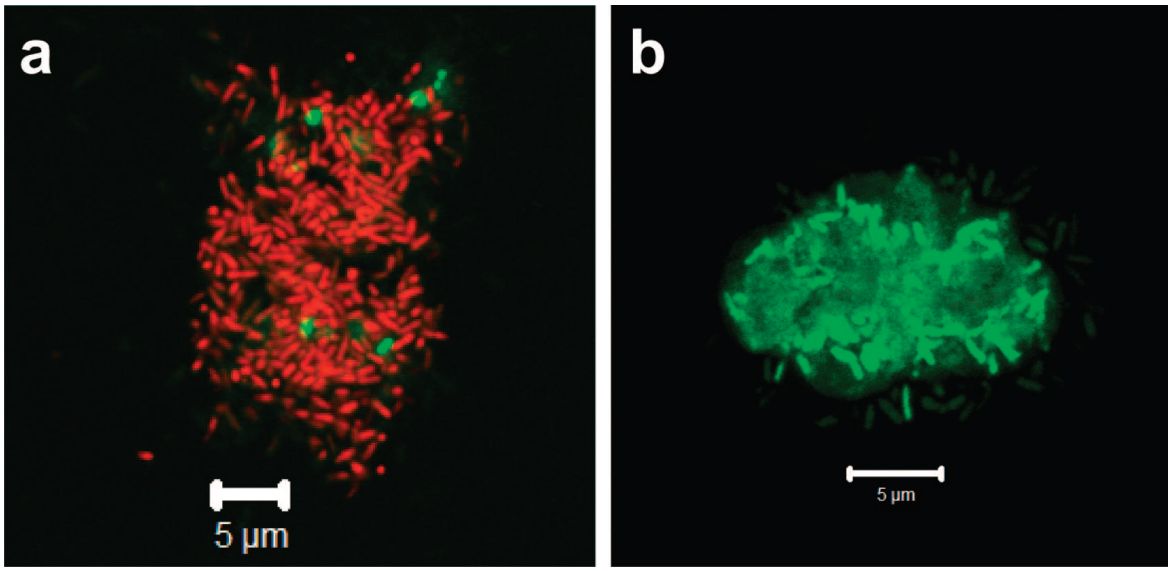

Figure 5-4. a) Confocal microscope image of a µRM cluster 10 minutes after introduction into a solution of *P. aeruginosa* (10^7/mL) kept in the dark. b) Central slice of 20 µm "z-stack" showing interior of µRM cluster with entrapped, killed bacteria after 1 hour exposure to white light.

These clusters, typically containing 4-12 µRM, form in the presence and absence of bacteria, as can be seen in the epifluorescence image in Figure 5-2c. Very prevalent

are clusters of four µRM that are approximately tetrahedral in shape; the cluster shown in Figure 5-4b appears to arise from fusion of two tetrahedral clusters. These µRM clusters are even more efficient in trapping bacteria than isolated µRM. As shown in Figure 5-4a one cluster exposed to a suspension of *P. aeruginosa* for ten minutes in the dark has entrapped hundreds of bacteria and almost all of the bacteria are live. As shown in Figure 5-4b, after irradiation with visible light for one hour all of the *P. aeruginosa* associated with a µRM cluster both within and on the surface have been killed.

It was previously shown that CPEs such as **2** and **3** are effective sensitizers of singlet oxygen in both aqueous and organic solutions.(36) We have also determined that the light-induced antimicrobial action of colloids containing **2** and similar cationic CPEs requires the presence of oxygen (Chapter 3). This has led us to conclude that the light-activated antimicrobial activity results from the generation of singlet oxygen and likely successor reactive oxygen intermediates. We suspect that the same mechanism for the light-activated activity is operative for the µRM. What likely accounts for the more rapid and effective killing for the µRM is their greater efficiency in entrapping the bacteria irreversibly, or for longer periods of time, compared to the solid colloids. As we have discussed above, the µRM should have a positive surface potential, yet also regions of negative charge density as well as hydrophobic regions. In other work we have noted that bacteria, including those studied here, attach in greater numbers to surfaces that contain both positive charged and hydrophobic groups. The heterogeneity of the materials comprising the µRM may thus contribute to their ability to attract and bind to bacteria. Another factor that may contribute to the irreversible nature of the binding is the potential for the material surface to reconstruct upon interaction with the bacterium. This

malleability of the surface is also indicated by the effects of shaking on samples containing bacteria, as evidenced in Figure 5-5, where samples held for the same time, one with shaking and one without, show distinctly different morphologies.

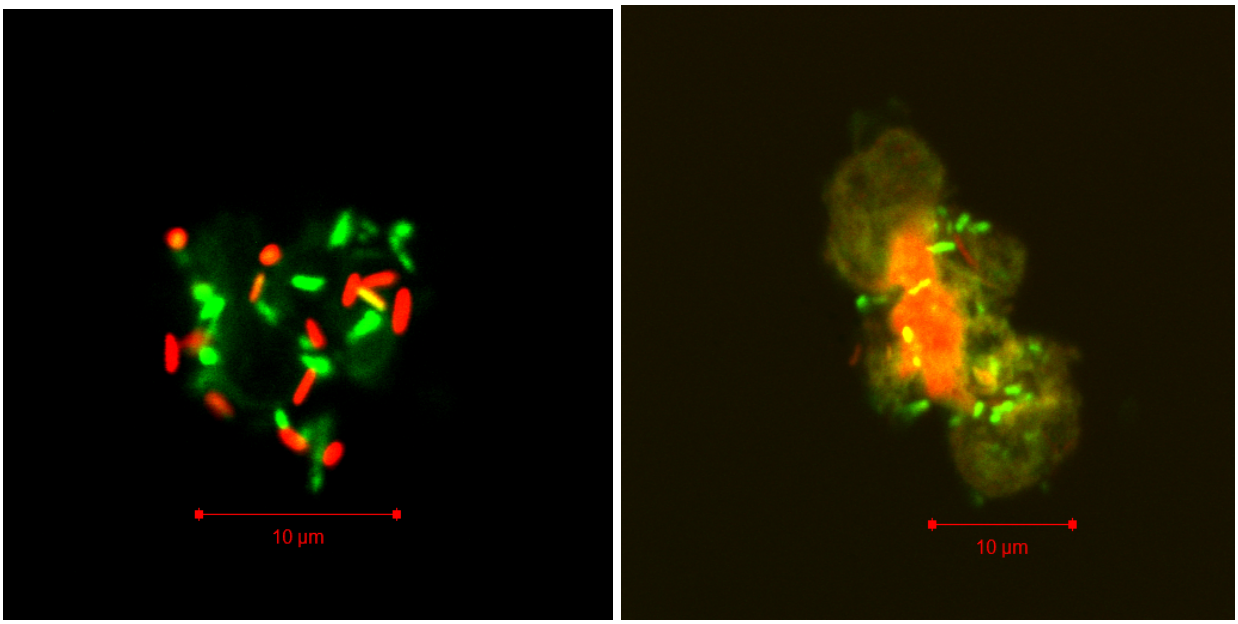

Figure 5-5. Effects of agitation on samples. The confocal image on the left (a) shows bacteria on the surface of a CPE-bacteria agglomerate not subjected to shaking during exposure to light for 30 minutes. The image on the right (b) is from a central slice of a z-stack of a shaken sample, indicating that the (mostly) dead bacteria seen here are on the interior of the agglomerate. The live/dead ratio for (a) is 1:1, while that of (b) is 1:5.

Another remarkable effect that is observed is the time evolution of the µRM/bacteria suspensions. As documented in a series of composite confocal images shown in Figure 5-6, over the course of several hours after being mixed with bacteria, the µRM exude fibrillar structures (Figure 5-6a) which appear to be especially effective in capturing bacteria. In addition to the fibrils, sheet-like structures which are very difficult to image with the confocal microscope (due to rapid photobleaching) are present, and these structures are also very effective at capturing bacteria (see Figure 5-6b and Figure

5-6c). Although the exact nature of these structures is not known at the present time, we believe that the material is likely a hydrogel consisting of the mixed CPEs.

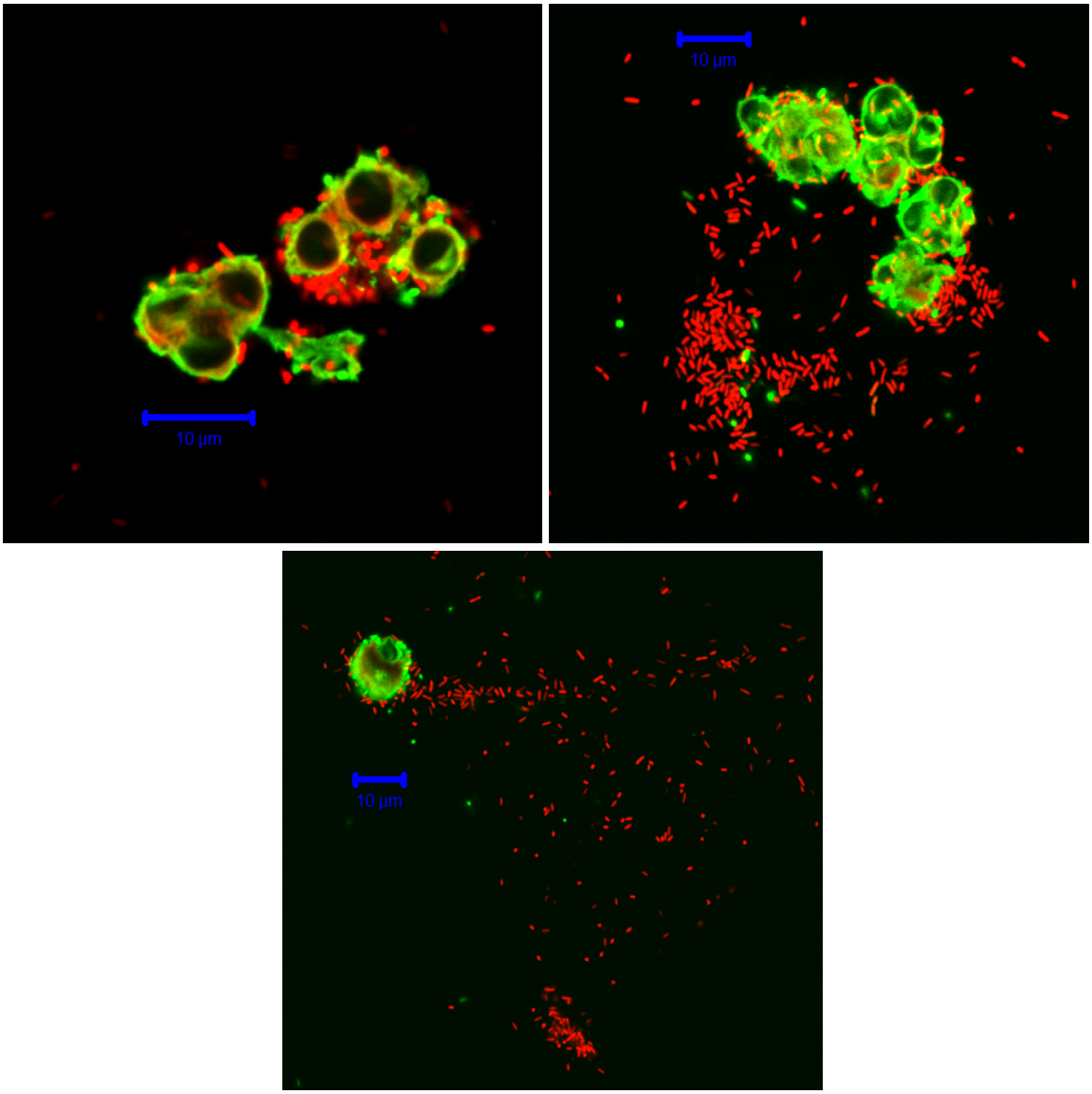

Figure 5-6. A collection of µRM images showing various forms of exuded filaments and possible films with entrapped bacteria.

The presence of this material may help to account for the extremely effective sequestration of the bacteria in the solution, as can be seen by the near absence of free bacteria in solution in a typical wide-field image after about one hour (Figure 5-7).

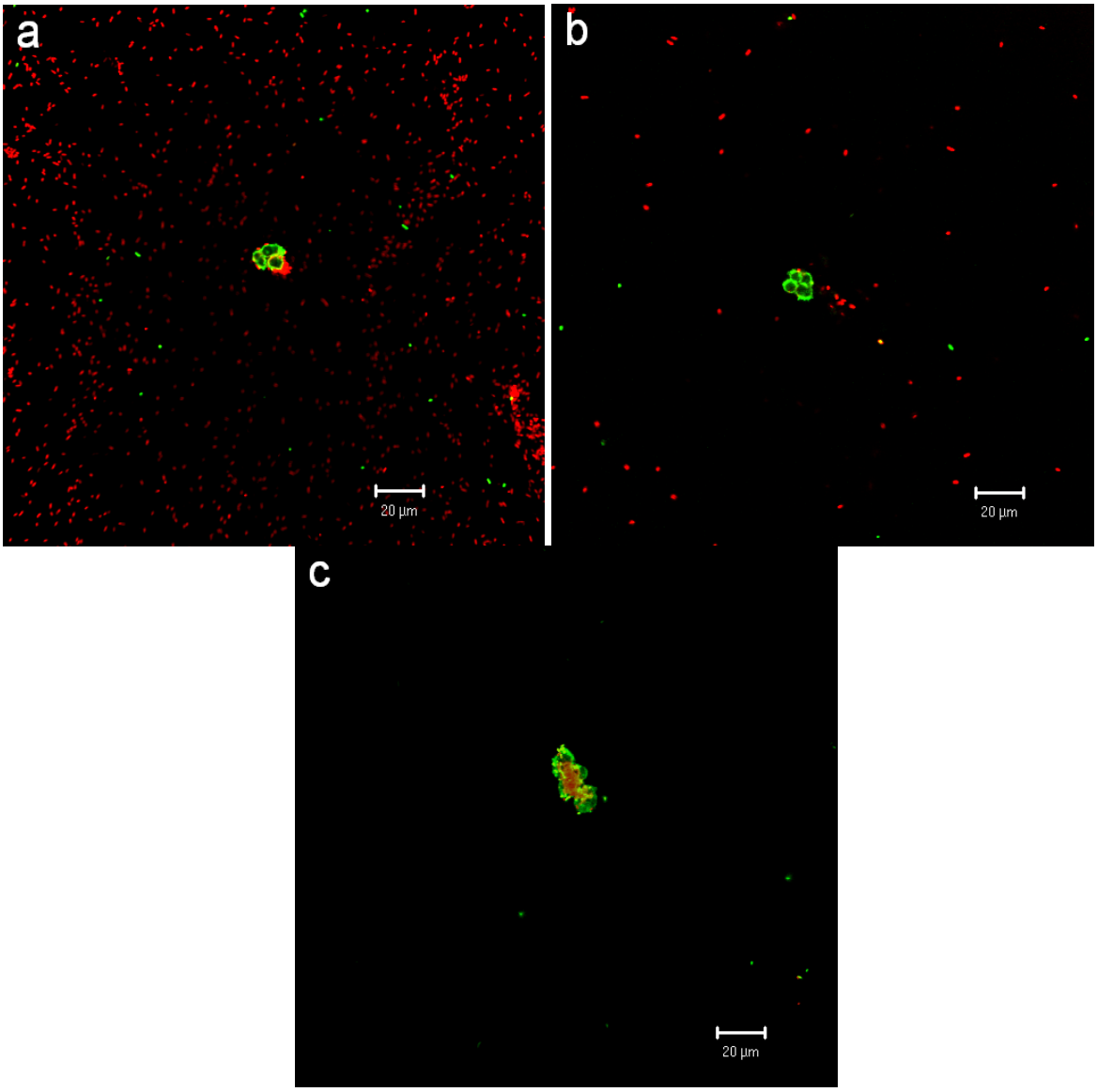

Figure 5-7. Wide-field images of the microcapsule/bacterial solution showing the dramatic decrease in free bacteria after exposure to the µRoach Motels for (a) 6 min. (b) 42 min. and (c) 65 min. There is some photobleaching (mostly of the red SYTO 60 stain) in the center of (a) from a previous scan.

Summary

Novel polyelectrolyte microcapsules consisting of the photoactive CPEs **2** and **3** were prepared and challenged with robust Gram negative bacteria. The microcapsules display strong green fluorescence indicating that the constituent conjugated polymers

retain their photophysical properties in the capsule structure. Experiments involving mixing of suspensions of polyelectrolyte capsules with *C. marina* and *P. aeruginosa* demonstrate that the materials act as highly effective light-activated micro "Roach Motels". In particular, live/dead assays indicate greater than 95% kill after exposure to ~1 hour of white light. The remarkable activity of the μRM is clearly due in part to the morphology of the capsule structures which leads to very effective capture and entrapment of the bacteria by the photoactive polymer material.

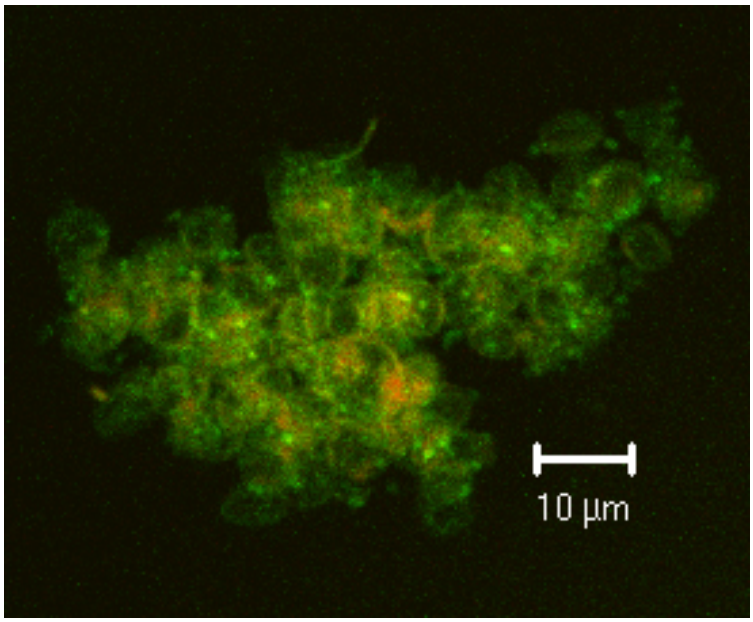

Figure 5-8. *B. atrophaeus* spores (brighter green dots) trapped within a μRM cluster.

More recently, these μRM showed significant trapping and killing potential when tested against *B. atrophaeus* spores—an anthrax simulant (Figure 5-8). In this ongoing work we seek to explore in more detail the mechanism and efficacy of these novel materials in potential antimicrobial applications.

Chapter 6

Flow Cytometry Studies of Antibacterial Activity

Introduction

The analysis of microorganisms can be carried out at a number of levels, from simple detection or identification to counting to characterization of viability, growth, metabolism, and interaction with various chemical and physical agents. The highest level of complexity would require an analytical technique that could detect, identify, count and characterize each of several organisms in a mixed population. Flow cytometry is such a technique—basically the generation of a particle stream by various means, usually in a liquid, which then undergoes sequential optical analysis. Although the instrumentation is somewhat flexible in its configuration, a typical setup might have a narrow (~10-100 μm) hydrodynamically (and more recently, acoustically) focused stream of particles passing through one or more illumination/excitation sources (usually laser) and a number of detectors (photomultiplier tubes-PMTs) for the light scattering and fluorescence generated. (Scheme 6-1)

At its simplest, flow cytometry is a type of microscopy: light scattering signals provide the same type of information as visual examination of a slide. Its power lies in the ability to analyze (almost) every cell in a given sample individually and rapidly. This greatly increases the speed, reliability and repeatability of sample analyses compared to conventional microscopy or even CLSM, with more simultaneously measured parameters (and it is carried out electronically rather than visually!).

History of flow cytometry

The concept of interrogating individual particles actually goes back quite some time, to a device created in the 1940s to analyze mine dust.(73) This apparatus was also used in World War II by the U.S. Army in experiments for the detection of bacteria and spores.(72) The Coulter Counter, an instrument that uses impedance across a small aperture to measure particle sizes was patented by W.H. Coulter(50) and introduced in the early 1950s. Cell analysis by flow cytometry began to develop in earnest in the mid 1960s with the first real flow cytometer(93), and working cell sorter(59, 60) in 1965, the first fluorescence-based flow cytometry device (ICP 11)(70) in 1968 and the first analysis of DNA cell cycle in 1969.(207) Rapid development of computers and digital electronics over the next couple of decades finally provided the processing power necessary to gather and manipulate the large quantities of data generated by this technique in a timely manner, and with enough flexibility to become useful in a number of fields.

Principles of Flow Cytometry

As shown in Scheme 6-1, modern flow cytometers have four main components:

1) a flow cell - liquid stream (sheath fluid), which carries and aligns the cells so that they pass single file through the light beam for sensing
2) an optical system - lamps or lasers (argon, krypton, dye laser)
3) a detector and analog-to-digital converters which convert scattering and fluorescence signals from light into electrical signals
4) a computer for analysis of the signals.

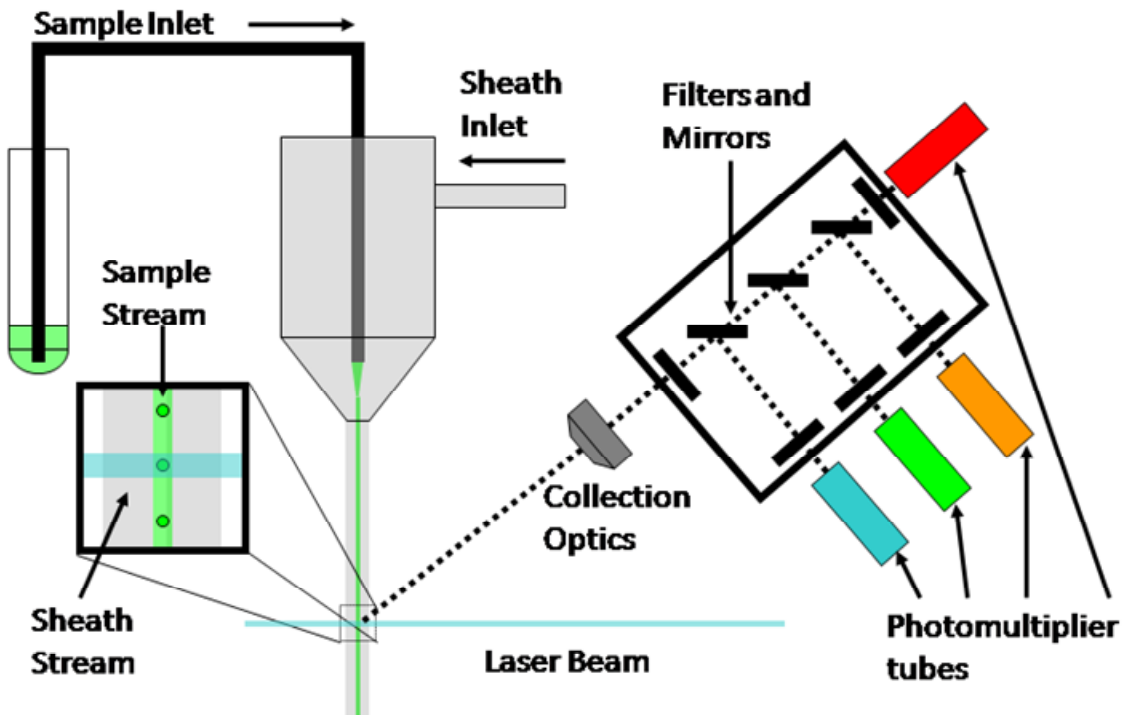

Scheme 6-1. Components of a flow cytometer. The computer system used to collect and analyze the data is not shown.

In a flow cytometer, each suspended particle from 0.2 to 150 micrometers passing through the incident beam scatters the light while fluorescent chemicals naturally present in the particle (intrinsic) or attached to the particle as a probe (extrinsic) may be excited into emitting light. Scattered light is evaluated in two distinct regimes: one is (nearly) axially aligned with the light beam and is referred to as Forward Scatter (FSC); another at much larger angles gauges what is called Side Scatter (SSC). Most instruments have the detectors (sometimes several) for these two parameters positioned roughly orthogonally to one another. Fluorescent emissions are picked up by one or more fluorescence detectors that are selected for wavelengths of interest.

All of these detectors are either aimed at the point where the stream passes through the light beam or are fed a portion of collected scatter by a train of band-pass optics. By analyzing fluctuations in brightness at each detector it is possible to derive

various types of information about the physical structure and chemical properties of each individual particle.

Forward scatter

This parameter is measured at narrow angles of 0.5 to 5˚ from the axis of the incident beam, usually by employing a beam stop of some sort to block the main portion of the beam. For our intended purpose of bacterial cell analysis, forward scatter measurements generally correlate with the cell size, and are quite useful in that regard if some important factors are considered:

1) optical properties of the system
    a. the wavelength of the incident beam
    b. the precise range of angles over which light is collected, determined by the focal lengths and numerical apertures of collecting lenses (see Figure 6-1)
    c. the size, shape, and position of irises, slits, and obscuration bars in the optical system

(Since there is no standard optical design for forward scatter measurements, it is likely that results will differ when measuring the same cells in different instruments.)

2) cellular properties
    a. a difference in refractive index between the sheath fluid and the cell suspension adds noise to scatter measurements and may cut accuracy (51)
    b. the presence of strongly absorbing material in cells tends to decrease the amplitude of scatter signals and
    c. highly textured surfaces or internal structures may have a similar effect (but often increase the amplitude of side scatter).

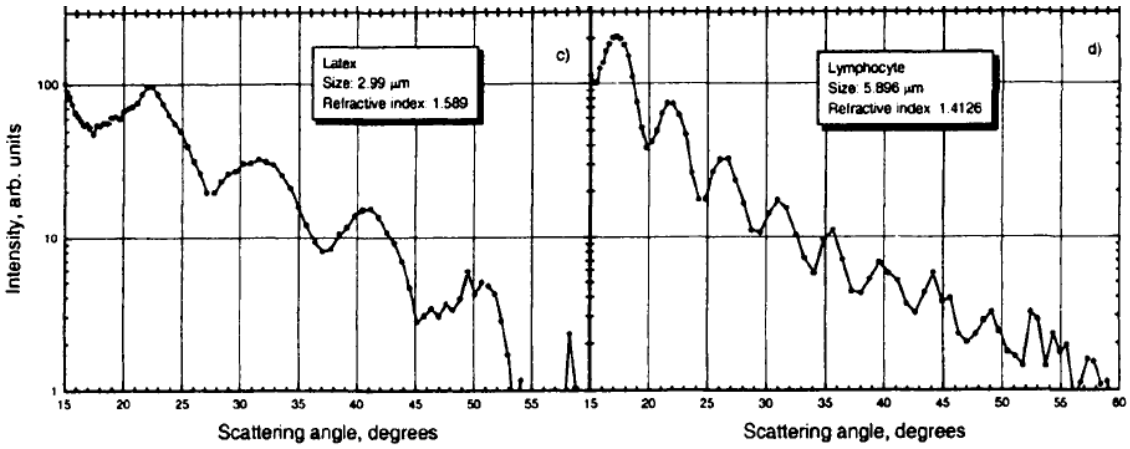

Figure 6-1. Plots of intensity vs. scattering angle of a latex bead (left) and a lymphocyte (right), illustrating the effect of scattering angles on signal intensity. (from ref.(188)) We can also infer from these data some influence from particle size and refractive index.

Side scatter

Side scatter is somewhat more reliably correlated to the surface complexity and granular structure of the particle (i.e., shape of the nucleus, the amount and type of cytoplasm granules or the membrane roughness). The light scattered at large angles to the incident beam is usually of higher intensity, probably from a combination of multiple reflections and the summation of single scattering events from individual granules.

Scatter signal arises from the difference in refractive index between cells and the medium that is maintained by the barrier of the cell membrane to water and solutes. The refractive index differential of cells with damaged membranes (which are permeable to dyes such as SYTOX Green or propidium iodide) is reduced, producing smaller forward scatter signals.

Fluorescence

Fluorescence measurements are advantageous because of their specificity and sensitivity, allowing for reliable and repeatable identification of labeled components even

at very low levels. In addition to single wavelength intensities, a number of other fluorescence parameters can be obtained, including total fluorescence, fluorescence polarization, fluorescence lifetimes and fluorescence emission spectra. The use of multiple fluorescence detection regimes (currently up to 13 channels available on one commercial instrument) can also increase the numbers and types of probes that can be deployed simultaneously. With fluorescence, flow cytometers are capable of detecting particles in the femtomolar range (100's of particles per mL), yet can collect data on up to 50,000 particles per second, with only µL volumes required for analysis.(146)

Once these data have been collected, they can be displayed in a variety of ways. The most common way to represent the distribution of events for a single detection parameter is a simple histogram. Somewhat more informative bivariate plots for two detection parameters can be constructed using color features to indicate event populations. These are quite useful for identifying the geometric mean of a population in order to properly set gates. More sophisticated software packages can produce contour diagrams and three-dimensional plots for multivariate analyses.

Special issues for bacterial analysis

As it turns out, despite the varied influences on scattering, size measurements with FSC are actually more reliable for bacteria than for eukaryotic cells, since many bacteria are close to either spherical or ellipsoidal and behave according to Mie theory.(128, 178, 88, 167)

Photobleaching is much less of a problem when using a flow cytometer to get precise quantitative measurements of fluorescence intensity from cells because each cell is exposed to excitation light for only a few microseconds as it passes through the

illuminating beam. Flow velocities are also very stable, so the period of exposure for a given cross-section is nearly constant. Nearly equal measurement values for cells with equal amounts of fluorescent material give very high precision. Still, as you might recall from Chapter 2, the relationship between staining conditions and viability must be judged carefully.

Some of the dyes used in staining may also bind to the flow cytometer tubing. If the system is not cleaned (with a recommended dilute soap solution) and flushed after use, there is a potential for cross-contamination by dyes used in previous runs (and other experimenters may be using stains with properties dramatically different from yours).

Sample processing in flow cytometry usually only takes a couple of minutes per sample. However, it is still a sequential process and time does pass between samples. This can be an important consideration if using a batch of bacteria obtained at the same time to do protracted experiments with multiple samples. Even with this constraint, flow cytometry is still much faster than either plate counting (overnight) or CLSM (see Chapter 2, Biocidal studies, Counting). On the other hand, plating unequivocally demonstrates reproductive viability and microscope slides have rarely been known to clog, as a flow cytometer occasionally does. Plate counting for bacterial susceptibility is usually correlated with flow cytometric evaluations, but can differ by more than a factor of five.(7)

Experimental methods

Instrument specifications

Flow cytometric studies herein were done using an Accuri C6 flow cytometer, a fairly new design with a small footprint (~2’ x 2’), four fluorescence and two scatter

detectors. This instrument has a 200 µm fused silica capillary with a maximum particle size limit of 40 µm and is capable of processing up to 10,000 events/second and sample concentrations near 10^7 cells/mL. (An added bonus is the pleasing musicality of this particular instrument during operation.) The C6 has an unconventional non-pressurized flow system employing peristaltic pumps for transport, allowing for precise metering of volume. The distinctly nice thing about this is that cell concentration can be measured without the need for adding beads to samples or performing time-consuming hemocytometer counts. The flow system will occasionally clog, (which is not too surprising given the agglomerative nature of our polymer/bacteria samples), but these clogs are usually quite easily cleared by executing a backflushing procedure that is integrated into the hardware.

The instrument has two lasers, a 488 nm solid state and a 640 nm diode. There are four fluorescence detectors, set up with the optical filters shown in Table 6-1. These have a linearity rating of 2.00 ± 0.05% with < 3.0% CV. Data are collected on FSC and SSC (from the 488 nm laser) and all four fluorescence channels in every run.

Table 6-1. Filters for fluorescence detection in the Accuri C6™. (from instrument manual)

filter name	excitation source (nm)	detection range (nm)
FL1	488	530 ± 15
FL2	488	585 ± 20
FL3	488	670 long pass
FL4	640	675 ± 12.5

The Accuri C6 was calibrated approximately monthly (more frequently in the initial phases of study) with 8 peak “rainbow” beads, and proved to be extremely stable in fluorescence as gauged by CV values over the course of one year.

Flow experiment parameters

P. aeruginosa and *B. atrophaeus* (vegetative) bacterial samples were derived from overnight batch cultures having a population of ~5 x 10^8 bacteria mL^{-1} and were diluted to between 10^6 and 10^7 mL^{-1} in 0.85% NaCl for flow samples. Spores were prepared as described in Chapter 2, Bacterial Growth and used at similar populations. The sample set was much the same as for other biocidal studies (Chapter 2, Biocidal studies-Experimental Parameters), with the exception of the live and dead controls, which are being split into multiple aliquots in the latest flow cytometry testing. In particular, unstained, propidium iodide (PI)-only stained and doubly stained (PI and the appropriate permeant SYTO dye) controls are being used to determine the autofluorescence of the *B. atrophaeus* vegetative cells. Biocidal candidate compounds were added to these samples at concentrations between 0.2 and 10 µg/mL. SYTO 9, 11, 21, 24 and propidium iodide stains were used in the flow cytometer experiments, with a 15 minute incubation period for the vegetative bacteria and 45 minutes for the spores. For the following samples, light exposures were 15-30 minutes—UV-365nm for the OPEs and broad-spectrum white light (Fiber-Lite 190) for the polymers.

With these stains, the most useful representation for gating the data was the bivariate plot of FL1 (530 nm) "green" vs. FL3 (670 nm) "red." These channels are FL1 (530 ± 15 nm—"green"—live) for the SYTO permeant stains and FL3 (670 nm long pass—"red"—dead) for the propidium iodide. For the flow cytometric bivariate plot graphics in this section, I have followed the convention of having the green fluorescence channel (FL1) on the Y axis and the red fluorescence channel (FL3) on the X axis. The state of samples through their virtual "lifetime" could be followed through the

progression of signals clockwise on these plots, starting in the lower left with unstained live controls (as in Figure 6-2), moving upward once stained, and then transitioning to the right and downward with the increase in membrane permeability and loss of integrity. With samples where the antimicrobial polymer compounds were free in solution, the signals tended to remain in the upper right quadrant, presumably due to the strong binding of the fluorescent polymers. An example of this type of progression can be seen in Figure 6-5.

In any given experimental set, consistent scattering thresholds were applied across all samples and 10K-120K events were collected per run. The experimental data were analyzed using the CFlow software available on the Accuri C6 and with FCS Express 3.0 from DeNovo Software.

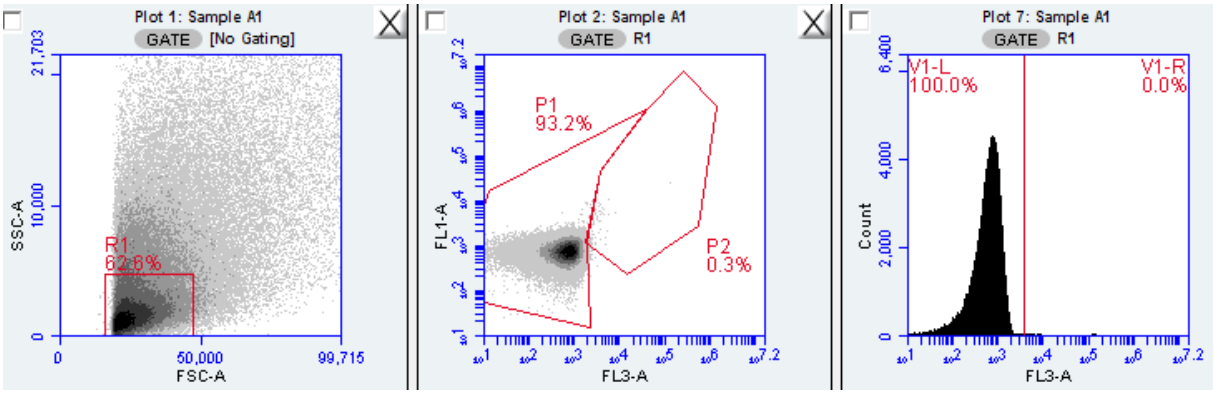

Figure 6-2. *Bacillus atrophaeus*. Live control, no stains.

Results

General observations

Despite the above caveats, the effects of the CPEs on the bacteria in most every case were easily observed. First and foremost, the signals for forward and side scatter tended to be dramatically spread out, sometimes with one affected more than the other. This spreading is most likely due to two factors: 1) the clumping and agglomeration that

was observed by CLSM in many prior experiments, and 2) the variability in the uptake of the stains among individual bacteria, clusters and debris particles (which may also be contained in the agglomerates). This contributed to a broadening in the distribution and increase in the range of intensities of both scatter and fluorescence, although this had to have been mitigated somewhat by the narrowing of the orifice (~40 µm maximum particle size(1)) through which any clustered material had to pass. This same reasoning would suggest that many agglomerated bacteria were probably not counted, due to the fact that the instrument rejects the acquisition of data if a pulse width exceeds a preset threshold. Also, for cells that were damaged and permeabilized to the "dead" stain, there was more of a change in FSC, likely due to the refractive index differential between the cells and the solution being diminished by equilibrium processes.

Gating optimization and threshold effects

Because of the pronounced spreading in the scatter, gate settings usually included <75% of total measured particles and were centered around mean values that were usually less than half of the maximum signals for both FSC and SSC. These settings were optimized by monitoring CV values for the fluorescent channels of interest (FL1 and FL3).

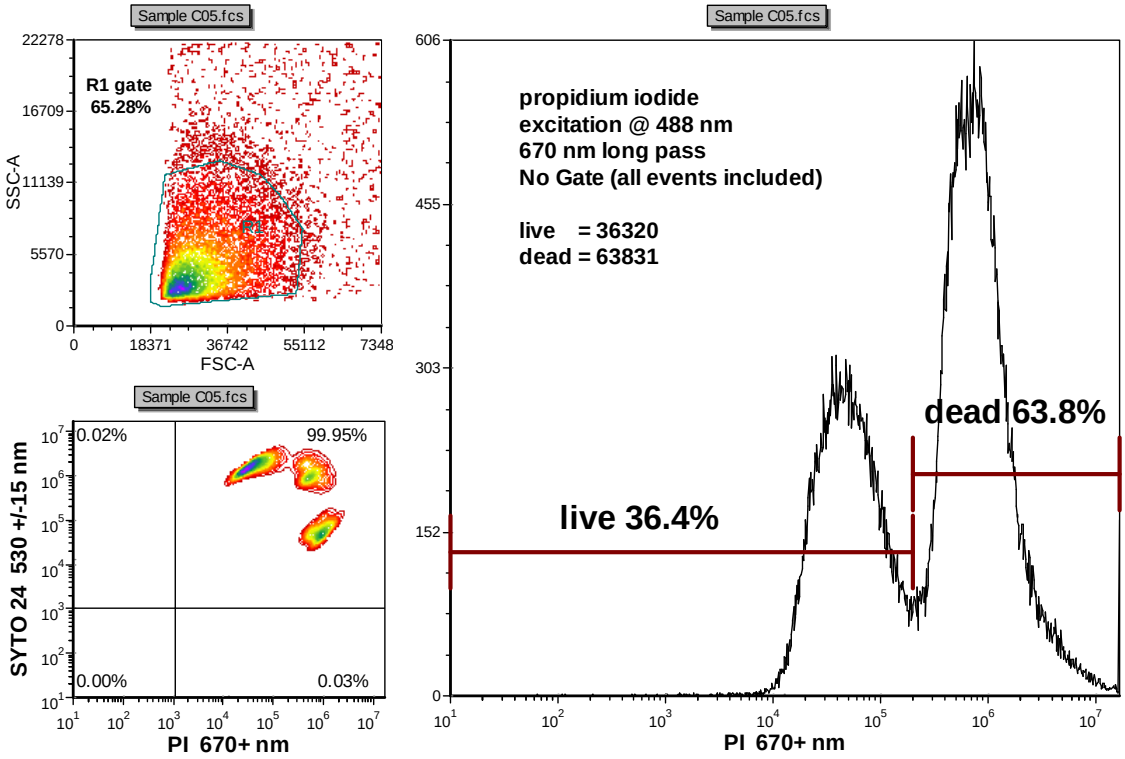

Figure 6-3. Gating optimization showing (lower left) three clearly delineated populations (left to right, live; "dying", and, lower right, dead) for this *B. atrophaeus* sample. Upper left is the roughly triangular gate, based on scatter parameters and on the right is the histogram showing the live/dead percentages, where the "dying" and dead populations are combined.

The choices of which channel and where to set the lower boundary (threshold) for signal intensity are also critical ones. A triggering threshold of 10-80K in FSC or 2-10K in SSC were usually sufficient for achieving CV values at or below 50%. Occasionally, these thresholds were combined with small valued fluorescence cutoffs (10-1000) in order to minimize triggering from cellular debris. Values higher than 1000 would typically begin to cut into legitimate data, since the particles of interest (bacteria) are already close to the lower size limits for the instrument. A comparison of triggering threshold effects is shown in Figure 6-4.

a) threshold: FSC-H @ 80000

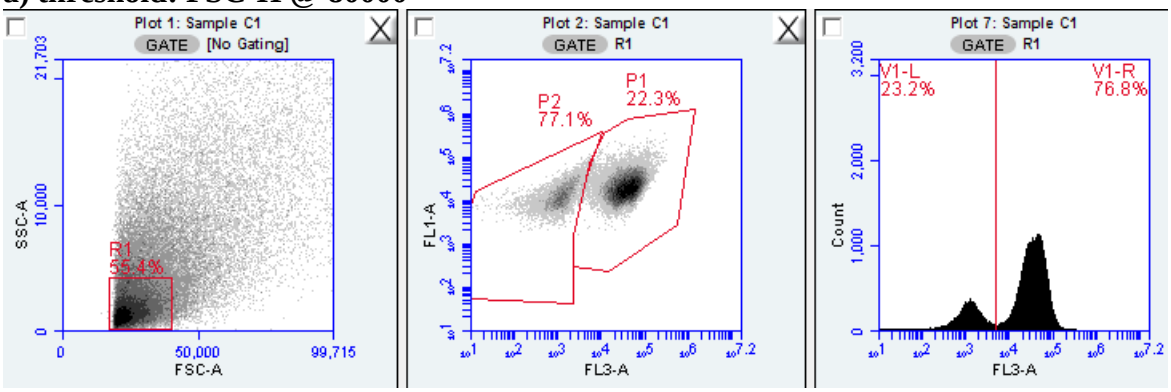

b) threshold: FL1-H @ 1000

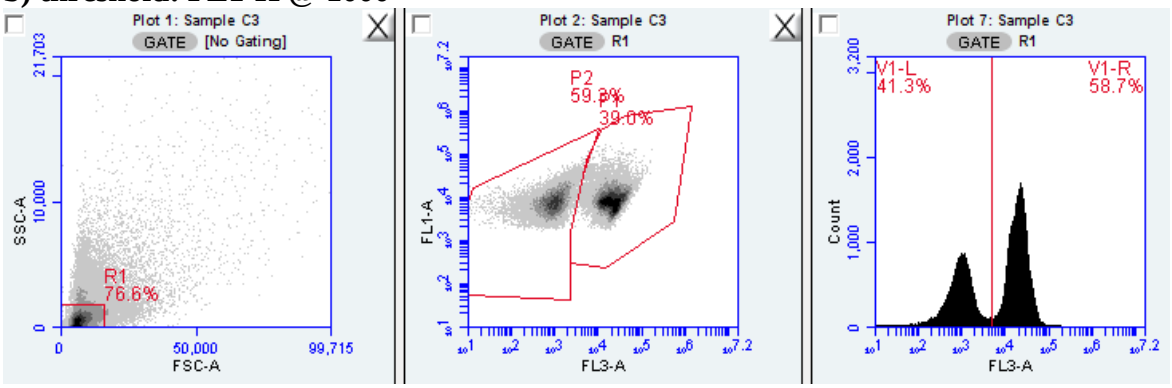

Figure 6-4. A comparison of forward scatter versus FL1 for triggering.

Here, the difference in live and dead values from one to the other is more than 18%. Obviously, there is "room for error" in assigning flow cytometric parameters, emphasizing the need for careful population identification and for setting thresholds and gating to optimize the capture of those populations.

Fluorescence factors

Some autofluorescence of bacteria was also observed, with *B. atrophaeus* being the brightest of the bunch (Figure 6-2). However, analysis of control samples (without CPEs) under the same gating conditions determined that the contribution of the bacteria to the overall signal intensity in FL1 (530 ± 15 nm) was somewhat less than 2%. This property of the bacteria allows analysis without a permeant stain, as seen in Figure 6-5.

This is quite useful, since the CPE polymers and the permeant SYTO stains have somewhat similar excitation and emission characteristics.

Fluorescence signal strength also shifts between samples with different polymers and with differing polymer concentrations; therefore the gating must shift between each sample to fit the new means of population. Usually, this is not a large shift and the population profiles or contour shapes tend to remain the same, so setting the new gates only requires sliding existing gates along one axis. An exception to this is seen in samples treated with OPE17 (**6**, Figure 1-6), where the bacteria appear heavily damaged, even with low exposure times. Here, we must assume that membrane integrity is highly impacted, causing rapid leakage of the SYTO permeant stain during equilibration with the suspension medium. This is reflected in the significant movement of the population by an order of magnitude lower in FL1 and about the same amount higher in FL3 (downward and to the right in the bivariate plot) as compared to OPE6 (**5**) and the PPE-DABCO complex (**2**). This effect can be seen in Figure 6-7.

Effect of CPE concentration

A study was carried out to determine the concentration dependent effects of PPE-DABCO (compound **2**, Figure 1-3) on *B. atrophaeus* in solution. A secondary purpose was to determine what effects the free polymers might have on fluorescence readings when using the green fluorescing SYTO permeant stains. Using only propidium iodide staining meant that any fluorescence observed in the FL1 parameter (530 ± 15 nm) would be due to the adherence/absorption of the polymer.

The raw flow data for this experiment are shown in Figure 6-5, with the gate windows labeled as to bacterial states. (Table 6-2 contains the numerical data from this

experiment, which are also graphed in Figure 6-5.) Here we note that the bacterial control is located mostly in the lower left quadrant, but did have some dead bacteria, possibly due to insufficient washing, that were stained by the PI and which appear in the lower right quadrant. It is interesting that even these already dead bacteria seem to become coated with the polymer as the concentration increases. This would indicate that the mechanism of polymer attachment is not dependent on any active process in the cells, such as nutrient uptake.

As the concentration is increased, the bacteria are coated more quickly, and are seen in the upper left quadrant at 2 mg/mL, where they have increased in green fluorescence, but have not all become permeable to the PI stain, as have those in the upper right quadrant. At concentrations of 3 mg/mL and higher, the bacteria are essentially all associated with the polymer and have all been killed.

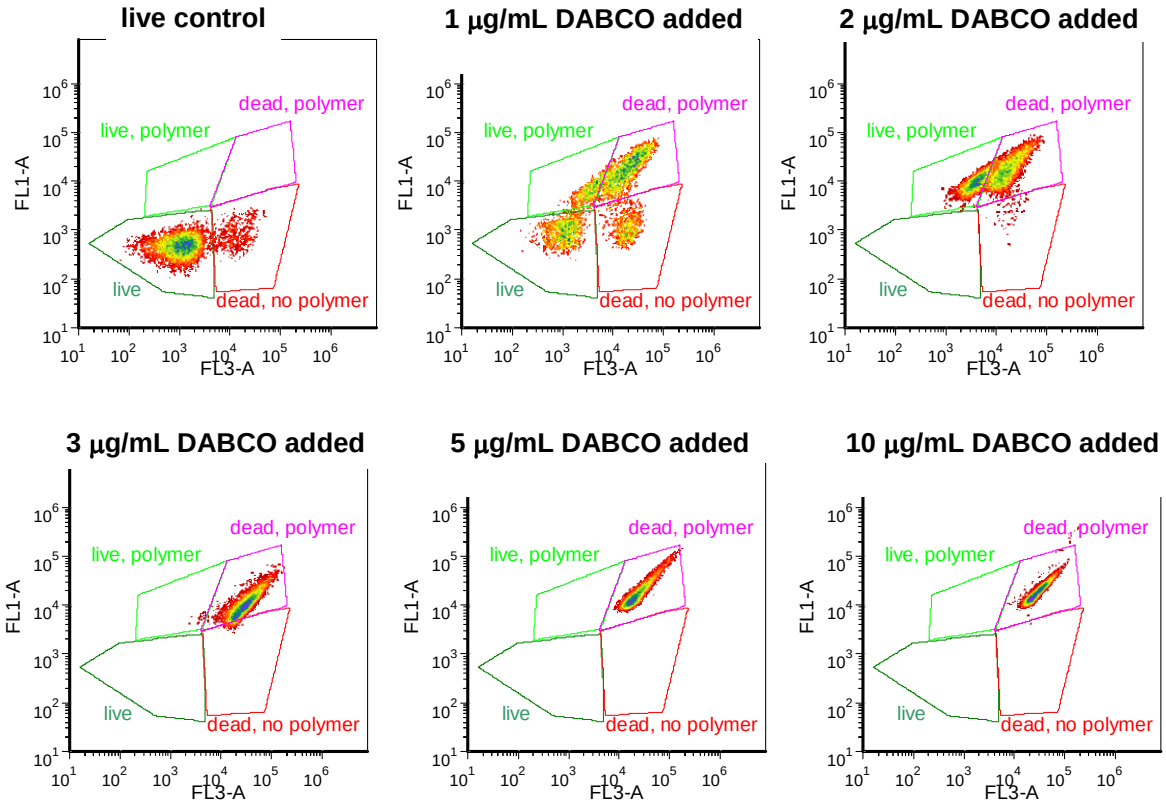

Figure 6-5. Concentration dependence of DABCO polymer (2) on killing of Bacillus atrophaeus in vegetative form. (From flow cytometry data). Only PI was used in staining.

Table 6-2. Data table for Figure 6-5 and Figure 6-6.

sample	%live no PE	%live + PE	%dead no PE	%dead + PE	**%total live**	**%total dead**
control	81.68	0.07	18.01	0.24	**81.76**	**18.24**
1 µg/mL	27.17	13.07	17.48	42.28	**40.24**	**59.76**
2 µg/mL	1.40	34.25	5.43	58.92	**35.65**	**64.35**
3 µg/mL	0.07	1.48	5.00	93.45	**1.55**	**98.45**
5 µg/mL	0.63	0.66	0.54	98.17	**1.29**	**98.71**
10 µg/mL	0.01	0.33	0.29	99.37	**0.34**	**99.66**

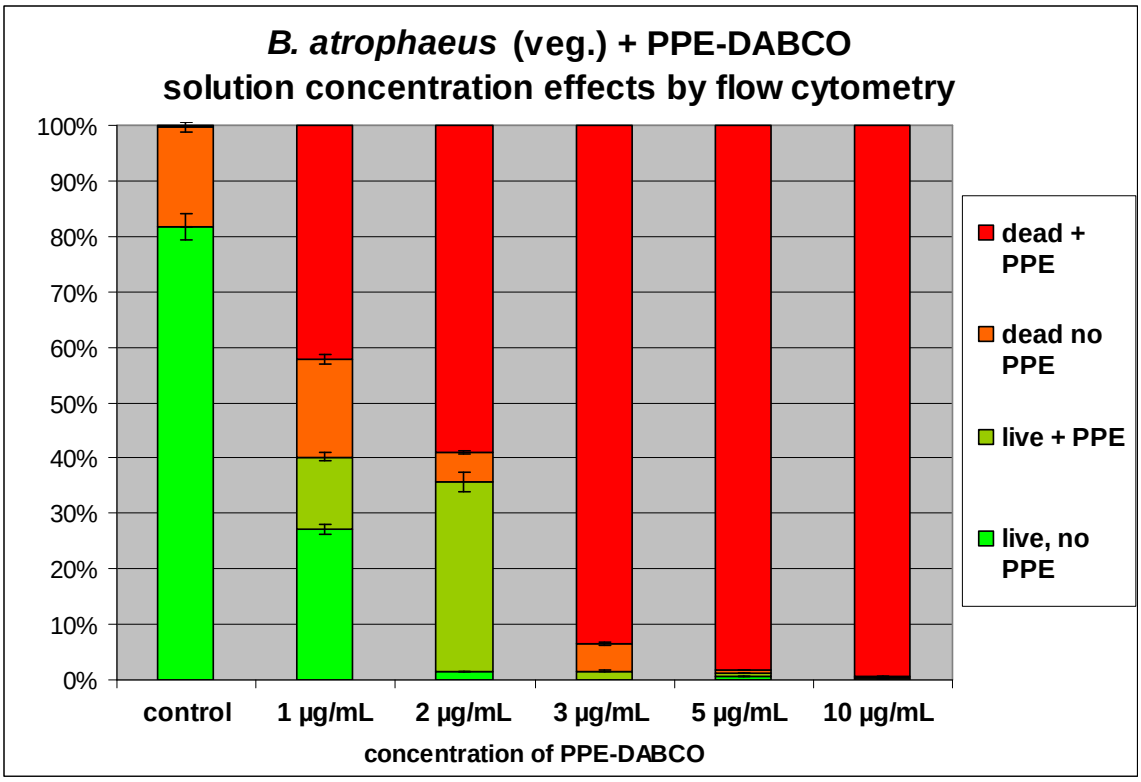

Figure 6-6. Flow cytometry data for *B. atrophaeus* survival after 30 min light exposure measured against PPE-DABCO (**2**) concentration in solution

The data in Figure 6-6 indicate that PPE-DABCO can be extremely cytotoxic with these Gram positive organisms. The very low remaining "live, no PPE" bacterial percentage in column 3 suggests that even at 2 µg/mL, the polymers have coated almost all of the bacteria, and will likely be lethal at longer exposure times.

Figure 6-7 shows some of the first data gathered on the oligomeric compounds **5** and **6** (Figure 1-6), by flow cytometry. This data indicates that the OPEs, particularly OPE17, can be effective biocides under dark and light conditions. OPE6 under dark conditions showed < 9% increase in bacterial death over the control, but this increased to ~25% following light exposure. The better performer (actually, the best we've tested so

far) was OPE17, which proved to be almost 100% lethal at 30 minutes, both in the dark and after light exposure.

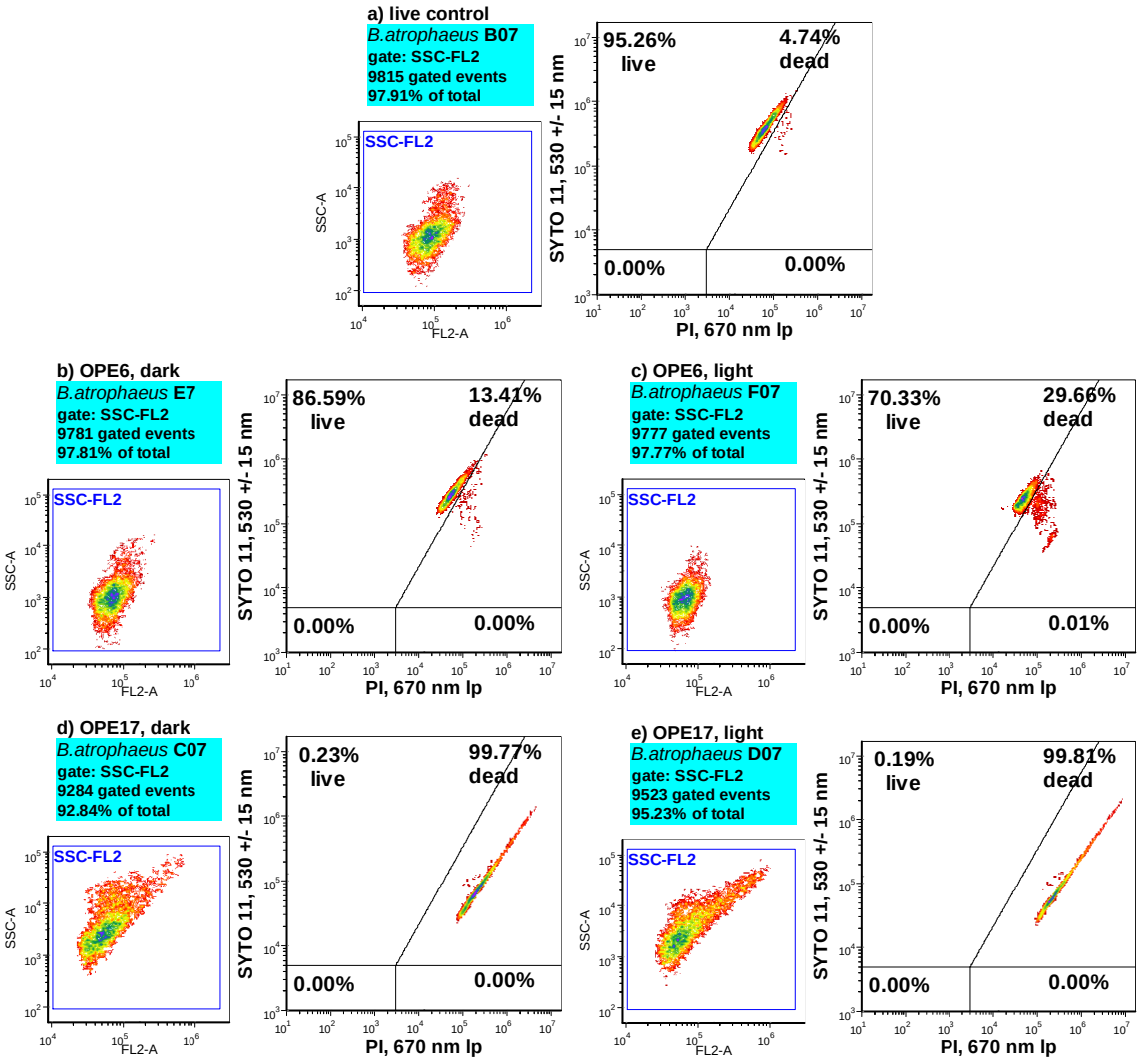

Figure 6-7. A series of SSC-gated contour plots showing the effect of OPE 6 & OPE17 (32 µg/mL)on *B.atrophaeus,* a) live bacterial control; b) OPE6 dark; c) OPE6 light; d) OPE17 dark; e) OPE17 light. The stain set used was SYTO 11/PI with light exposures of 30 min. FSC threshold for this series was 80,000.

Evaluation of control samples that had undergone light exposure were also important with the oligomers, since these molecules require shorter wavelength excitation for activation. This did seem to affect some of the bacterial samples more than others,

and may have been due to the method of exposure of samples with the portable UV lamp. In some instances, the attrition of the bacteria was significant; this is not surprising, since UV light is used for sterilization in some applications. More problematic was that the attrition rate varied, possibly from lowered or heightened exposure caused by sample placement. In the worst case, cell death in the live control was measured at 22% (Figure 6-8). Even with this handicap, significant differences between the experimental samples and the controls can still be observed, but more uniform exposure conditions in the new rotating carousel photochamber should certainly help to normalize sample exposures and reduce some of the variation observed in light-exposed control samples.

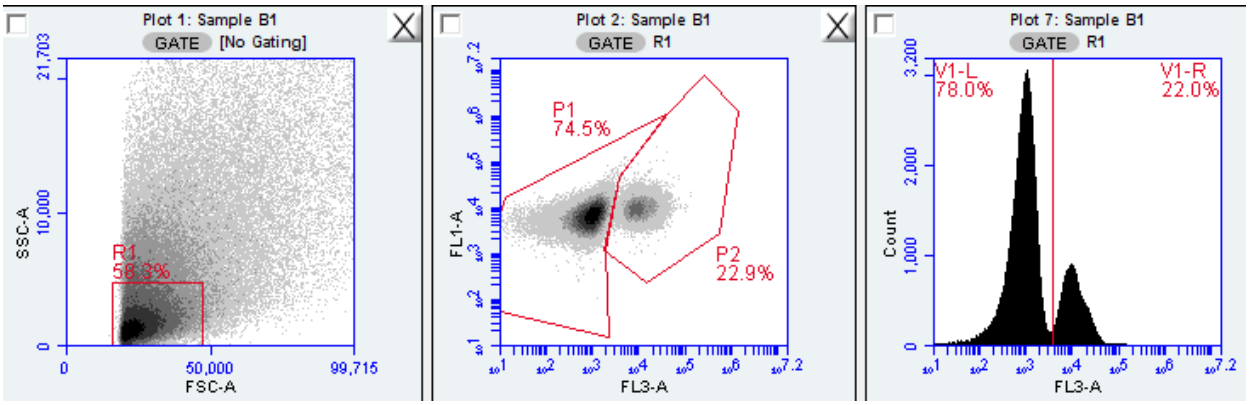

Figure 6-8. Live (UV-365nm) light-exposed *B. atrophaeus* control with stains.

However, even at lower concentrations (2 µg/mL) the light activated effects of the oligomers were unambiguous, as can be seen in Figure 6-9. Here the PI staining is quantitative and the indicative red fluorescence has increased by 3 orders of magnitude over the live control. This suggests that OPE17 with light exposure is extremely effective in permeabilizing the bacterial membrane of Gram positive bacteria.

a) OPE 17 dark

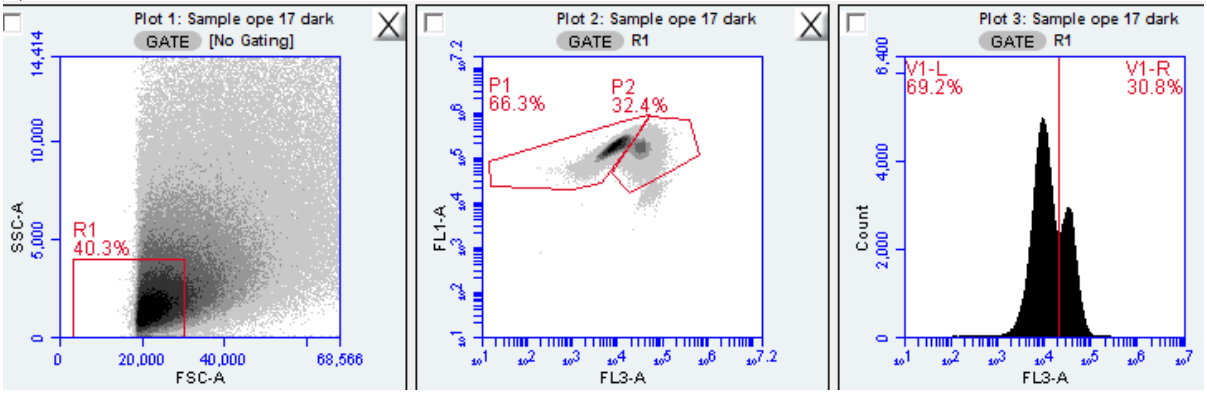

b) OPE17 light

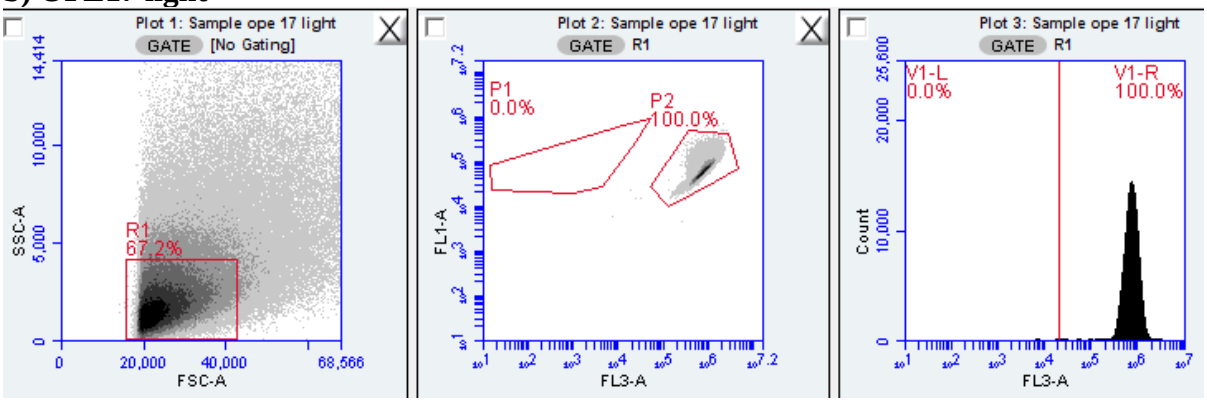

Figure 6-9. Effects of light exposure on *B. atrophaeus* treated with **6** at a concentration of 2 µg/mL.

Summary

Progress so far

A large number of compounds, including 2, 3, 4, 5, 6, the µRM and some newly synthesized polyampholytes have all undergone preliminary screening with flow cytometry, confirming the observations of antimicrobial effects on bacterial cells made in earlier experiments with confocal microscopy. Some of the oligomers seem especially potent and are seen to cause quantitative or near quantitative permeabilization of the bacteria. The PPE-DABCO complex in solution (Figure 6-5 and Figure 6-6) and grafted onto cotton and fabric samples shows significant activity as well.

The samples with fibers have so far yielded more complex information that indicate the existence of other processes, almost certainly moderated by surface attachment of the bacteria. Since flow cytometry can only measure what remains in solution, which can be valuable information, this precludes any conclusive analysis at the present time. More studies are under way that involve simultaneous CLSM imaging matched to the flow data from the same sample, but protocols for sample handling [rinsing, staining (loss of stains to fibers is observed)] still need to be optimized.

Bacteria: Confusion Reigns [borrowed from Shapiro (186)]

After describing in detail the instrumental capabilities and lauding the advantages of flow cytometry, it now seems somewhat disingenuous not to state that there is something of an art to this science. While the measurement of particle characteristics can be very precise, selection of gating parameters, triggering thresholds, sample concentrations, staining protocols, flow rates and other factors all have impacts (sometimes quite significant) on the results obtained, making it difficult to determine what the overall optimum protocol should be. Keeping as many of the variables as stable as possible is the recommended course of action for a project of this type. (And for science in general, I suppose.)

At this point in the development of flow cytometry, and, based on our current understanding of bactericidal processes, it is probably not reasonable to expect that changes in one flow cytometric parameter will accurately indicate general bacterial susceptibility to a given antimicrobial compound.(166) Since different antibacterial agents may have different direct and indirect impacts on various functions in different bacteria, it is obviously important to be able to track more than one parameter to

understand the effects of the CPEs on the bacteria. The multiple parameters available in flow cytometry do help to accurately discriminate certain properties, but these properties may be difficult to uncouple from each other, so it seems unlikely that a single set of testing parameters will be found that fits all bacteria, or even the same bacteria under somewhat different sample conditions.

An important part of refining the process is analysis of the cells in a comparable medium (meaning matched pH and ionic strengths) without the challenge of antibacterial compounds.(184) However, once the intrinsic properties of bacterial cells are sufficiently characterized, flow cytometry, with or without a given set of stains, may yield much useful information.(185, 7) However, these observations can still shed light on both direct and indirect impact of antimicrobials on microorganisms and enable identification of mechanisms involved in bacterial death.(5, 6, 165, 147, 157, 215) Given its rapid analysis times, low volume requirements, high sensitivity and synchronous measurement of fluorescence sensitivity, flow cytometry can be a powerful tool for the evaluation of bacterial responses and may aid in the discovery of new antimicrobial agents.

Chapter 7

Polyelectrolyte-coated Fabric-Preliminary Studies

Introduction

Progress in the development of applications for the CPE compounds under study is always encouraging. It had long been considered within the group that grafting of the polymers to fabrics and/or fiber material would be a good way to explore the potential for protective clothing, bandages, filtration devices, etc. (I recall discussions from 2008 of "Whitten mittens.") In some environments, fibers with these types of coatings may also offer significant resistance to the attachment and buildup of biofilms.

K. Ogawa, then at the University of Florida, and now a professor at Cal State Northridge, was able to accomplish this using a coupling reaction similar to the one employed for grafting the polymers onto silica microspheres. By attaching a siloxane linkage to any exposed hydroxyl groups, with the other end of the linkage having a phenyl iodide moiety, growing a PPE from the surface becomes a simple matter of supplying the monomers for polymerization.

Experimental methods

Polymer grafting to fabric samples

Samples of Battle Dress Uniform (BDU) fabric were supplied by the U.S. Army Natick Soldier Systems Center. These samples were camouflage patterned, with the coloring primarily on the outer surface. These samples were treated according to the procedure outlined in Scheme 7-1. This same process was also later performed on plain cotton fibers.

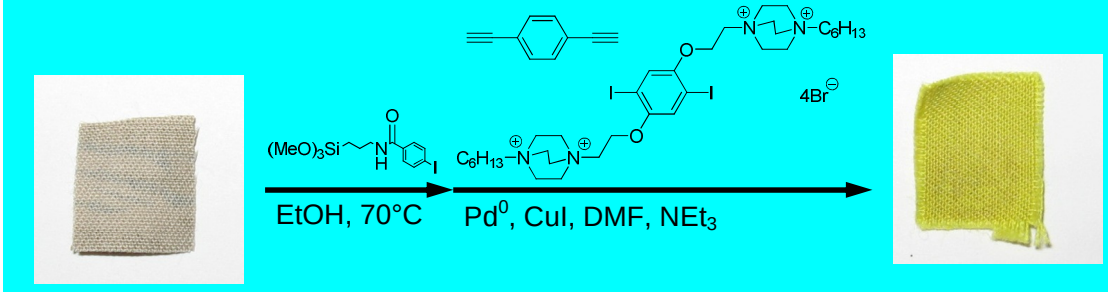

nylon and cotton fabric
treated with silane reagent in ethanol at 70℃
rinsed with methanol, dried in a vacuum oven at 90℃.
DABCO polymer grafted via *in situ* polymerization.
rinsed with methanol.
treated with aqueous solution of SDS to remove unattached residual polymer
rinsed with water, methanol and dried in a vacuum oven at 90℃.

Scheme 7-1. Description of grafting method used on fabric samples by K. Ogawa.

Exposure to a UV lamp shows bright fluorescence corresponding closely to the wavelength of the unbound CPE polymer (Figure 7-1). Confocal microscopic examination also confirmed the presence of the polymer, but only on some of the fibers (Figure 7-2).

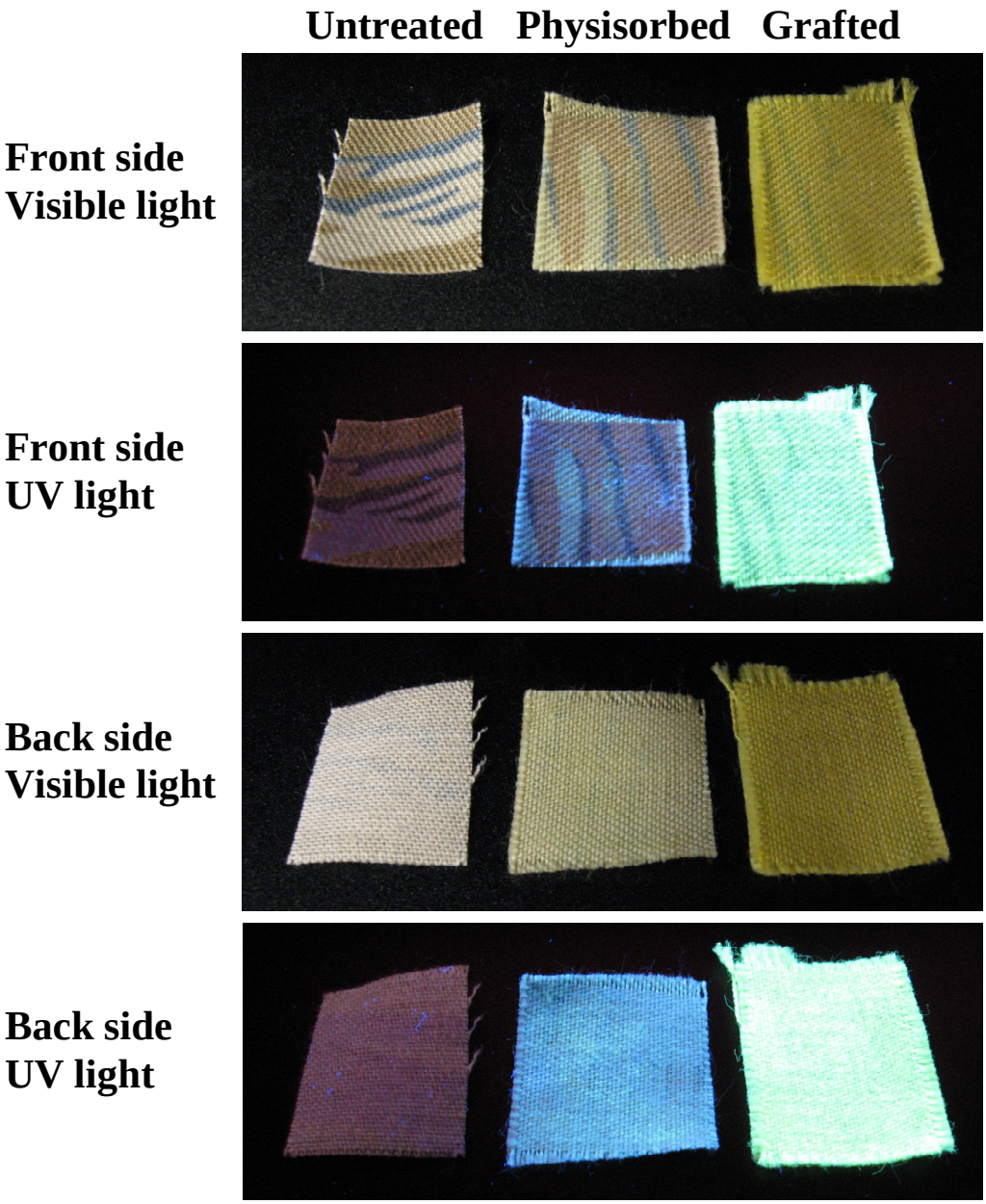

Figure 7-1. Physical appearance of fabric samples. Leftmost samples are untreated, middle samples have polymer **2** physisorbed and samples on the right are polymer **2** grafted.

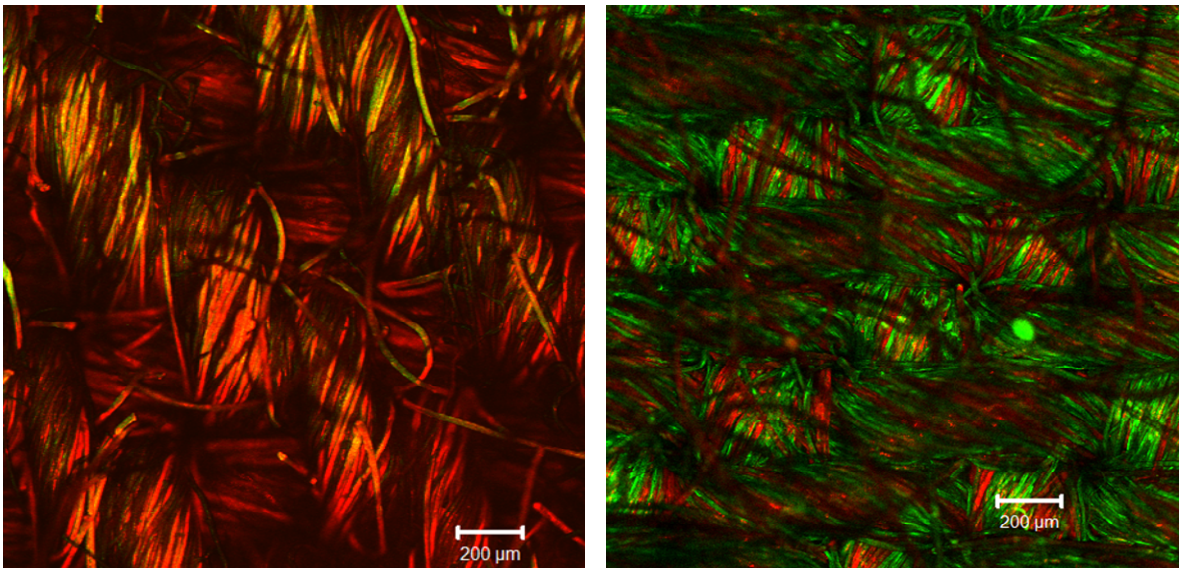

Figure 7-2. CLSM images of uniform fabric supports—left: untreated Natick fabric, right: polymer-grafted (DABCO) Natick fabric

Biocidal experiments

Bacterial sample preparation was carried out as described in Chapter 2. Fabric samples were placed in microcentrifuge tubes and submerged with the bacterial suspension. The Fiber Lite 190 was used for irradiation and light exposure times were increased to 30 minutes to offset occlusion of the radiation source by the fabrics. This is based on the assumption of a 15 minute average exposure per side while shaking in situ with the vortex mixer, during which the microcentrifuge tubes are observed to rotate more or less continuously.

The sample set for fabrics was expanded compared to other biocidal studies (Chapter 2, Biocidal studies-Experimental Parameters), with the addition of the split live and dead controls for flow cytometry testing (see Chapter 6, Flow experiment parameters) and rinse samples, prepared by rinsing the fabric coupons with 0.5 mL buffer after removal from suspension, creating a more dilute sample (rinseate) for each trial, along with the original, more concentrated suspension. The rinseate is considered to be

more representative of the attached bacteria, which are much more likely to have been affected by the CPE antimicrobial activity. Some concerns arise at this point, related to the uncertainty in the rinsing step and the degree of agitation that can or should be applied for accurate assessment of the attached bacteria. Seven experiments so far, with both the fabrics and cotton fibers (20 samples total) have not yielded consistent results. Our experience is not unique in this regard, as indicated by similar problems encountered at Natick relating to spore assessment. (H. Schreuder-Gibson, personal communication).

Results and discussion

Photophysical properties of grafted fabrics

Spectroscopic analysis indicates strong fluorescence in both the physisorbed and grafted samples. Figure 7-3 shows the emission spectra of the grafted and physisorbed fabrics, with a comparison to the untreated fabric. The much lower emission intensity of the physisorbed product is attributable to its likely binding orientation lateral to the surface of the polymer, driven by the electrostatic attachment. The grafted product, on the other hand, is probably more brush-like in nature, with some lateral orientation and cross-linking likely, but not to the extent of the physisorbed material. The surface grafted fabric exhibits bright fluorescence centered at 502 nm; this emission band is red-shifted in comparison to its solution emission profile (λ_{max} = ~440 nm).

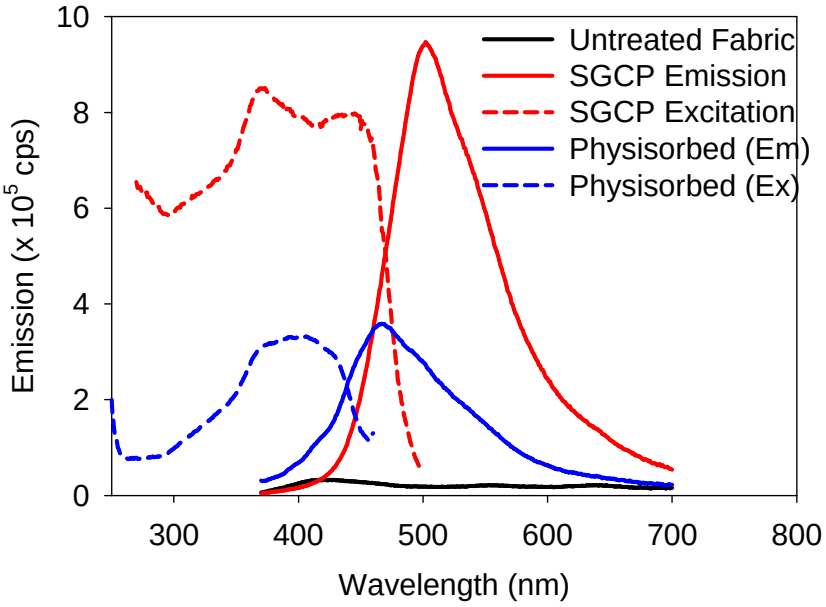

Figure 7-3. Photophysical Properties of Fabrics. Excited @ 360 nm, Emission λ_{max} = 502 nm. (K. Ogawa)

Antimicrobial activity

At this stage, only the grafted fabrics and cotton fibers have been tested for biocidal activity. *P. aeruginosa* and *B. atrophaeus* (vegetative and spore forms) have been exposed to the substrates in solution. Both these species (in vegetative form) show marked proclivity for attachment to the polymer coated samples as compared to the untreated samples (Figure 7-4). Dead bacteria (as identified by the uptake of impermeant stain (PI in all the experiments listed here). are most numerous on the fiber surfaces, while, in general, very few are observed in solution relative to the live population.

The accumulation on the fibers of what is assumed to be bacterial decomposition products creates a "plaque" of sorts that is strongly fluorescent in the region of PI emission (indicating high DNA content) as seen in Figure 7-6. This type of deposit has also been observed in previous experiments with the CPE coated microspheres (Figure 3-6 and Figure 3-7) and possibly is the source of the red fluorescence contained within

the interior of the µRM in Figure 5-5b. This material is obviously very "sticky" and is thought to contribute to the aggregation of particles in solution.

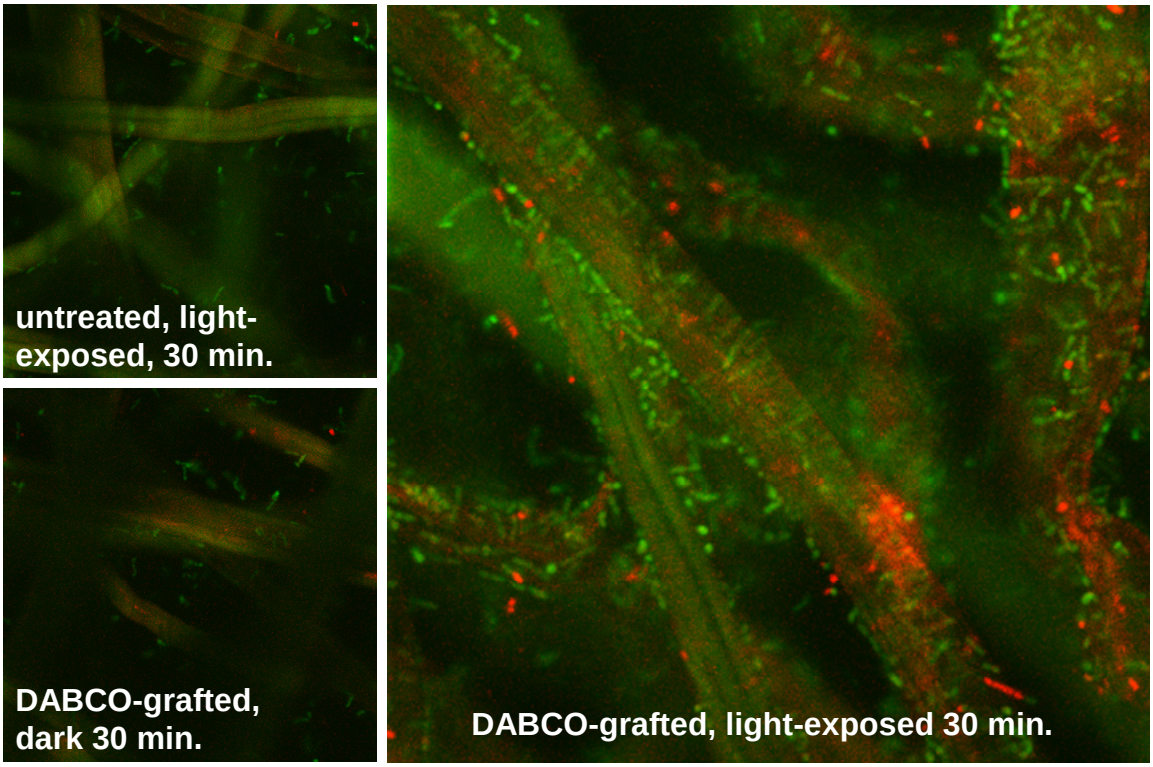

Figure 7-4. CLSM images of *B. atrophaeus* on PPE-DABCO grafted cotton fibers, stained with Syto 11 and propidium iodide.

Confocal imaging, due to time limitations, has been mainly of the fibers themselves, while solution populations and staining characteristics have been quantified using the flow cytometer. Setting up reliable protocols for exposure and live/dead assaying is ongoing: Some of the fabric samples, most especially the polymer-coated ones, tend to float during exposure in the suspensions; some fibers, particularly the raw cotton, absorb one or both stains quite effectively. This is the likely source of much of the dim red fluorescence of the fibers in Figure 7-5.

B. atrophaeus spores, as might be expected, proved difficult to stain, requiring 45 minutes incubation time. Also, the spore samples tested did not exhibit nearly the degree

of attachment shown by the vegetative cells. Very little killing of the spores was observed, most likely because of their innate hardiness in conjunction with these two external factors.

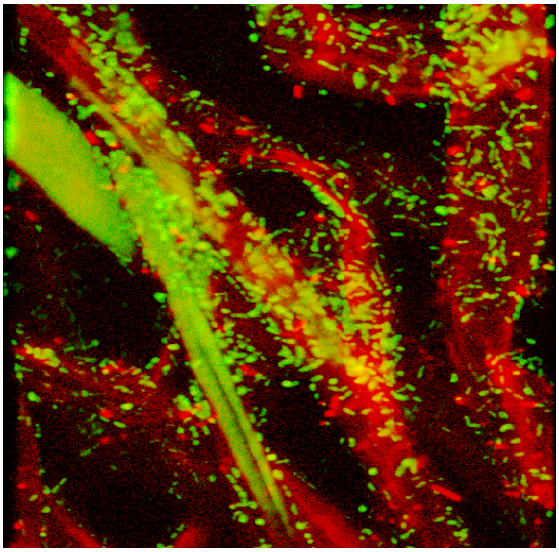

Figure 7-5. A CLSM image of SYTO 11/PI stained *B. Atrophaeus* on PPE-DABCO grafted cotton fibers. This 3D projection of a z-stack reveals the dense attachment of the bacteria, with numerous live (green) and dead cells (brighter red particles).

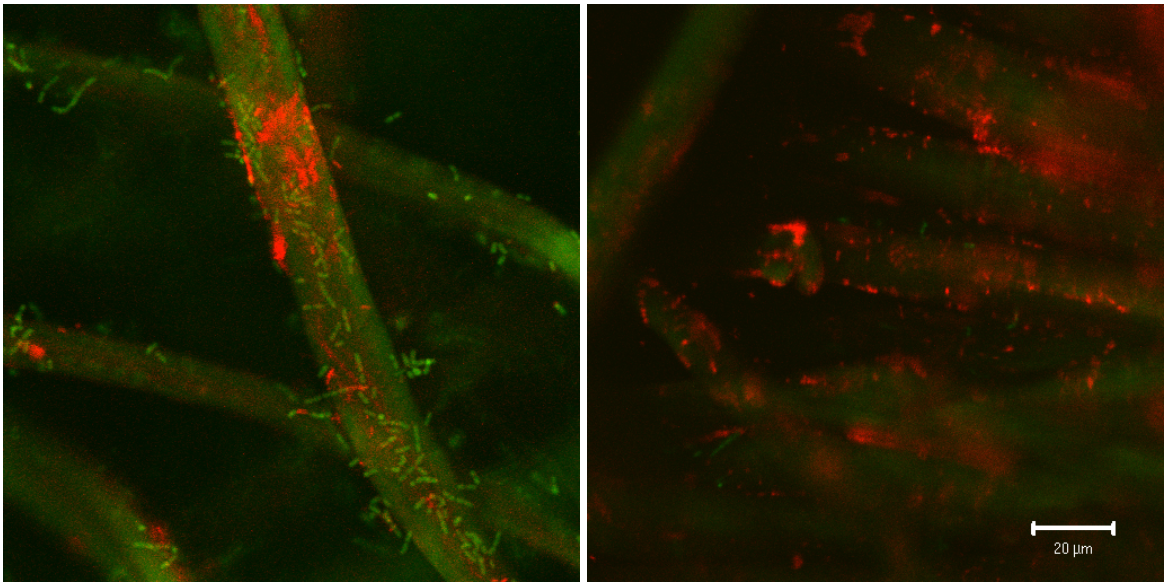

Figure 7-6. Images of red "plaque," believed to be composed of PI stained bacterial decomposition products.

The effects of bacterial exposure to PPE-DABCO-grafted cotton fibers over time under dark and light-exposed conditions are shown in Figure 7-7. Bear in mind that these particular data represent the populations of bacteria *not* attached to the fibers, but remaining in solution after the fibers were removed after the indicated exposure times. The data from the flow cytometry measurements suggest that the fibers (submerged in the suspension) continue to acquire adherent bacteria up to and perhaps beyond a 2 hr exposure time, as indicated by the blue bacterial population lines.

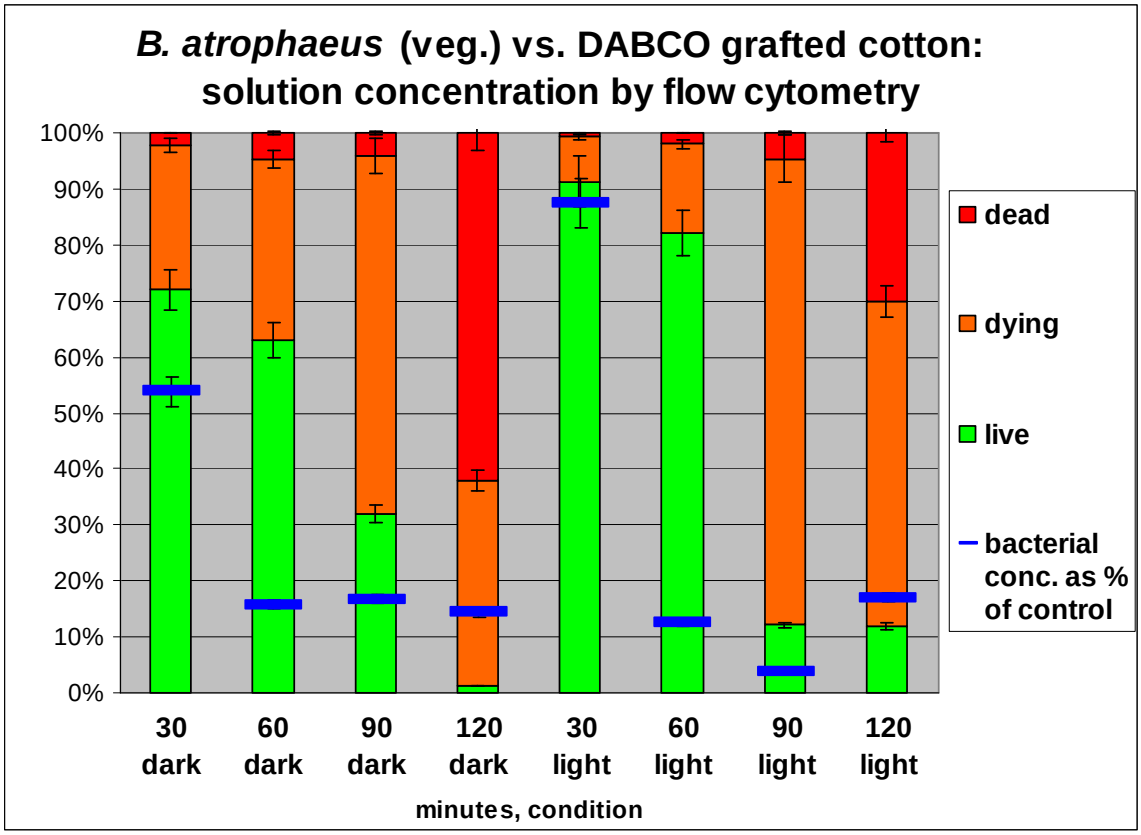

Figure 7-7. A graph of live, dying and dead *B. atrophaeus* vegetative cells remaining in (original suspension) solution after exposure to PPE-DABCO (**2**)-grafted cotton under both dark and light conditions. Bacterial populations relative to the control are represented by the blue bars.

The majority of the bacteria remaining in suspension after 2 hours are dead or dying (~90%), as compared to the control (~7.5%, not shown). Again, we hesitate to

declare quantitative values for the "true" antimicrobial activity, as this is still a work in progress (especially as related to the rinsing, agitation, and access to light exposure aspects of the experimental protocols), but the trends are certainly valid and appear to be quite promising.

To offer a final curiosity, the survival of the light-exposed bacteria at longer times (120 minutes), as seen in Figure 7-7, is a persistent phenomenon for which I currently have no explanation. Studies of the effects of visible light on bacteria are sparse in the literature, with most focusing more on UV wavelengths for decontamination purposes. This effect seems to be independent of polymer type and may in fact be predominantly cell dependent. If this is the case, one explanation might be a bacterial response to damage induced by intense light exposure that also affords protection from the CPEs. Experiments involving irradiation of a number of types of live controls (without CPEs) of both Gram positive and Gram negative organisms are planned to further delineate the nature and extent of the phenomenon.

Summary

These experiments on the PPE-grafted fabrics lend support to their use in antimicrobial applications. The bacteria *P. aeruginosa* and *B. atrophaeus* (in vegetative form) adhere well to the substrates, as established by CLSM imaging and by the drop in the bacterial populations in solution as measured by flow cytometry. Bacterial damage and killing are certainly taking place on the fiber surfaces, as evidenced by CLSM observation in numerous experiments, but I am hesitant to report quantitative data because of the need for refinement of the light exposure, rinsing, agitation and measurement protocols.

Further studies are needed to establish polymer loading and retention under various conditions. Analogously, the bacterial loading and retention (and potential for cleaning) need to be determined. Part of the difficulty in completing these studies is due to the lack of accepted protocols for measuring these parameters. Aerosol spraying of the bacterial solutions may be one way to control dosing (and avoid the flotation of the sample coupons. Personnel at Natick are working to establish such protocols, but are mainly focused on the spore form of the bacteria, which do have quite different properties.

Our few initial tests on the spore form of *B. atrophaeus* with the fibers did not indicate a high degree of spore attachment and/or deactivation. Staining of the spores is known to be much more of a challenge, since they are essentially dormant, hardened shells with increased Ca^{2+} and Mg^{2+} content that inhibit the transport of many dyes. It is likely that these same properties will inhibit infiltration of our CPE complexes as well, though some spores are known to be susceptible to reactive oxygen species.(110, 67)

Since starting the fabric experiments it has been a goal to run parallel sample analyses using both the confocal microscope and the flow cytometer. While this is a sound concept, successful execution has only occurred a few times so far. Once the new protocols have been fully developed and verified, we hope to generate more directly comparative (and quantitative!) data sets that can elucidate the bacterial attachment and killing processes on the grafted fibers.

Chapter 8

Conclusions & Future Directions

Conclusions

A number of innovative and effective antimicrobial compounds have been produced based on isolation from environmental sources. By mimicking these and extrapolation of structure-activity relationships gleaned from the analysis of these compounds and their primary and secondary structures, artificial compounds with singlet oxygen sensitization properties and quaternary ammonium functionalized end caps and/or side chains have been identified, synthesized and refined. Several related studies were carried out on this family of organic phenylene ethynylene compounds investigating their antimicrobial effectiveness when incorporated into ordered structures on microspheres, as hollow, multi-layer capsules, grafted to fibers and free in solution. Analyses of the impacts of these compounds on several species of bacteria exposed under a variety of conditions indicate that this is a fruitful approach, worthy of continued research efforts. Further work in this area is driven by the rapid emergence of resistance in multiple pathogenic species.

These studies determined that this group of CPE compounds has biocidal activity toward certain bacterial species in the absence and/or presence of light in aqueous media. Determination of bacterial viability by live-dead (permeabilization) assays in the dark versus in the light has been used to determine if the polymers are inherently biocidal under various conditions: with and without oxygen and with and without photo-induced enhancement of their activity.

It is fairly well-established that irradiation of potential sensitizers of singlet oxygen can result in damage or death of microorganisms, and in several cases, the site of damage produced by the reactive species can be determined or inferred. However, in many cases it is not clear as to what the degradation is or how and where it is initiated. It seems probable that in many cases involving light-induced activation of oxygen in microbial systems there is an initial generation of singlet oxygen followed by its reaction with some component of the cell to generate reactive species that are potentially more reactive and longer lived than singlet oxygen and that these are the likely source of cell killing. The mechanisms for surface binding and infiltration of polymers into bacterial cells are quite variegated and often not well understood. This is evidenced by the variations in permeabilization, staining intensities and cell agglomeration and the difficulty that these and other factors presented in most all experiments and in determining a working regime for the flow cytometry experiments in particular.

Evaluation of goals

The following goals and objectives of this research project have been met:

Organisms to be tested were selected on the basis of their availability, ease of culturing, pathogenicity (or lack thereof, for the laboratory strains) and Gram staining characteristics. These were then grown, harvested and used in multiple experiments.

Rapid and effective assays for evaluation of the biocidal activity were developed using confocal microscopy and flow cytometry to corroborate quantitative data. Bacterial samples with appropriate stain sets were run with live controls using flow cytometry, showing an increase in throughput and allowing for normalization to account for any

natural attenuation of bacterial populations over time due to lack of nutrients and/or oxygen.

The presence of oxygen was confirmed to enhance bacterial killing relative to ambient conditions, and, conversely, the absence of oxygen reduced the biocidal effectiveness of the CPE complexes in solution. The issue of light activation has turned out to be a bit more complex than originally expected, as expounded on in Chapter 4 and in recent experiments with a thiophenyl oligomer (Figure 8-3).

The CPE compounds have proven effective at retaining their recognized biocidal capabilities when grafted onto silica microspheres and cotton fibers, and appear to be even more effective, especially at bacterial sequestration, when formed into LbL capsules. Some time and concentration dependence of biocidal activity has also been determined.

Examination of structure/activity relationships, as determined by these studies (and by the membrane studies mentioned earlier) has been quite valuable. It has been used to guide synthetic objectives, especially for the numerous new oligomers that have been synthesized, with more recent synthetic targets designed with the impact of OPE17 (**6**) in mind.

Final comments

My original hypothesis that the antimicrobial activity of this family of CPE compounds can be analytically measured, modified and incorporated into various relevant material substrates has been affirmed. It is hoped that, collectively, these studies will inform future synthetic design goals for CPEs and antimicrobial compounds in general. Studies of these and other CPE compounds may be helpful in determining

antimicrobial resistance mechanisms, especially if investigated for dosage, binding and membrane effects and interrogated in conjunction with currently developing genetic analysis techniques.

It is encouraging to know that, in some small way, these current lines of inquiry are supporting the rapid development of antimicrobial compounds that appear to circumvent standard antibiotic resistance mechanisms. There is urgent need for these and other compounds and their delivery methods/applications to be developed, refined and put into service in novel ways in the fight against disease.

Future Directions—Near Term

Mechanistic studies

Determining the critical properties of the active CPEs and elucidation of their biocidal mechanism will be a key part of future investigations. More oxygenation and deoxygenation experiments could help determine the factors affecting the role of oxygen in the biocidal activity. This will help in deciding if future spectroscopic experiments will focus on oxygen species or on other potential intermediates. A commercially available, highly selective fluorescent reagent for singlet oxygen known as singlet oxygen sensor green (SOSG) has been applied to a range of biological systems that are known to generate singlet oxygen. Increases in SOSG fluorescence closely follow the increase in the concentration of conjugated dienes, which is stoichiometrically related to singlet oxygen production. During *in vivo* tests on liposomal systems, algae and wounded leaves showed an increase in SOSG fluorescence, even in the dark. SOSG or other fluorescent indicators can be evaluated with confocal microscopy and/or flow cytometry and thus may serve as a probe in our experimental system for the detection of singlet oxygen. (58)

Once the mechanism has been deduced, there are several options for maximizing the activity of the system. The light source, frequency and exposure times can be varied, along with variations in polymer length and functionalization. There is also potential for species selectivity, wherein different species of Gram positive and Gram negative bacteria may be tested for susceptibility to different solution conditions and to variations in polymer structure with the objective of optimizing biocidal activity of the beads. The parameters of light exposure, activity in the presence of inhibitors, the addition of quenching agents or other conditions found to enhance activity may also be explored.

Evaluation of the morphological changes in the multilayer systems may be another avenue to investigate. The transition of the μRoach Motels over time and upon exposure to bacterial solutions is intriguing (see Figure 5-6) and may yield information about the "capture" mechanism and the sequestration of bacterial species in more general cases.

Refinement of flow cytometric techniques

The flow cytometer has proven to be an excellent resource for rapid evaluation of the CPE complexes' antibacterial action. Although numerous reliable qualitative assessments are in hand, several refinements are being made to the flow cytometry protocols in order to bolster the reliability of the quantitative data. The sample preparation, threshold and gating parameters, dosing of CPEs and experimental time constraints (especially for experiments involving simultaneous CLSM imaging) are all under review.

A number of other dyes and staining protocols are also being considered, with the goal of utilizing the second (647 nm) laser on the Accuri C6 as another excitation source.

This would extend the spectral range for data acquisitions, increasing the number of parameters simultaneously measurable. The library of dyes is ever expanding and now includes many with a high level of specificity for targets in cell structure and metabolism.

For example, bacteria considered "dead" by dye exclusion criteria are presumed to have significantly diminished membrane integrity. If this is a direct indication of membrane porosity, the loss of membrane potential due to the dissipation of ion concentration gradients across the membrane may be observable; a number of membrane potential measurements by flow cytometry have been reported in the literature.(184, 215, 189, 28) Issues of staining relating to membrane integrity, permeability, and "viability" have been discussed in the Chapter 2 section on Staining, and these concepts will still require careful evaluation of how they relate to bacterial cell death as determined by flow cytometry.

Matching the sheath fluid in the flow cytometer to the buffer composition of the samples may result in more accurate analyses, with less distortion resulting from the mismatch of refractive indices between the standard sheath (water) and the sample buffer, especially for particle sizes of < 1 µm.(139, 7) According to the user's manual, this should be easily implemented on the Accuri C6.

The problem of pulse width exclusion of agglomerated bacteria (Chapter 6, Results-General observations) is also being considered. Alteration of the pulse width limitations by hardware or software may be possible. Assessment of the pulse width as it relates to other measured parameters might also help to reveal the extent of data loss by signal rejection.

Synthesis of new CPEs

Polyampholytes. Ampholytes are a class of zwitterionic compounds that contain a mixture of positively and negatively charged moieties. These should not be confused with amphiphiles, which are compounds with segregated regions of hydrophilicity and hydrophilicity. The charged groups of polyampholytes can be placed along the polymer chain in stoichiometrically controlled ratios, either directly on the polymer backbone, or, more frequently, in side groups pendant to the polymer chain. Three such compounds, shown in Scheme 8-1, have been synthesized by E. Ji in our group. Bacterial suspensions exposed to each of the two molecules with opposite stoichiometry from Scheme 8-1b gave some very complex readings in the flow cytometer; an example is shown in Figure 8-1. The samples were observed to have completely coagulated after only a few minutes (making data acquisition by flow cytometry a bit uncertain), leaving the previously turbid solution completely clear. These and similar types of ampholytic complexes certainly merit further attention.

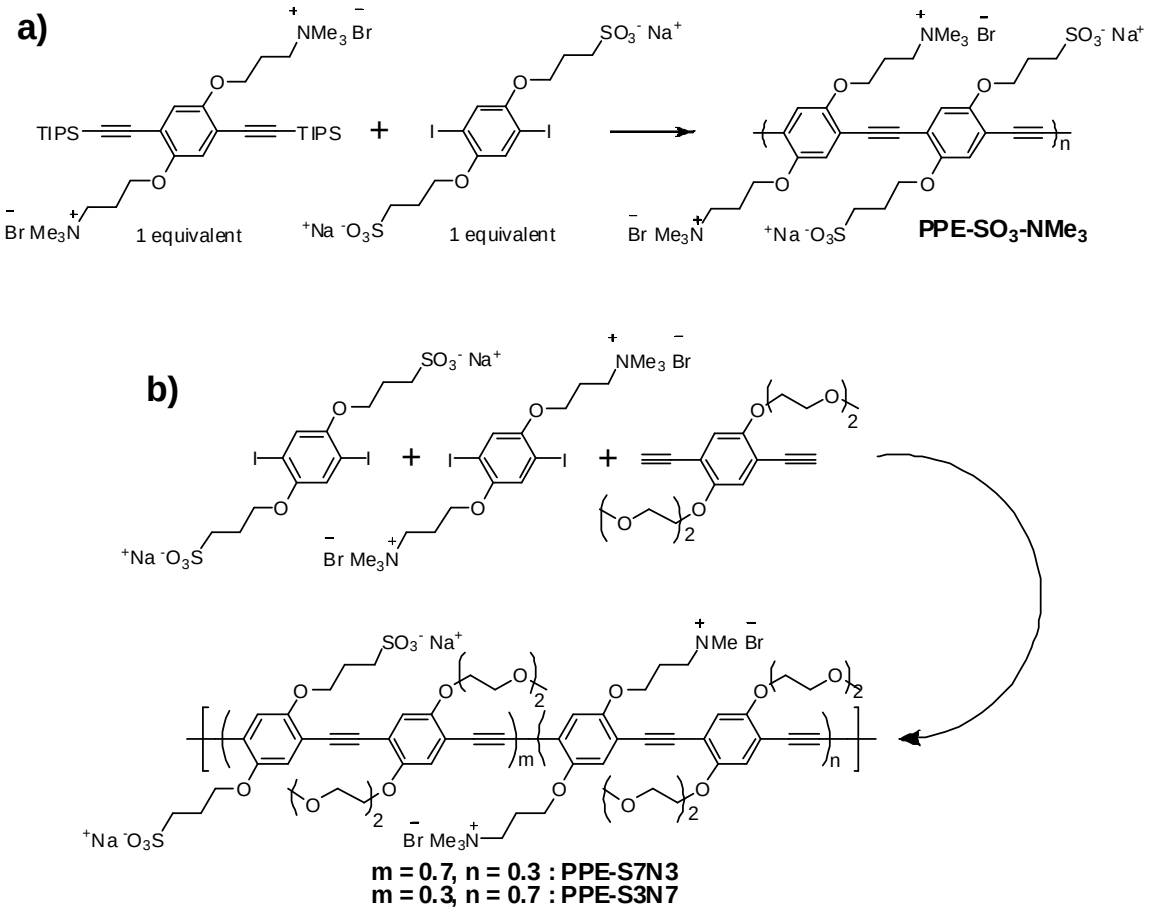

Scheme 8-1. Starting materials and the target complex structures for conjugated phenylene ethynylene polyampholytes to be investigated in this study. The equimolar version is shown in a; the two complexes in b have 7:3 (PPE-S7N3) and 3:7 (PPE-S3N7) ratios of sulfonate to quaternary ammonium.

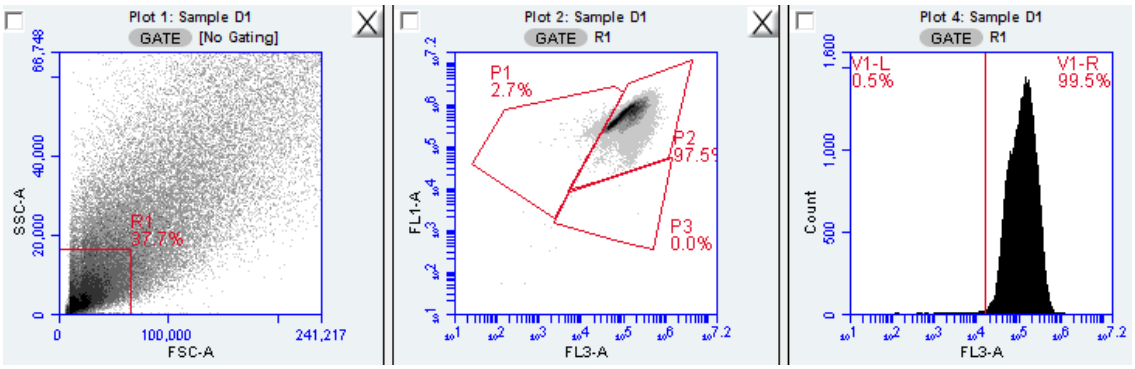

Figure 8-1. Flow cytometry results for B. atrophaeus exposed to the polyampholyte PPE-S7N3. It is obviously quite effective in killing the bacteria, but the bivariate plot of fluorescence shows unexpected complexity, with at least 5 different populations distinguishable.

Oligomers. I alluded earlier to the ongoing testing of a large number of oligomeric compounds by flow cytometry. These have been synthesized in our group by Z. Zhou and Y. Tang. Substitutions have been made in the end group and side chain chemistries and symmetric and asymmetric configurations have been explored.

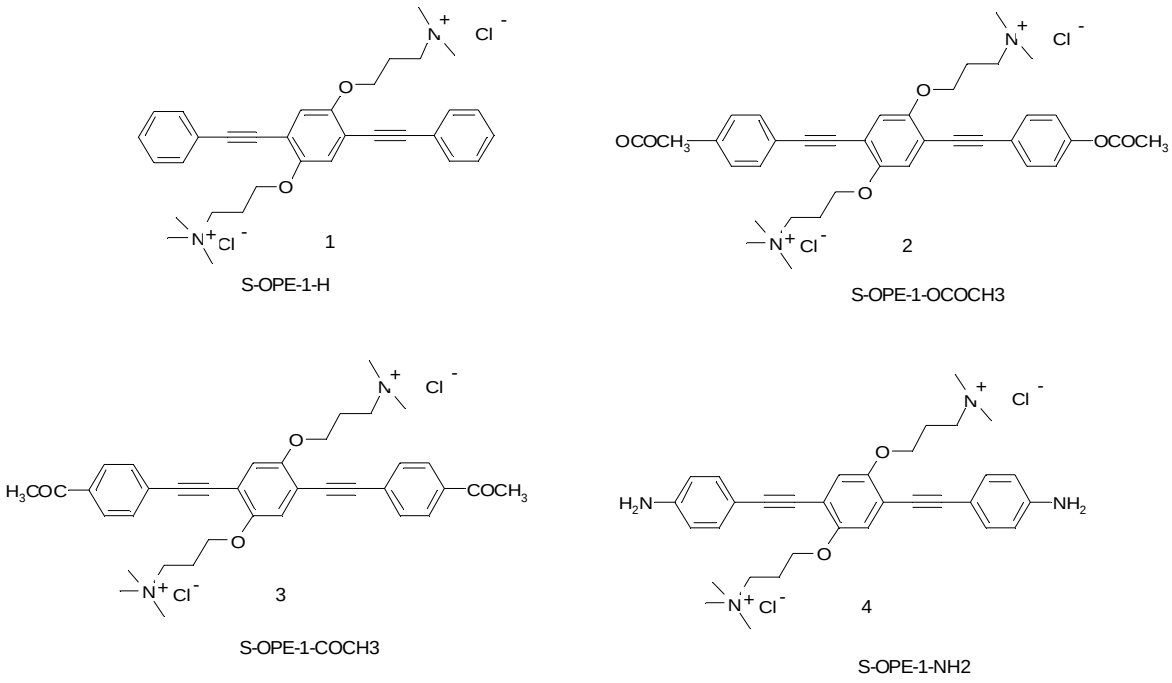

Figure 8-2. Structures of some of the new symmetric oligomeric compounds based on phenylene ethynylene linkages.

More recent oligomeric targets have been synthesized that were designed with the biocidal success of the OPE17 compound in mind. Figure 8-3 shows the structure of an analog of OPE17 with a thiophenyl ring substituting for the central phenyl group. In preliminary tests, this compound seems to follow the trend for the PPE-Th compound, showing much more effective antimicrobial activity (possibly more than OPE17 itself) when not exposed to an excitation source.

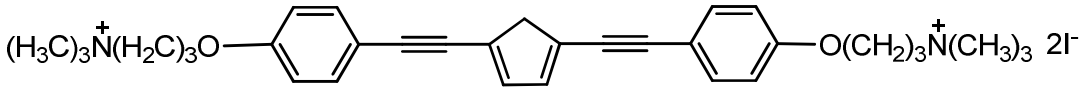

Figure 8-3. A recently synthesized oligomeric CPE, designated as OPE17-Th.

Membrane modeling

Various lipid bilayers and vesicles can be used to form complex biophysical systems that closely mimic biological cell membranes. The simulation of bacterial membranes is another way to investigate the likely disruptions, reordering and associations resulting from bacterial exposure to the CPE compounds. Carried out by L. Ding and Y. Wang in our group, these studies have already provided some understanding of the mechanisms of membrane disruption, insertion characteristics of the complexes and quantification of membrane permeabilization.(46, 54)

In considering the interaction of any antimicrobial system with a cell membrane, it is important to keep in mind the variations in (and adaptability of) the organisms. In light of this, matching the activity in the model systems to the *actual* components of cell membranes will be critical as the research progresses.

Table 8-1. Lipid distribution for several different bacterial cell types. (65) RBC = red blood cells. Lipid designations are PC-phosphatidylcholine; PE-phosphatidylethanolamine; PG-phosphatidylglycerol; PS-phosphatidyl-serine; SM-sphingomyelin; CL-cardiolipin; CH-cholesterol.

Cell type	PC (%)	PE (%)	PG (%)	PS (%)	SM (%)	CL (%)	CH (%)
E. coli (Gram-negative)	–	80	20	–	–	5	–
S. typhimurium (Gram-negative)	–	60	33	–	–	7	–
P. cepacia (Gram-negative)	–	82	18	–	–	–	–
B. subtilis (Gram-positive)	–	12	70	–	–	4	–
S. aureus (Gram-positive)	–	–	57	–	–	43	–
RBC (outer leaflet)	33	9	–	–	18	–	25
RBC (inner leaflet)	10	25	–	10	5	–	–

As seen in Table 8-1, the type and quantity of phospholipids in a given organism can vary considerably. Bacterial membranes contain substantial amounts of negatively charged phospholipids, such as phosphatidylglycerol (PG) and cardiolipin (CL). In contrast, the outer leaflet of the mammalian cell membrane is composed mainly of phosphatidylcholine (PC), phosphatidylethanolamine (PE), and cholesterol (CH), which are all charge-neutral at physiological pH. Future antimicrobial design, particularly design for bacterial specificity, will need to be vetted thoroughly against this wide range of parameters, as will the consideration for impact on human tissue and systems.

One of the initial membrane modeling experiments performed by L. Ding shows a substantial increase in surface pressure in a PG film upon injection of PPE-Th (**4**) underneath the film, indicating insertion into the monolayer. Under the same circumstances, there appears to be a distinct lack of interaction between complex **4** and the PC and PE lipids most commonly found in mammalian cells (Figure 8-4). This indicates that **4** may have potential selectivity in penetrating and killing bacteria over mammalian cells.

The early stages of mammalian cytotoxicity tests also look promising, with no significant bovine aortic endothelial cell deaths after extended incubation with several of the oligomeric and polymeric compounds (K.Wilde, UNM, unpublished results).

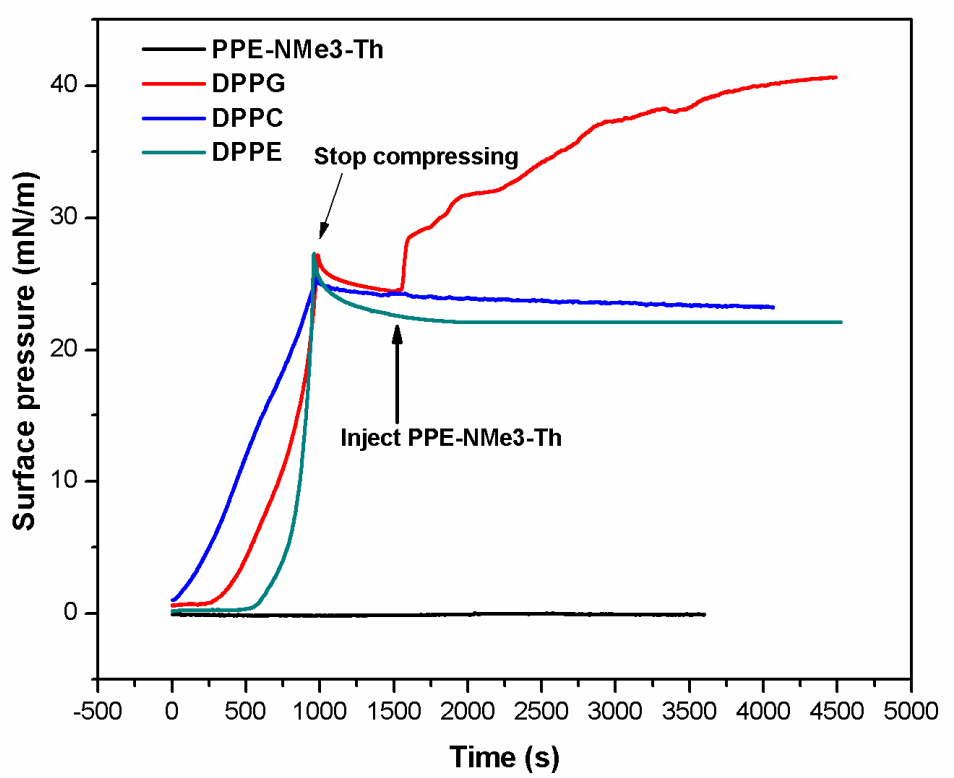

Figure 8-4. Data from a Langmuir trough experiment, indicating selective insertion of the PPE-Th polymer into a PG monolayer, with no apparent influence on PC or PE.

Structural calculations

Theoretical and computational modeling are an essential part of modern antibiotic design. Models providing explanations of the interaction of the CPE compounds with cell membrane components, analogous to the biophysical studies described above, are highly desired. An understanding of the interaction of cationic, anionic, zwitterionic and neutral complexes with lipids (in all their complex permutations, but especially for bacterial lipid components) would be very useful. The difficulties may lie in relating

binding affinities to charge, ionic strength and other basic properties of the system, since charged systems are notoriously difficult to model *ab initio*.

An effort to model oligomeric CPE chemical structures has been undertaken within the group by E. Hill, using GAUSSIAN with various basis sets. This already has revealed potential conformational variations away from ring coplanarity and from strict rigidity (linearity) along the conjugated chain, even for the smallest oligomers.(81) These might be matched with empirically determined or calculated spectrophotometric properties to inform synthetic goals.

Bacterial targets

Of course, direct experimentation with living microorganisms will still be necessary and probably most immediately relevant for development and implementation of antimicrobial regimes. Testing across a range of organisms, including those generating a majority of the nosocomial infections should be quite informative in that regard. *Staphylococcus aureus, Streptococcus mutans* and other potential candidates of various Gram positive and negative dispositions are listed in Table 8-2. Organisms on this list are subject to the limitations of availability, space, virulency and pathogenicity (as designated by BSL and the University Biosafety Committee).

Table 8-2. A list of potential bacterial targets for antimicrobial candidate compounds. Those highlighted have been examined at some point in current and previous studies by our research group.

scientific name	Gram	vegetative/spore
Cobetia marina	**-**	**veg**
Pseudomonas aeruginosa	**-**	**veg**
Escherichia coli	**-**	**veg**
Streptococcus mutans	**+**	**veg**
Staphylococcus aureus	**+**	**veg**
Staphylococcus epidermidis	**+**	**veg**
Bacillus cereus	**+**	**both**
Bacillus atrophaeus	**+**	**both**
Klebsiella pneumoniae	**-**	**veg**
Enterococcus sp	**+**	**veg**
Bacillus anthracis (Sterne)	**+**	**spore**
Clostridium difficile	**+**	**both**

Plating and colony-counting of exposed bacterial samples would strongly supplement the CLSM and flow cytometry analyses. Minimum inhibitory concentration testing results could be correlated to the concentrations and applications used in clinical situations to determine what concentrations are adequate to kill the given pathogens.

Future Directions—Longer Term

Molecular design for specific applications

The fact that a number of the CPE compounds are high molecular weight polymers with a proven surface attachment protocol (167) suggests that they may be practical and robust as coatings for medical devices, fabrics, surfaces used for food preparation, bandages, filter elements and other components. Having an immobilized antimicrobial coating could reduce the incidence of microbial transfer on doorknobs, countertops and other fomites. Applications for these types of compounds may be extensive (Table 8-3), especially if they are found to be environmentally stable and benign to mammalian species.

To further these ends, the material properties of the beads and of the CPE coatings, including the molecular weight, charge per repeat unit, pendant functional groups and method of attachment/immobilization can potentially be adjusted to maximize the activity and robustness for real world use.

With the controlled formation of extended structures such as monolayers, multilayers, vesicles, surface coatings on fibers and planar substrates, etc., these materials may make viable, adjustable and stable components for macroscale biocidal systems and even for nanotechnological devices such as biosensors. These products and applications would culminate the search for the practical, functional, non-leaching and potentially selective biocidal components described in Chapter 1.

Table 8-3. Potential Uses for Antimicrobial CPEs

Non-leaching coatings for:
Surgical instruments
Catheters
Countertops
Bandages/sterile dressings
Bedding (sheets, mattress covers, pillow cases)
Surgical furniture/dividers/curtains
Orthopedic prostheses
Filter elements
Recoverable bacterial absorbents (by filtration or magnetic components) in the form of coated beads or other suitable substrates
Separation membranes for bacterial exclusion/extraction/immobilization
Disposal bags for biological waste
Could also be incorporated into:
Paints
Sealants
Coagulants/Flocculants
Device components (via casting or electrospinning)
Electrospun fibers for woven fabrics/filters
Biosensors

There is also tremendous potential for combining these compounds into new forms (such as the LbL capsules in Chapter 5) or incorporating them into applications such as drug delivery (one of the motivations for research on LbL constructs) or direct use as topical disinfectants or even internally active pharmaceuticals. (Although a great deal of work would obviously have to be done before the latter uses might be realized.)

Matching the design of these complexes to new substrates could also enhance their utility for certain applications. For example, beads with superparamagnetic centers are another type of substrate that may be considered as a support. These might afford the means to manipulate, isolate or otherwise alter the position or activity of CPE-grafted particles in solution or on surfaces. Ideally, this avenue of inquiry might yield a system that may be used, for example, to treat contaminated water sources by dispersing them into the water and magnetically removing them at the end of such a treatment process, minimizing loss and perhaps allowing them to be cleaned and reused.

Surface morphology

Effects of surface morphology, which have been found to be important for microbial attachment and propagation, can also be explored by changing bead sizes and solution concentration, grafting oligomers or polymers of mixed lengths, creating textured materials using electrospun fibers or by applying the polymer as a film on various patterned surfaces.

Other types of bacterial studies

Isolation of any surviving bacteria could also contribute to the identification of mutant strains that could then be screened for susceptibility to other biocides and antibiotics to determine antimicrobial resistance/susceptibility traits. Spores, viruses,

fungi, protozoa and other pathogens might also be evaluated, if an intrepid graduate student is found who is able to culture them and find a working protocol for analysis…

References

1. Accuri_Cytometers: C6 Flow Cytometer Instruction Manual. ver. 1.32, rev. A, 2008.
2. Alakomi, H-L, Paananen, A, Suihko, M-L, Helander, IM & Saarela, M: Weakening Effect of Cell Permeabilizers on Gram-Negative Bacteria Causing Biodeterioration. *Applied and Environmental Microbiology,* 72**:** 4695-4703, 2006.
3. Alam, AR, Rhoades, AM, Elasri, MO & Wicks, DA: Impact of surfactant structure on biocide efficacy. *Abstracts of Papers American Chemical Society,* 229**:** U541, 2005.
4. Alberts, B, Johnson, A, Lewis, J & al., e: *Molecular Biology of the Cell,* New York, Garland Science 2002.
5. Alekshun, MN & Levy, SB: Molecular mechanisms of antibacterial multidrug resistance. *Cell,* 128**:** 1037-1050, 2007.
6. Allegra, S, Berger, F, Berthelot, P, Grattard, F, Pozzetto, B & Riffard, S: Use of Flow Cytometry To Monitor Legionella Viability. *Applied and Environmental Microbiology,* 74**:** 7813-7816, 2008.
7. Alvarez-Barrientos, A, Arroyo, J, Canton, R, Nombela, C & Sanchez-Perez, M: Applications of flow cytometry to clinical microbiology. *Clinical Microbiology Reviews,* 13**:** 167-+, 2000.
8. Andresen, M, Stenstad, P, Moretro, T, Langsrud, S, Syverud, K, Johansson, LS & Stenius, P: Nonleaching antimicrobial films prepared from surface-modified microfibrillated cellulose. *Biomacromolecules,* 8**:** 2149-2155, 2007.
9. Antipov, AA, Shchukin, D, Fedutik, Y, Petrov, AI, Sukhorukov, GB & Mohwald, H: Carbonate microparticles for hollow polyelectrolyte capsules fabrication. *Colloids and Surfaces a-Physicochemical and Engineering Aspects,* 224**:** 175-183, 2003.
10. Antipov, AA & Sukhorukov, GB: Polyelectrolyte multilayer capsules as vehicles with tunable permeability. *Advances in Colloid and Interface Science,* 111**:** 49-61, 2004.
11. Arcidiacono, S, Mello, CM & Senecal, K: Incorporation of antimicrobial peptides into polymeric films and coatings. *Abstracts of the General Meeting of the American Society for Microbiology,* 103**:** A-020, 2003.
12. Arciola, CR: Opportunistic bacteria in implant infections - Knowing them to plan their control. *International Journal of Artificial Organs,* 29**:** 341-342, 2006.
13. Babayan, A & Nikaido, H: In Pseudomonas aeruginosa ethidium bromide does not induce its own degradation or the assembly of pumps involved in its efflux. *Biochemical and Biophysical Research Communications,* 324**:** 1065-1068, 2004.
14. Baciu, M, Sebai, SC, Ces, O, Mulet, X, Clarke, JA, Shearman, GC, Law, RV, Templer, RH, Plisson, C, Parker, CA & Gee, A: Degradative transport of cationic amphiphilic drugs across phospholipid bilayers. *Philosophical Transactions of the Royal Society a-Mathematical Physical and Engineering Sciences,* 364**:** 2597-2614, 2006.
15. Baier, J, Maisch, T, Maier, M, Engel, E, Landthaler, M & Baumler, W: Singlet oxygen generation by UVA light exposure of endogenous photosensitizers. *Biophysical Journal,* 91**:** 1452-1459, 2006.

16. Banin, E, Brady, KM & Greenberg, EP: Chelator-induced dispersal and killing of Pseudomonas aeruginosa cells in a biofilm. *Applied and Environmental Microbiology,* 72**:** 2064-2069, 2006.
17. Bar, W, Bade-Schumann, U, Krebs, A & Cromme, L: Rapid method for detection of minimal bactericidal concentration of antibiotics. *Journal of Microbiological Methods,* 77**:** 85-89, 2009.
18. Barbeau, J, Gauthier, C & Payment, P: Biofilms, infectious agents, and dental unit waterlines: A review. *Canadian Journal of Microbiology,* 44**:** 1019-1028, 1998.
19. Bashford, CL, Alder, GM & Pasternak, CA: Fluctuation of surface charge in membrane pores. *Biophysical Journal,* 82**:** 2032-2040, 2002.
20. Berg, MC, Zhai, L, Cohen, RE & Rubner, MF: Controlled drug release from porous polyelectrolyte multilayers. *Biomacromolecules,* 7**:** 357-364, 2006.
21. Bjarnsholt, T, Kirketerp-Moller, K, Kristiansen, S, Phipps, R, Nielsen, AK, Jensen, PO, Hoiby, N & Givskov, M: Silver against Pseudomonas aeruginosa biofilms. *Apmis,* 115**:** 921-928, 2007.
22. Bjergbaek, LA & Roslev, P: Formation of nonculturable Escherichia coli in drinking water. *Journal of Applied Microbiology,* 99**:** 1090-1098, 2005.
23. Black, JG: *Microbiology-Principles and Applications,* Upper Saddle River, New Jersey, Prentice Hall 1996.
24. Blaser, SA, Scheringer, M, MacLeod, M & Hungerbuhler, K: Estimation of cumulative aquatic exposure and risk due to silver: Contribution of nano-functionalized plastics and textiles. *Science of the Total Environment,* 390**:** 396-409, 2008.
25. Bloomfield, SF, Stewart, G, Dodd, CER, Booth, IR & Power, EGM: The viable but non-culturable phenomenon explained? *Microbiology-Uk,* 144**:** 1-3, 1998.
26. Blot, S: Limiting the attributable mortality of nosocomial infection and multidrug resistance in intensive care units. *Clinical Microbiology and Infection,* 14**:** 5-13, 2008.
27. Botes, M & Cloete, TE: The potential of nanofibers and nanobiocides in water purification. *Critical Reviews in Microbiology,* 36**:** 68-81, 2010.
28. Bouhdid, S, Abrini, J, Zhiri, A, Espuny, MJ & Manresa, A: Investigation of functional and morphological changes in Pseudomonas aeruginosa and Staphylococcus aureus cells induced by Origanum compactum essential oil. *Journal of Applied Microbiology,* 106**:** 1558-1568, 2009.
29. Brunt, KD & Thompson, SM: Surface bioactivation by silver ions. *Advances in Coating Technology***:** 35/1-35/18, 1998.
30. Bryers, JD: Medical biofilms. *Biotechnol. Bioeng.,* 100**:** 1-18, 2008.
31. Burrows, LL & Khoury, AE: Issues surrounding the prevention and management of device-related infections. *World Journal of Urology,* 17**:** 402-409, 1999.
32. Campanac, C, Pineau, L, Payard, A, Baziard-Mouysset, G & Roques, C: Interactions between biocide cationic agents and bacterial biofilms. *Antimicrobial Agents and Chemotherapy,* 46**:** 1469-1474, 2002.
33. Casey, DR, Sebai, SC, Shearman, GC, Ces, O, Law, RV, Templer, RH & Gee, AD: Formulation affects the rate of membrane degradation catalyzed by cationic amphiphilic drugs. *Industrial & Engineering Chemistry Research,* 47**:** 650-655, 2008.

34. Cen, L, Neoh, KG & Kang, ET: Surface functionalization technique for conferring antibacterial properties to polymeric and cellulosic surfaces. *Langmuir,* 19**:** 10295-10303, 2003.
35. Cheeseman, KE, Denyer, SP, Hosein, IK, Williams, GJ & Maillard, JY: Evaluation of the bactericidal efficacy of three different alcohol hand rubs against 57 clinical isolates of S-aureus. *Journal of Hospital Infection,* 72**:** 319-325, 2009.
36. Chemburu, S, Corbitt, TS, Ista, LK, Ji, E, Fulghum, J, Lopez, GP, Ogawa, K, Schanze, KS & Whitten, DG: Light-Induced Biocidal Action of Conjugated Polyelectrolytes Supported on Colloids. *Langmuir***:** 11053-11062, 2008.
37. Chemburu, S, Corbitt, TS, Ista, LK, Ji, E, Fulghum, J, Lopez, GP, Ogawa, K, Schanze, KS & Whitten, DG: Light-induced biocidal action of conjugated polyelectrolytes supported on colloids. *Langmuir,* 24**:** 11053-11062, 2008.
38. Chemburu, S, Ji, E, Casana, Y, Wu, Y, Buranda, T, Schanze, KS, Lopez, GP & Whitten, DG: Conjugated Polyelectrolyte Supported Bead Based Assays for Phospholipase A(2) Activity. *Journal of Physical Chemistry B,* 112**:** 14492-14499, 2008.
39. Chen, CZ, Beck-Tan, NC, Dhurjati, P, Dyk, TKV, LaRossa, RA & Cooper, SL: Quaternary ammonium functionalized poly(propyleneimine) dendrimers as effective antimicrobials. *Biomacromolecules,* 1**:** 473-480, 2000.
40. Chen, LH, McBranch, DW, Wang, HL, Helgeson, R, Wudl, F & Whitten, DG: Highly sensitive biological and chemical sensors based on reversible fluorescence quenching in a conjugated polymer. *Proceedings of the National Academy of Sciences of the United States of America,* 96**:** 12287-12292, 1999.
41. Cloete, TE: Resistance mechanisms of bacteria to antimicrobial compounds. *International Biodeterioration & Biodegradation,* 51**:** 277-282, 2003.
42. Codling, CE, Maillard, J-Y & Russell, AD: Aspects of the antimicrobial mechanisms of action of a polyquaternium and an amidoamine. *Journal of Antimicrobial Chemotherapy,* 51**:** 1153-1158, 2003.
43. Collins, TJ, Banerjee, D, Khetan, SK & Yano, T: Abstracts of Papers. *226th National Meeting of the American Chemical Society.* New York, American Chemical Society: Washington, DC, 2003 pp IEC-158.
44. Cooke, RPD: Hazards of water. *Journal of Hospital Infection,* 57**:** 290-293, 2004.
45. Corbitt, TS, Ding, L, Ji, E, Ista, LK, Ogawa, K, Lopez, GP, Schanze, KS & Whitten, DG: Light and Dark Biocidal Activity of Cationic Poly(arylene ethylene) Conjugated Polyelectrolytes. *Photochem. Photobiol. Sci.***:** 998-1005, 2009.
46. Corbitt, TS, Ding, LP, Ji, EY, Ista, LK, Ogawa, K, Lopez, GP, Schanze, KS & Whitten, DG: Light and dark biocidal activity of cationic poly(arylene ethynylene) conjugated polyelectrolytes. *Photochemical & Photobiological Sciences,* 8**:** 998-1005, 2009.
47. Corbitt, TS, Sommer, JR, Chemburu, S, Ogawa, K, Ista, LK, Lopez, GP, Whitten, DG & Schanze, KS: Conjugated Polyelectrolyte Capsules: Light-Activated Antimicrobial Micro "Roach Motels". *ACS Applied Materials & Interfaces,* 1**:** 48-52, 2009.
48. Cosa, G, Focsaneanu, KS, McLean, JRN, McNamee, JP & Scaiano, JC: Photophysical properties of fluorescent DNA-dyes bound to single- and double-

stranded DNA in aqueous buffered solution. *Photochemistry and Photobiology,* 73**:** 585-599, 2001.
49. Costerton, JW: The role of bacterial exopolysaccharides in nature and disease (Originally published in Developments in Industrial Microbiology, volume 26, pages 249-261). *Journal of Industrial Microbiology and Biotechnology,* 22**:** 551-563, 1999.
50. Coulter, WH: *Method for Electronically Determining Particle Sizes,* 1952.
51. Cucci, TL & Sieracki, ME: Effects of mismatched refractive indices in aquatic flow cytometry. *Cytometry,* 44**:** 173-178, 2001.
52. De Geest, BG, Sanders, NN, Sukhorukov, GB, Demeester, J & De Smedt, SC: Release mechanisms for polyelectrolyte capsules. *Chemical Society Reviews,* 36**:** 636-649, 2007.
53. DeQueiroz, GA & Day, DF: Disinfection of Bacillus subtilis spore-contaminated surface materials with a sodium hypochlorite and a hydrogen peroxide-based sanitizer. *Letters in Applied Microbiology,* 46**:** 176-180, 2008.
54. Ding, LP, Chi, EY, Chemburu, S, Ji, E, Schanze, KS, Lopez, GP & Whitten, DG: Insight into the Mechanism of Antimicrobial Poly(phenylene ethynylene) Polyelectrolytes: Interactions with Phosphatidylglycerol Lipid Membranes. *Langmuir,* 25**:** 13742-13751, 2009.
55. Donelli, G, Francolini, I, Piozzi, A, Di Rosa, R & Marconi, W: New polymer-antibiotic systems to inhibit bacterial biofilm formation: A suitable approach to prevent central venous catheter-associated infections. *Journal of Chemotherapy,* 14**:** 501-507, 2002.
56. Farley, RT: Dissertation. Gainesville, Florida, University of Florida, 2007.
57. Ficici, SE, Durmaz, G, Ilhan, S, Akgun, Y & Kosgeroglu, N: Bactericidal effects of commonly used antiseptics/disinfectans against nosocomial pathogens and relationship between antibacterial and biocide resistance. *Mikrobiyoloji Bulteni,* 36**:** 259-269, 2002.
58. Flors, C, Fryer, MJ, Waring, J, Reeder, B, Bechtold, U, Mullineaux, PM, Nonell, S, Wilson, MT & Baker, NR: Imaging the production of singlet oxygen in vivo using a new fluorescent sensor, Singlet Oxygen Sensor Green□. *Journal of Experimental Botany,* 57**:** 1725–1734, 2006.
59. Fulwyler, MJ: AN ELECTRONIC PARTICLE SEPARATOR WITH POTENTIAL BIOLOGICAL APPLICATION. *Science,* 150**:** 371-&, 1965.
60. Fulwyler, MJ: ELECTRONIC SEPARATION OF BIOLOGICAL CELLS BY VOLUME. *Science,* 150**:** 910-&, 1965.
61. Funston, AM, Silverman, EE, Schanze, KS & Miller, JR: Spectroscopy and transport of the triplet exciton in a terthiophene end-capped poly(phenylene ethynylene). *Journal of Physical Chemistry B,* 110**:** 17736-17742, 2006.
62. Fuster-Valls, N, Hernadez-Herrero, M, Marin-De-Mateo, M & Rodriguez-Jerez, JJ: Effect of different environmental conditions on the bacteria survival on stainless steel surfaces. *Food Control,* 19**:** 308-314, 2008.
63. Fux, CA, Costerton, JW, Stewart, PS & Stoodley, P: Survival strategies of infectious biofilms. *Trends in Microbiology,* 13**:** 34-40, 2005.
64. Gabriel, GJ, Pool, JG, Som, A, Dabkowski, JM, Coughlin, EB, Muthukurnar, M & Tew, GN: Interactions between Antimicrobial Polynorbornenes and Phospholipid

Vesicles Monitored by Light Scattering and Microcalorimetry. *Langmuir,* 24**:** 12489-12495, 2008.
65. Gabriel, GJ, Som, A, Madkour, AE, Eren, T & Tew, GN: Infectious disease: Connecting innate immunity to biocidal polymers. *Materials Science & Engineering R-Reports,* 57**:** 28-64, 2007.
66. Gabriel, GJ & Tew, GN: Conformationally Rigid Proteomimetics: A Case Study in Designing Antimicrobial Aryl Oligomers. *Org. Biomol. Chem.***:** 417–423, 2008.
67. Garcia-De-Lomas, J, Lerma, M, Cebrian, L, Esteban, E, Gimenez, MJ, Aguilar, L, Dominguez, V & Randez, JJ: Evaluation of the in-vitro cidal activity and toxicity of a novel peroxygen biocide: 2-butanone peroxide. *Journal of Hospital Infection,* 68**:** 248-254, 2008.
68. Garg, S, Zaneveld, LJD, Anderson, RA, Jr. & Waller, DP: Compositions and methods for trapping and inactivating pathogenic microbes and spermatozoa. Rush-Presbyterian-St. Luke's Medical Center, 2004.
69. Goebbert, C, Schichtel, M & Nonninger, R: Disinfectant coatings Ag/TiO2 nanoparticles as biocides. *Farbe und Lack,* 108**:** 20-25, 2002.
70. Göhde, W: USE OF FLOW CUVETTES FOR EVALUATING DENSITY GRADIENTS IN PREPARATIVE ULTRACENTRIFUGATION. *Zeitschrift Fur Naturforschung Part B-Chemie Biochemie Biophysik Biologie Und Verwandten Gebiete,* B 24**:** 250-&, 1969.
71. Grapski, JA & Cooper, SL: Synthesis and characterization of non-leaching biocidal polyurethanes. *Biomaterials,* 22**:** 2239-2246, 2001.
72. Gucker, FT, Okonski, CT, Pickard, HB & Pitts, JN: A PHOTOELECTRONIC COUNTER FOR COLLOIDAL PARTICLES. *Journal of the American Chemical Society,* 69**:** 2422-2431, 1947.
73. Gucker, FT, Pickard, HB & Okonski, CT: A PHOTOELECTRIC INSTRUMENT FOR COMPARING THE CONCENTRATIONS OF VERY DILUTE AEROSOLS, AND MEASURING LOW LIGHT INTENSITIES. *Journal of the American Chemical Society,* 69**:** 429-438, 1947.
74. Guerin-Mechin, L, Dubois-Brissonnet, F, Heyd, B & Leveau, JY: Quaternary Ammonium Compound stresses induce specific variations in fatty acid composition of Pseudomonas aeruginosa. *International Journal of Food Microbiology,* 55**:** 157-159, 2000.
75. Hall-Stoodley, L, Costerton, WJ & Stoodley, P: Bacterial biofilms: from the natural environment to infectious diseases. *Nature Reviews,* 2**:** 95-108, 2004.
76. Hamouda, T & J. R. Baker, J: Antimicrobial mechanism of action of surfactant lipid preparations. *Journal of Applied Microbiology,* 89**:** 397-403, 2000.
77. Hazziza-Laskar, J, Helary, G & Sauvet, G: Biocidal polymers active by contact. 4. Polyurethanes based on polysiloxanes with pendant primary alcohols and quaternary ammonium groups. *Journal of Applied Polymer Science,* 58**:** 77-84, 1995.
78. Henning, J, Muller, F & Peggau, J: Cationic and anionic surfactants - compatabilities.. *SOFW Journal,* 127**:** 30-35, 2001.
79. Hetrick, EM & Schoenfisch, MH: Reducing implant-related infections: active release strategies. *Chemical Society Reviews,* 35**:** 780-789, 2006.

80. Heydorn, A, Nielsen, AT, Hentzer, M, Sternberg, C, Givskov, M, Ersboll, BK & Molin, S: Quantification of biofilm structures by the novel computer program COMSTAT. *Microbiology-Uk,* 146**:** 2395-2407, 2000.
81. Hill, E, Evans, D & Whitten, DG: Modeling of CPEs with GAUSSIAN. unpublished, 2010.
82. Hirahara, Y, Ueno, H & Nakamuro, K: Aqueous photodegradation of fenthion by ultraviolet B irradiation: contribution of singlet oxygen in photodegradation and photochemical hydrolysis. *Water Research,* 37**:** 468-476, 2003.
83. Ho, HA, Najari, A & Leclerc, M: Optical detection of DNA and proteins moth cationic polythiophenes. *Accounts of Chemical Research,* 41**:** 168-178, 2008.
84. Hoskisson, PA & Hobbs, G: Continuous culture - making a comeback? *Microbiology,* 151**:** 3153-3159, 2005.
85. Huang, JY, Koepsel, RR, Murata, H, Wu, W, Lee, SB, Kowalewski, T, Russell, AJ & Matyjaszewski, K: Nonleaching antibacterial glass surfaces via "Grafting Onto": The effect of the number of quaternary ammonium groups on biocidal activity. *Langmuir,* 24**:** 6785-6795, 2008.
86. Ibrahim, MK, Kamel, AI, Abou Shady, MR & Afyfy, HI: Role of Pseudomonas aeruginosa and Klebsiella pneumoniae in nosocomial infections and their susceptibility to antibiotics and disinfectants. *Egyptian Journal of Microbiology,* 34**:** 645-657, 1999.
87. Ignatova, M, Labaye, D, Lenoir, S, Strivay, D, Jerome, R & Jerome, C: Immobilization of silver in polypyrrole/polyanion composite coatings: Preparation, characterization, and antibacterial activity. *Langmuir,* 19**:** 8971-8979, 2003.
88. Impellitteri, CA, Tolaymat, TM & Scheckel, KG: The Speciation of Silver Nanoparticles in Antimicrobial Fabric Before and After Exposure to a Hypochlorite/Detergent Solution. *Journal of Environmental Quality,* 38**:** 1528-1530, 2009.
89. Ista, LK, Perez-Luna, VH & Lopez, GP: Surface-grafted, environmentally sensitive polymers for biofilm release. *Applied and Environmental Microbiology,* 65**:** 1603-1609, 1999.
90. Jiang, H, Zhao, XY, Shelton, AH, Lee, SH, Reynolds, JR & Schanze, KS: Variable-Band-Gap Poly(arylene ethynylene) Conjugated Polyelectrolytes Adsorbed on Nanocrystalline TiO2: Photocurrent Efficiency as a Function of the Band Gap. *ACS Applied Materials & Interfaces,* 1**:** 381-387, 2009.
91. Johnston, MD, Hanlon, GW, Denyer, SP & Lambert, RJW: Membrane damage to bacteria caused by single and combined biocides. *Journal of Applied Microbiology,* 94**:** 1015-1023, 2003.
92. Jones, G, Jackson, WR, Kanoktanaporn, S & Bergmark, WR: PHOTOPHYSICAL AND PHOTOCHEMICAL PROPERTIES OF COUMARIN DYES IN AMPHIPHILIC MEDIA. *Photochemistry and Photobiology,* 42**:** 477-483, 1985.
93. Kamentsky, LM, Melamed, MR & Derman, H: SPECTROPHOTOMETER - NEW INSTRUMENT FOR ULTRARAPID CELL ANALYSIS. *Science,* 150**:** 630-&, 1965.
94. Kang, S, Pinault, M, Pfefferle, LD & Elimelech, M: Single-walled carbon nanotubes exhibit strong antimicrobial activity. *Langmuir,* 23**:** 8670-8673, 2007.

95. Kato, N, Schuetz, P, Fery, A & Caruso, F: Thin multilayer films of weak polyelectrolytes on colloid particles. *Macromolecules,* 35**:** 9780-9787, 2002.
96. Kenawy, ER, Worley, SD & Broughton, R: The chemistry and applications of antimicrobial polymers: A state-of-the-art review. *Biomacromolecules,* 8**:** 1359-1384, 2007.
97. Kersters, K: The genus *Deleya*. In: *The Prokaryotes.* edited by BALOWS, A., TRUPER, H. G., DWORKIN, M., HARDER, W. & SCHLEIFER, K. H., New York, Springer Verlag, 1992, pp 3189-3197.
98. Koper, OB, Klabunde, JS, Marchin, GL, Klabunde, KJ, Stoimenov, P & Bohra, L: Nanoscale powders and formulations with biocidal activity towards spores and begetative cells of Bacillus species, viruses and toxins. *Current Microbiology,* 44**:** 49-55, 2002.
99. Krishnan, S, Ober, CK, Lee, KL, Angert, ER, Hexemer, A & Kramer, EJ: Antibacterial coatings based on quaternized poly(4-vinylpyridine) block copolymers. *Abstracts of Papers American Chemical Society,* 228**:** U496, 2004.
100. Kugler, R, Bouloussa, O & Rondelez, F: Evidence of a charge-density threshold for optimum efficiency of biocidal cationic surfaces. *Microbiology,* 151**:** 1341-1348, 2005.
101. Kugler, R, Bouloussa, O & Rondelez, F: Evidence of a charge-density threshold for optimum efficiency of biocidal cationic surfaces. *Microbiology-Sgm,* 151**:** 1341-1348, 2005.
102. Kumar, R & Muenstedt, H: Silver ion release from antimicrobial polyamide/silver composites. *Biomaterials,* 26**:** 2081-2088, 2005.
103. Kurt, P, Wood, L, Ohman, DE & Wynne, KJ: Highly effective contact antimicrobial surfaces via polymer surface modifiers. *Langmuir,* 23**:** 4719-4723, 2007.
104. Kwon, DH & Lu, CD: Polyamines increase antibiotic susceptibility in Pseudomonas aeruginosa. *Antimicrobial Agents and Chemotherapy,* 50**:** 1623-1627, 2006.
105. Lam, KLH, Ishitsuka, Y, Cheng, YS, Chien, K, Waring, AJ, Lehrer, RI & Lee, KYC: Mechanism of supported membrane disruption by antimicrobial peptide protegrin-1. *Journal of Physical Chemistry B,* 110**:** 21282-21286, 2006.
106. Lambert, RJW, Graf, JF & Sedlak, RI: Antimicrobial resistance and cross-resistance in several bacterial species between 1989 and 2000. *Abstracts of the Interscience Conference on Antimicrobial Agents and Chemotherapy,* 42**:** 103, 2002.
107. Lambert, RJW & Johnston, MD: The effect of interfering substances on the disinfection process: A mathematical model. *Journal of Applied Microbiology,* 91**:** 548-555, 2001.
108. Lambert, RJW, Joynson, J & Forbes, B: The relationships and susceptibilities of some industrial, laboratory and clinical isolates of Pseudomonas aeruginosa to some antibiotics and biocides. *Journal of Applied Microbiology,* 91**:** 972-984, 2001.
109. Lamberts, JJM, Schumacher, DR & Neckers, DC: Novel Rose-Bengal Derivatives - Synthesis and Quantum Yield Studies. *Journal of the American Chemical Society,* 106**:** 5879-5883, 1984.
110. Landa-Solis, C, Gonzalez-Espinosa, D, Guzman-Soriano, B, Snyder, M, Reyes-Teran, G, Torres, K & Gutierrez, AA: Microcyn (TM): a novel super-oxidized

water with neutral pH and disinfectant activity. *Journal of Hospital Infection,* 61**:** 291-299, 2005.
111. Laopaiboon, L, Hall, SJ & Smith, RN: The effect of a quaternary ammonium biocide on the performance and characteristics of laboratory-scale rotating biological contactors. *Journal of Applied Microbiology,* 93**:** 1051-1058, 2002.
112. Lear, JC, Maillard, JY, Dettmar, PW, Goddard, PA & Russell, AD: Chloroxylenol- and triclosan-tolerant bacteria from industrial sources - susceptibility to antibiotics and other biocides. *International Biodeterioration & Biodegradation,* 57**:** 51-56, 2006.
113. Lee, SB, Koepsel, RR, Morley, SW, Matyjaszewski, K, Sun, YJ & Russell, AJ: Permanent, nonleaching antibacterial surfaces. 1. Synthesis by atom transfer radical polymerization. *Biomacromolecules,* 5**:** 877-882, 2004.
114. Lenoir, S, Pagnoulle, C, Galleni, M, Compere, P, Jerome, R & Detrembleur, C: Polyolefin matrixes with permanent antibacterial activity: Preparation, antibacterial activity, and action mode of the active species. *Biomacromolecules,* 7**:** 2291-2296, 2006.
115. Lenoir, S, Pagnoulle, C, Galleni, M, Compere, P, Jerome, R & Detrembleur, C: Polyolefin Matrixes with Permanent Antibacterial Activity: Preparation, Antibacterial Activity, and Action Mode of the Active Species. *Biomacromolecules***:** 2291-2296, 2006.
116. Lepecq, JB & Paoletti, C: A FLUORESCENT COMPLEX BETWEEN ETHIDIUM BROMIDE AND NUCLEIC ACIDS - PHYSICAL-CHEMICAL CHARACTERIZATION. *Journal of Molecular Biology,* 27**:** 87-&, 1967.
117. Lewis, K & Klibanov, AM: Surpassing nature: rational design of sterile-surface materials. *Trends in Biotechnology,* 23**:** 343-348, 2005.
118. Lichter, JA & Rubner, MF: Polyelectrolyte Multilayers with Intrinsic Antimicrobial Functionality: The Importance of Mobile Polycations. *Langmuir,* 25**:** 7686-7694, 2009.
119. Lichter, JA, Van Vliet, KJ & Rubner, MF: Design of Antibacterial Surfaces and Interfaces: Polyelectrolyte Multilayers as a Multifunctional Platform. *Macromolecules,* 42**:** 8573-8586, 2009.
120. Lin, J, Murthy, SK, Olsen, BD, Gleason, KK & Klibanov, AM: Making thin polymeric materials, including fabrics, microbicidal and also water-repellent. *Biotechnology Letters,* 25**:** 1661-1665, 2003.
121. Lin, J, Qiu, SY, Lewis, K & Klibanov, AM: Bactericidal properties of flat surfaces and nanoparticles derivatized with alkylated polyethylenimines. *Biotechnology Progress,* 18**:** 1082-1086, 2002.
122. Lin, J, Qiu, SY, Lewis, K & Klibanov, AM: Mechanism of bactericidal and fungicidal activities of textiles covalently modified with alkylated polyethylenimine. *Biotechnology and Bioengineering,* 83**:** 168-172, 2003.
123. Lithner, D, Damberg, J, Dave, G & Larsson, A: Leachates from plastic consumer products - Screening for toxicity with Daphnia magna. *Chemosphere,* 74**:** 1195-1200, 2009.
124. Liu, B & Bazan, GC: Homogeneous fluorescence-based DNA detection with water-soluble conjugated polymers. *Chemistry of Materials,* 16**:** 4467-4476, 2004.

125. Loughlin, MF, Jones, MV & Lambert, PA: Pseudomonas aeruginosa cells adapted to benzalkonium chloride show resistance to other membrane-active agents but not to clinically relevant antibiotics. *Journal of Antimicrobial Chemotherapy,* 49**:** 631-639, 2002.
126. Lu, LD, Rininsland, FH, Wittenburg, SK, Achyuthan, KE, McBranch, DW & Whitten, DG: Biocidal activity of a light-absorbing fluorescent conjugated polyelectrolyte. *Langmuir,* 21**:** 10154-10159, 2005.
127. Lucio, M, Ferreira, H, Lima, J & Reis, S: Use of liposomes as membrane models to evaluate the contribution of drug-membrane interactions to antioxidant properties of etodolac. *Redox Report,* 13**:** 225-236, 2008.
128. Madkour, AE & Tew, GN: Perspective - Towards self-sterilizing medical devices: controlling infection. *Polymer International,* 57**:** 6-10, 2008.
129. Maeyama, R, Kwon, IIK, Mizunoe, Y, Anderson, JM, Tanaka, M & Matsuda, T: Novel bactericidal surface: Catechin-loaded surface-erodible polymer prevents biofilm formation. *Journal of Biomedical Materials Research,* 75A**:** 146-155, 2005.
130. Maillard, J-Y: Bacterial target sites for biocide action. *Society for Applied Microbiology Symposium Series,* 31**:** 16S-21S, 2002.
131. Maillard, J-Y: Antimicrobial biocides in the healthcare environment: efficacy, usage, policies, and perceived problems. *Therapeutics and Clinical Risk Management,* 1**:** 307-320, 2005.
132. Maillard, JY: Bacterial resistance to biocides in the healthcare environment: should it be of genuine concern? *Journal of Hospital Infection,* 65**:** 60-72, 2007.
133. Maisch, T, Baier, J, Franz, B, Maier, M, Landthaler, M, Szeimies, RM & Baumler, W: The role of singlet oxygen and oxygen concentration in photodynamic inactivation of bacteria. *Proceedings of the National Academy of Sciences of the United States of America,* 104**:** 7223-7228, 2007.
134. Maisch, T, Bosl, C, Szeimies, RM, Lehn, N & Abels, C: Photodynamic effects of novel XF porphyrin derivatives on prokaryotic and eukaryotic cells. *Antimicrobial Agents and Chemotherapy,* 49**:** 1542-1552, 2005.
135. Maisch, T, Franz, B, Baier, J, Maier, M, Landthaler, M, Szeimies, R & Baumler, W: Investigation of photodynamic inactivation of bacteria using the detection of singlet oxygen luminescence. *Experimental Dermatology,* 15**:** 230-230, 2006.
136. Maisch, T, Szeimies, RM, Jori, G & Abels, C: Antibacterial photodynamic therapy in dermatology. *Photochemical & Photobiological Sciences,* 3**:** 907-917, 2004.
137. Makal, U, Wood, L, Ohman, DE & Wynne, KJ: Polyurethane biocidal polymeric surface modifiers. *Biomaterials,* 27**:** 1316-1326, 2006.
138. Malik, Z, Hanania, J & Nitzan, Y: Bactericidal Effects of Photoactivated Porphyrins - an Alternative Approach to Antimicrobial Drugs. *Journal of Photochemistry and Photobiology B-Biology,* 5**:** 281-293, 1990.
139. Maltsev, VP: Scanning flow Cytometry for advanced analysis of cells. *Cytometry***:** 124-125, 2002.
140. Mandeville, R, Kournikakis, B, Brousseau, P & Richard, L: Use of tetramisole and its derivatives against spore-producing microorganisms. *PCT Int. Appl.,* 2003.
141. Mantareva, V, Angelov, I, Kussovski, V, Woehrle, D & Dimitrov, S: METALLOPHTHALOCYANINES AS PHOTODYNAMIC SENSITIZERS

FOR TREATMENT OF PATHOGENIC BACTERIA. SYNTHESIS AND SINGLET OXYGEN FORMATION. *Comptes Rendus De L Academie Bulgare Des Sciences,* 62**:** 1521-1526, 2009.
142. Marini, M, De Niederhausern, S, Iseppi, R, Bondi, M, Sabia, C, Toselli, M & Pilati, F: Antibacterial activity of plastics coated with silver-doped organic-inorganic hybrid coatings prepared by sol-gel processes. *Biomacromolecules,* 8**:** 1246-1254, 2007.
143. Marshall, BM & McMurry, LM: Biocides and resistance. In: *Frontiers in Antimicrobial Resistance: A Tribute to Stuart B. Levy.* 2005, pp 174-190.
144. Martens, ACM, Vandenengh, GJ & Hagenbeek, A: THE FLUORESCENCE INTENSITY OF PROPIDIUM IODIDE BOUND TO DNA DEPENDS ON THE CONCENTRATION OF SODIUM-CHLORIDE. *Cytometry,* 2**:** 24-25, 1981.
145. Martin, DJH, Denyer, SP, McDonnell, G & Maillard, JY: Resistance and cross-resistance to oxidising agents of bacterial isolates from endoscope washer disinfectors. *Journal of Hospital Infection,* 69**:** 377-383, 2008.
146. Martin, JC: The Basics of Flow Cytometry. *32nd Annual Flow Cytometry Course.* University of New Mexico, Albuquerque, NM, 2009 pp 27.
147. Mason, DJ & Gant, VA: THE APPLICATION OF FLOW-CYTOMETRY TO THE ESTIMATION OF BACTERIAL ANTIBIOTIC SUSCEPTIBILITY. *Journal of Antimicrobial Chemotherapy,* 36**:** 441-443, 1995.
148. Mathai, S, Smith, TA & Ghiggino, KP: Singlet oxygen quantum yields of potential porphyrin-based photosensitisers for photodynamic therapy. *Photochemical & Photobiological Sciences,* 6**:** 995-1002, 2007.
149. Matyjaszewski, K, Huang, J, Wu, W, Kowalewski, T, Koepsel, RR, Russell, AD, Lee, SB & Murata, H: Non-leaching Antibacterial Glass Surfaces via Grafting onto: the Effects of Number of QA on Biocidal Activity. *Langmuir,* in press, 2008.
150. McQuade, DT, Hegedus, AH & Swager, TM: Signal amplification of a "turn-on" sensor: Harvesting the light captured by a conjugated polymer. *Journal of the American Chemical Society,* 122**:** 12389-12390, 2000.
151. McQuade, DT, Pullen, AE & Swager, TM: Conjugated polymer-based chemical sensors. *Chemical Reviews,* 100**:** 2537-2574, 2000.
152. Mecke, A, Majoros, InJ, Patri, AK, James R. Baker, J, Holl, MMB & Orr, BG: Lipid Bilayer Disruption by Polycationic Polymers: The Roles of Size and Chemical Functional Group. *Langmuir,* 21**:** 10348-10354, 2005.
153. Mirata, H, Koepsel, RR, Matyjaszewski, K & Russell, AJ: Permanent, non-leaching antibacterial surfaces--2: How high density cationic surfaces kill bacterial cells. *Biomaterials,* 28**:** 4870-4879, 2007.
154. Molecular_Probes: Nucleic Acid Stains—Section 8.1. *Molecular Probes-The Handbook.* Invitrogen (web site), 2010.
155. Monod, J: *Recherches sur la Croissance des Cultures Bacte´riennes,* Paris, Hermann & Co. 1942.
156. Monod, J: The growth of bacterial cultures. *Annu Rev Microbiological Research,* 3**:** 371-394, 1949.

157. Mortimer, FC, Mason, DJ & Gant, VA: Flow cytometric monitoring of antibiotic-induced injury in Escherichia coli using cell-impermeant fluorescent probes. *Antimicrobial Agents and Chemotherapy,* 44**:** 676-681, 2000.
158. Mulyukin, AL, Demkina, EV, Kryazhevskikh, NA, Suzina, NE, Vorob'eva, LI, Duda, VI, Galchenko, VF & El-Registan, GI: Dormant forms of Micrococcus luteus and Arthrobacter globiformis not platable on standard media. *Microbiology,* 78**:** 407-418, 2009.
159. Murata, H, Koepsel, RR, Matyjaszewski, K & Russell, AJ: Permanent, non-leaching antibacterial surfaces - 2: How high density cationic surfaces kill bacterial cells. *Biomaterials,* 28**:** 4870-4879, 2007.
160. Mutlu, GM & Wunderink, RG: Severe pseudomonal infections. *Current Opinion in Critical Care,* 12**:** 458-463, 2006.
161. Nardello, V, Azaroual, N, Cervoise, I, Vermeersch, G & Aubry, JM: Synthesis and photooxidation of sodium 1,3-cyclohexadiene-1,4-diethanoate: A new colorless and water-soluble trap of singlet oxygen. *Tetrahedron,* 52**:** 2031-2046, 1996.
162. Nardello, V, Azaroual, N, Cervoise, I, Vermeersch, G & Aubry, JM: Synthesis and photooxidation of sodium 1,3-cyclohexadiene-1,4-diethanoate: A new colorless and water-soluble trap of singlet oxygen. *Tetrahedron,* 52**:** 2031-2046, 1996.
163. Nardello, V, Brault, D, Chavalle, P & Aubry, JM: Measurement of photogenerated singlet oxygen (O-1(2) ((1)Delta(g))) in aqueous solution by specific chemical trapping with sodium 1,3-cyclohexadiene-1,4-diethanoate. *Journal of Photochemistry and Photobiology B-Biology,* 39**:** 146-155, 1997.
164. Nebe-von-Caron, G, Stephens, PJ, Hewitt, CJ, Powell, JR & Badley, RA: Analysis of bacterial function by multi-colour fluorescence flow cytometry and single cell sorting. *Journal of Microbiological Methods,* 42**:** 97-114, 2000.
165. Nikaido, H: Molecular basis of bacterial outer membrane permeability revisited. *Microbiology and Molecular Biology Reviews,* 67**:** 593-+, 2003.
166. Novo, DJ, Perlmutter, NG, Hunt, RH & Shapiro, HM: Multiparameter flow cytometric analysis of antibiotic effects on membrane potential, membrane permeability, and bacterial counts of Staphylococcus aureus and Micrococcus luteus. *Antimicrobial Agents and Chemotherapy,* 44**:** 827-834, 2000.
167. Ogawa, K, Chemburu, S, Lopez, GP, Whitten, DG & Schanze, KS: Conjugated polyelectrolyte-grafted silica microspheres. *Langmuir,* 23**:** 4541-4548, 2007.
168. Partee, J, Frankevich, EL, Uhlhorn, B, Shinar, J, Ding, Y & Barton, TJ: Delayed fluorescence and triplet-triplet annihilation in pi-conjugated polymers. *Physical Review Letters,* 82**:** 3673-3676, 1999.
169. Pecson, BM, Martin, LV & Kohn, T: Quantitative PCR for Determining the Infectivity of Bacteriophage MS2 upon Inactivation by Heat, UV-B Radiation, and Singlet Oxygen: Advantages and Limitations of an Enzymatic Treatment To Reduce False-Positive Results. *Applied and Environmental Microbiology,* 75**:** 5544-5554, 2009.
170. Pinto, MR, Kristal, BM & Schanze, KS: A water-soluble poly(phenylene ethynylene) with pendant phosphonate groups. Synthesis, photophysics, and layer-by-layer self-assembled films. *Langmuir,* 19**:** 6523-6533, 2003.
171. Pinto, MR & Schanze, KS: Conjugated polyelectrolytes: Synthesis and applications. *Synthesis-Stuttgart***:** 1293-1309, 2002.

172. Poole, K: Mechanisms of bacteria biocide and antibiotic resistance. *Society for Applied Microbiology Symposium Series***:** 55S-64S, 2002.
173. Prakash, B, Veeregowda, BM & Krishnappa, G: Biofilms: A survival strategy of bacteria. *Current Science (Bangalore)*, 85**:** 1299-1307, 2003.
174. Prats, C, Lopez, D, Giro, A, Ferrer, J & Valls, J: Individual-based modelling of bacterial cultures to study the microscopic causes of the lag phase. *Journal of Theoretical Biology*, 241**:** 939-953, 2006.
175. Qiu, Y, Zhang, N, An, YH & Wen, X: Biomaterial strategies to reduce implant-associated infections. *International Journal of Artificial Organs*, 30**:** 828-841, 2007.
176. Rashid, F & Horobin, RW: ACCUMULATION OF FLUORESCENT NON-CATIONIC PROBES IN MITOCHONDRIA OF CULTURED-CELLS - OBSERVATIONS, A PROPOSED MECHANISM, AND SOME IMPLICATIONS. *Journal of Microscopy-Oxford*, 163**:** 233-241, 1991.
177. Rechinger, KB & Siegumfeldt, H: Rapid assessment of cell viability of Lactobacillus delbrueckii subsp. bulgaricus by measurement of intracellular pH in individual cells using fluorescence ratio imaging microscopy. *International Journal of Food Microbiology*, 75**:** 53-60, 2002.
178. Richards, JJ, Ballard, TE & Melander, C: Inhibition and dispersion of Pseudomonas aeruginosa biofilms with reverse amide 2-aminoimidazole oroidin analogues. *Organic & Biomolecular Chemistry*, 6**:** 1356-1363, 2008.
179. Russell, AD: Bacterial resistance to disinfectants: Present knowledge and future problems. *Journal of Hospital Infection*, 43**:** S57-S68, 1999.
180. Russell, AD, Tattawasart, U, Maillard, JY & Furr, JR: Possible link between bacterial resistance and use of antibiotics and biocides. *Antimicrobial Agents and Chemotherapy*, 42**:** 2151-2151, 1998.
181. Sauvet, G, Fortuniak, W, Kazmierski, K & Chojnowski, J: Amphiphilic block and statistical siloxane copolymers with antimicrobial activity. *Journal of Polymer Science, Part A: Polymer Chemistry*, 41**:** 2939-2948, 2003.
182. Schreier, S, Malheiros, SVP & de Paula, E: Surface active drugs: self-association and interaction with membranes and surfactants. Physicochemical and biological aspects. *Biochimica Et Biophysica Acta-Biomembranes*, 1508**:** 210-234, 2000.
183. Senthilikumar, S, Nath, S & Pal, H: Photophysical properties of coumarin-30 dye in aprotic and protic solvents of varying polarities. *Photochemistry and Photobiology*, 80**:** 104-111, 2004.
184. Shapiro, HM: Membrane potential estimation by flow cytometry. *Methods*, 21**:** 271-279, 2000.
185. Shapiro, HM: Multiparameter flow cytometry of bacteria: Implications for diagnostics and therapeutics. *Cytometry*, 43**:** 223-226, 2001.
186. Shapiro, HM: *Practical Flow Cytometry*, Hoboken, New Jersey, Wiley-Liss 2003.
187. Shirai, A, Maeda, T, Masayo, K, Kawano, G & Kourai, H: Control of Legionella species and host amoeba by bis-quaternay ammonium compounds. *Biocontrol Science*, 5**:** 97-102, 2000.
188. Shvalov, AN, Surovtsev, IV, Chernyshev, AV, Soini, JT & Maltsev, VP: Particle classification from light scattering with the scanning flow cytometer. *Cytometry*, 37**:** 215-220, 1999.

189. Silverman, JA, Perlmutter, NG & Shapiro, HM: Correlation of daptomycin bactericidal activity and membrane depolarization in Staphylococcus aureus. *Antimicrobial Agents and Chemotherapy,* 47**:** 2538-2544, 2003.
190. Som, A, Vemparala, S, Ivanov, I & Tew, GN: Synthetic mimics of antimicrobial peptides. *Biopolymers,* 90**:** 83-93, 2008.
191. Stickler, DJ: Susceptibility of antibiotic-resistant Gram-negative bacteria to biocides: A perspective from the study of catheter biofilms. *Society for Applied Microbiology Symposium Series***:** 163S-170S, 2002.
192. Stoimenov, PK, Klinger, RL, Marchin, GL & Klabunde, KJ: Metal oxide nanoparticles as bacteriocidal agents. *Langmuir,* 18**:** 6679-6686, 2002.
193. Suschke, U, Sporer, F, Schneele, J, Geiss, HK & Reichling, J: Antibacterial and cytotoxic activity of Nepeta cataria L., N-cataria var. citriodora (Beck.) Balb. and Melissa officinalis L. essential oils. *Natural Product Communications,* 2**:** 1277-1286, 2007.
194. Suzuki, N, Mizumoto, I, Itami, T, Takahashi, Y, Tanaka, R, Hatate, H, Nomoto, T & Kozawa, A: Virucidal effect of singlet oxygen on penaeid white spot syndrome virus. *Fisheries Science,* 66**:** 166-168, 2000.
195. Tan, CY, Alas, E, Muller, JG, Pinto, MR, Kleiman, VD & Schanze, KS: Amplified quenching of a conjugated polyelectrolyte by cyanine dyes. *Journal of the American Chemical Society,* 126**:** 13685-13694, 2004.
196. Tan, CY, Pinto, MR & Schanze, KS: Photophysics, aggregation and amplified quenching of a water-soluble poly(phenylene ethynylene). *Chemical Communications***:** 446-447, 2002.
197. Taranekar, P, Qiao, Q, Jiang, H, Ghiviriga, I, Schanze, KS & Reynolds, JR: Hyperbranched conjugated polyelectrolyte bilayers for solar-cell applications. *Journal of the American Chemical Society,* 129**:** 8958-+, 2007.
198. Thomas, SW, Joly, GD & Swager, TM: Chemical sensors based on amplifying fluorescent conjugated polymers. *Chemical Reviews,* 107**:** 1339-1386, 2007.
199. Thorsteinsson, T, Masson, M, Kristinsson, KG, Hjalmarsdottir, MA, Hilmarsson, H & Loftsson, T: Soft antimicrobial agents: Synthesis and activity of labile environmentally friendly long chain quaternary ammonium compounds. *Journal of Medicinal Chemistry,* 46**:** 4173-4181, 2003.
200. Tiller, JC, Liao, CJ, Lewis, K & Klibanov, AM: Designing surfaces that kill bacteria on contact. *Proceedings of the National Academy of Sciences of the United States of America,* 98**:** 5981-5985, 2001.
201. Tortora, GJ, Funke, BR & Case, CL: *Microbiology-An Introduction,* Redwood City, CA, The Benjamin/Cummings Publishing, Co., Inc. 1995.
202. Tratnyek, PG, Elovitz, MS & Colverson, P: PHOTOEFFECTS OF TEXTILE DYE WASTEWATERS - SENSITIZATION OF SINGLET OXYGEN FORMATION, OXIDATION OF PHENOLS AND TOXICITY TO BACTERIA. *Environmental Toxicology and Chemistry,* 13**:** 27-33, 1994.
203. Tsuang, YH, Sun, JS, Huang, YC, Lu, CH, Chang, WHS & Wang, CC: Studies of photokilling of bacteria using titanium dioxide nanoparticles. *Artificial Organs,* 32**:** 167-174, 2008.

204. Tzeng, DD, Lee, MH, Chung, KR & Devay, JE: Products in Light-Mediated Reactions of Free Methionine Riboflavin Mixtures That Are Biocidal to Microorganisms. *Canadian Journal of Microbiology,* 36**:** 500-506, 1990.
205. Vaara, M & Vaara, T: Poly Cations Sensitize Enteric Bacteria to Antibiotics. *Antimicrobial Agents and Chemotherapy,* 24**:** 107-113, 1983.
206. Valduga, G, Bertoloni, G, Reddi, E & Jori, G: EFFECT OF EXTRACELLULARLY GENERATED SINGLET OXYGEN ON GRAM-POSITIVE AND GRAM-NEGATIVE BACTERIA. *Journal of Photochemistry and Photobiology B-Biology,* 21**:** 81-86, 1993.
207. Vandilla, MA, Trujillo, TT, Mullaney, PF & Coulter, JR: CELL MICROFLUOROMETRY - A METHOD FOR RAPID FLUORESCENCE MEASUREMENT. *Science,* 163**:** 1213-&, 1969.
208. Walsh, SE, Maillard, JY, Russell, AD, Catrenich, CE, Charbonneau, DL & Bartolo, RG: Activity and mechanisms of action of selected biocidal agents on Gram-positive and -negative bacteria. *Journal of Applied Microbiology,* 94**:** 240-247, 2003.
209. Walsh, SE, Maillard, JY, Russell, AD, Catrenich, CE, Charbonneau, DL & Bartolo, RG: Development of bacterial resistance to several biocides and effects on antibiotic susceptibility. *Journal of Hospital Infection,* 55**:** 98-107, 2003.
210. Walters, KA, Ley, KD & Schanze, KS: Triplet state photophysics in an aryleneethynylene pi-conjugated polymer. *Chemical Communications***:** 1115-1116, 1998.
211. Wang, H-H & Lin, MS: QAS polymers as biocides. *Journal of Polymer Research,* 5**:** 177-186, 1998.
212. Wang, YS & Schanze, KS: Photochemical Probes of Intramolecular Electron and Energy-Transfer. *Chemical Physics,* 176**:** 305-319, 1993.
213. Werle, P, Trageser, M & Stober, R: *German patent application.* 1991.
214. Whitman, WB, Coleman, DC & Wiebe, WJ: Prokaryotes: The unseen majority. *Proc. Natl. Acad. Sci. USA,* 95**:** 6578-6583, 1998.
215. Wickens, HJ, Pinney, RJ, Mason, DJ & Gant, VA: Flow cytometric investigation of filamentation, membrane patency, and membrane potential in Escherichia coli following ciprofloxacin exposure. *Antimicrobial Agents and Chemotherapy,* 44**:** 682-687, 2000.
216. Wilkinson, F, Helman, WP & Ross, AB: Quantum Yields for the Photosensitized Formation of the Lowest Electronically Excited Singlet-State of Molecular-Oxygen in Solution. *Journal of Physical and Chemical Reference Data,* 22**:** 113-262, 1993.
217. Worley, SD, Eknoian, M, Bickert, J & Williams, JF: Abstracts of Papers. *216th National Meeting of the American Chemical Society.* Boston, MA, American Chemical Society, Wahington, DC, 1998 pp POLY-410.
218. Wozniak, E, Mozrzymas, A, Czarny, A, Kocieba, M, Rozycka-Roszak, B, Dega-Szafran, Z, Dulewicz, E & Petryna, M: Antimicrobial activity of N-alkoxycarbonylmethyl-N-alkyl-piperidinium chlorides. *Zeitschrift Fur Naturforschung C-a Journal of Biosciences,* 59**:** 782-786, 2004.

219. Zeineldin, R, Piyasena, ME, Bergstedt, TS, Sklar, LA, Whitten, D & Lopez, GP: Superquenching as a detector for microsphere-based flow cytometric assays. *Cytometry Part A,* 69A**:** 335-341, 2006.
220. Zeineldin, R, Piyasena, ME, Sklar, LA, Whitten, D & Lopez, GP: Detection of membrane biointeractions based on fluorescence superquenching. *Langmuir,* 24**:** 4125-4131, 2008.
221. Zhao, XY, Pinto, MR, Hardison, LM, Mwaura, J, Muller, J, Jiang, H, Witker, D, Kleiman, VD, Reynolds, JR & Schanze, KS: Variable band gap poly(arylene ethynylene) conjugated polyelectrolytes. *Macromolecules,* 39**:** 6355-6366, 2006.
222. Zhou, Q & Swager, TM: Fluorescent chemosensors based on energy migration in conjugated polymers: The molecular wire approach to increased sensitivity. *Journal of the American Chemical Society,* 117**:** 12593-12602, 1995.
223. Zhu, HG, Stein, EW, Lu, ZH, Lvov, YM & McShane, MJ: Synthesis of size-controlled monodisperse manganese carbonate microparticles as templates for uniform polyelectrolyte microcapsule formation. *Chemistry of Materials,* 17**:** 2323-2328, 2005.

Appendix A

Syntheses of Conjugated Electrolytes

Reagents

All chemicals used for synthesis were of reagent grade and purchased from Sigma-Aldrich Chemical Company or from J.T. Baker. Unless otherwise noted, chemicals and reagents were used without further purification. Reactions were carried out under a nitrogen atmosphere using freshly distilled solvents. Tetrahydrofuran and triethylamine were distilled over sodium hydride under nitrogen prior to use. Dichloromethane was distilled over phosphorus pentoxide. 1 M tetrabutylammonium fluoride THF solution (Aldrich), copper(I) iodide, iodine monochloride, diisopropylamine (Acros), trimethylsilylacetylene (GFS), and tetrakis(triphenylphosphine)- palladium(0) (Strem) were used as received. All other analyticalgrade chemicals and solvents were used without any further treatment.

Monomers

1,4-Diiodo-2,5-bis[2-(2-methoxyethoxy)ethoxy]benezene (4a). 2,5-Diiodohydroquinone (**3**) (5.79 g, 16 mmol), (2-Methoxyethoxy)ethyl tosylate (11.0 g, 40 mmol), and potassium carbonate (5.52 g, 40 mmol) were combined in a flask with100 mL of acetone. The mixture was heated to 70°C and kept stirring for overnight. The mixture was filtered and filtrate concentrated by rotary evaporation. Water was added and product was extracted with chloroform. The product was purified by column chromatography on silica using 2:3 mixture of ethyl acetate and hexane. Solvent was removed by rotary evaporation to give yellow oil. ^{1}H NMR (300 MHz, $CDCl_3$): δ 3.40 (s,

6H), 3.58 (m, 4H), 3.78 (m, 4H), 3.88 (m, 4H), 4.11 (m, 4H), 7.23 (s, 2H). ^{13}C NMR (75 MHz, $CDCl_3$): δ 59.5, 69.9, 70.7, 71.4, 72.4, 86.7, 123.8, 153.4.

1,4-diethynyl-2,5-bis[2-(2-methoxyethoxy)ethoxy]benezene (5a). Compound **4a** (5.65 g, 10 mmol), trimethylsilylacetylene (3.1 mL, 22 mmol), CuI (57 mg, 0.3 mmol), and $Pd(PPh_3)_4$ (0.35 g, 0.3 mmol) were dissolved in 60 mL of THF and 40 mL of diisopropyl amine. The mixture was warmed to 70°C and kept stirring overnight. Water was added and the mixture was extracted with ether followed by several washings with water. Solvent was removed *in vacuo*. The product was purified by column chromatography on silica using 1:4 mixture of ethyl acetate and hexane. Solvent was removed by rotary evaporation to give a white solid.

The white solid was dissolved in 50 mL of methanol. To the solution, 50 mL of 1M NaOH(aq) was added and refluxed for 2 hours. Water was added to the mixture and extracted with ether. The organic layer was washed with water several times, then dried with Na_2SO_4. Solvent was removed by rotary evaporation to give reddish solid. The product was purified column chromatography on silica using 2:3 mixture of ethyl acetate and hexane to give white solid after evaporation of the solvent. ^{1}H NMR (300 MHz, CDCl3): δ 3.32 (s, 2H), 3.38 (s, 6H), 3.56 (m, 4H), 3.75 (m, 4H), 3.87 (m, 4H), 4.15 (m, 4H), 6.99 (s, 2H). ^{13}C NMR (75 MHz, CDCl3): δ 59.4, 69.9, 69.9, 71.3, 72.4, 79.9, 83.1, 113.9, 118.6, 154.4.

3,3'-[(2,5-diiodo-1,4-phenylene)bis(oxy)]bis[N,N,N-triethyl-1-propanaminium] bromide salt (**7b**). Compound 4 (3.01 g 5 mmol) was suspended in a mixture of 100 mL of triethylamine, 38 mL of water, 56 mL of ethanol, and 56 mL of acetone. The mixture was refluxed overnight. The solvent was evaporated and the residue

was washed with acetone several times to yield white solid. ^{1}H NMR (300 MHz, CD_3OD): δ 1.30 (t, 12H), 2.16 (m, 4H), 3.33 (q, 8H), 3.45 (m, 4H), 4.04 (m, 4H), 7.30 (s, 2H). ^{13}C NMR (75 MHz, CD_3OD): δ 8.1, 23.3, 54.3, 55.9, 67.9, 87.2, 124.1, 154.1.

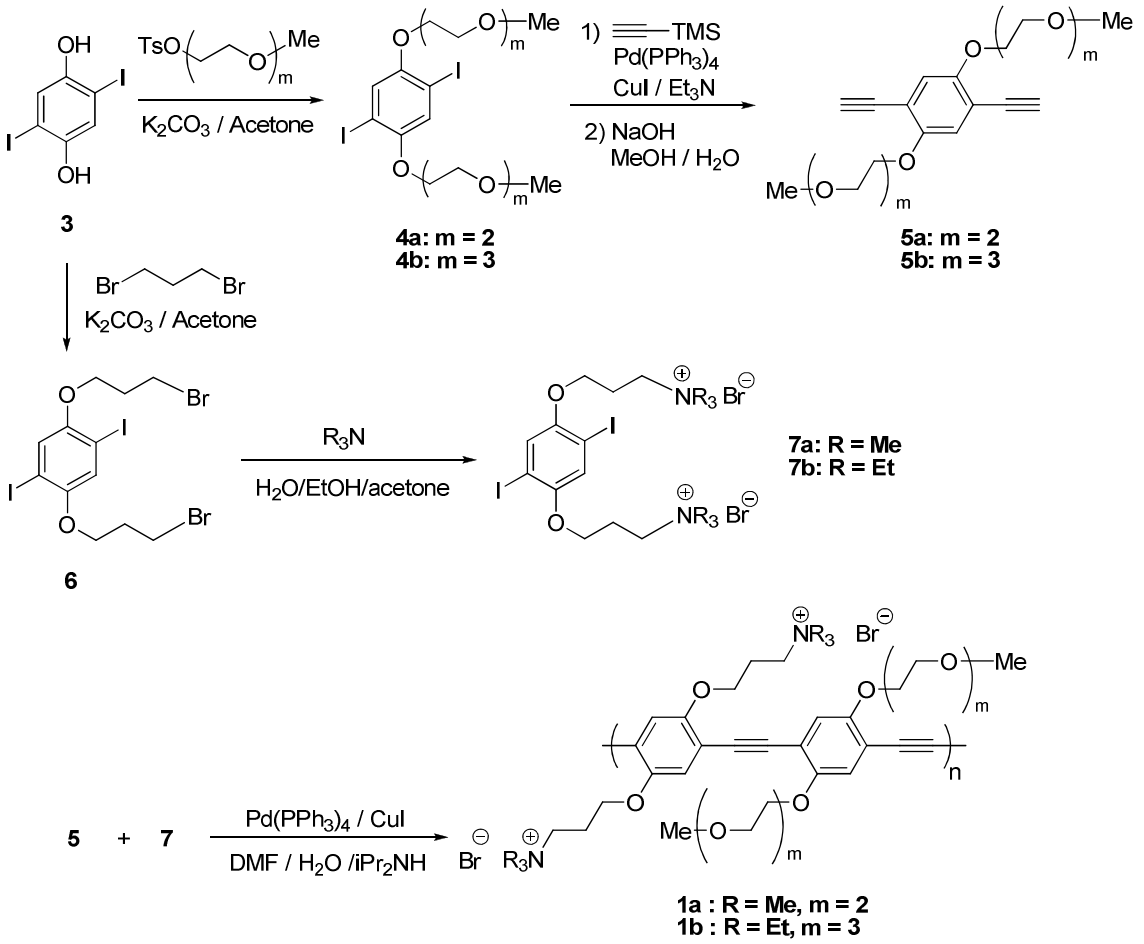

Scheme A-1**.** General synthetic scheme for polymers **1a** and **1b**. (NOTE: compound numbering, with the exception of **1a** and **1b**, is unique to this appendix.)

Polymers

PPE-OR8 (1a) and -OR11 (1b)

Compound **5a** (362 mg, 1 mmol), compound **7a** (722 mg, 1 mmol), CuI (5.7 mg, 0.03 mmol), and $Pd(PPh_3)_4$ (35 mg, 0.03 mmol) were dissolved in a mixture of 30 mL of DMF, 20 mL of water, and 10 mL of diisopropylamine. The mixture was heated to 70°C

and kept stirring overnight. The reaction mixture was concentrated by rotary evaporation and added dropwise into 250 mL of acetone. The precipitate was dissolved in a small amount of Millipore water and filtered through quantitative filter paper, followed by a 25 µm glass filter. The solution was dialyzed against water using 6-8 kD MWCO cellulose membrane. The solution was concentrated via rotary evaporation and the polymer was precipitated with acetone. The precipitate was collected by centrifugation and washed with acetone. The product was a bright yellow powder and it was dried under vacuum for 5 hours. ^{1}H NMR (300 MHz, CD_3OD): δ 2.46 (br), 3.05 (br), 3.14 (br), 3.44 (br), 3.60 (br), 3.79 (br), 4.16 (br), 7.16 (br). **Polymer 1b** was synthesized in a similar procedure using compound **5b** (451 mg, 1 mmol), compound **7b** (806 mg, 1 mmol) ^{1}H NMR (300 MHz, CD_3OD): δ 1.37 (br), 2.22 (br), 3.02 (br), 3.39 (br), 3.52 (br), 3.75 (br), 4.11 (br), 7.37 (br).

PPE-DABCO (2)

Polymer **2**, (221). A deoxygenated solution of 69 mg (60 µmol) of $Pd(PPh_3)_4$ and 11 mg (60 µmol) of CuI in 25 mL of DMF/ diisopropylamine 1:1 mixture was added via canula to a deoxygenated solution of 0.380 g (2.00 mmol) of 4 and 1.62 g (2.00 mmol) of 6 in 150 mL of a DMF/water mixture (1:1 v/v) contained in a Schlenk flask. The resulting solution was purged with argon for 10 min and then stirred at 70 °C for 24 h. After cooling, the polymerization reaction was terminated by pouring the reaction mixture into 700 mL of diethyl ether/acetone/methanol (3:1:1 v/v/v). The precipitated polymer was collected by vacuum filtration and redissolved in 50 mL of DMF/water (2:1 v/v). (This solution was not treated with NaCN.) The polymer was again precipitated by addition to 700 mL of diethyl ether/acetone/methanol. The precipitate was isolated by

filtration, and it was purified by dialysis against water using a 6000-8000 MWCO cellulose membrane. After dialysis, the polymer solution was filtered through a 0.45 µm nylon membrane, and the concentration was adjusted to ca. 1.0 mg mL-1. The polymer was stored in this format and diluted as appropriate for spectroscopic studies. 2,5-Diiodohydroquinone(196) (**3**), 1,4-diiodo-2,5-bis[2-[2-(2-methoxyethoxy)ethoxy]ethoxy]benzene(167) (**4b**), 1,4-diethynyl-2,5-bis[2-[2-(2-methoxyethoxy)ethoxy]ethoxy]benzene(167) (**5b**), 1,4-bis(3-bromopropoxy)-2,5-diiodobenzene(150) (**6**), and 3,3'-[(2,5-diiodo-1,4-phenylene)bis(oxy)]bis[N,N,N-trimethyl-1-propanaminium] bromide salt(150) (**7a**), sodium 1,3-cyclohexadiene 1,4-diethanoate (CHDDE)(162) were synthesized according to the literature procedure. Unless otherwise noted, ^{1}H and ^{13}C NMR spectra were recorded on either a Varian Gemini 300, VXR 300, or Mercury 300 spectrometer, and chemical shifts are reported in ppm relative to TMS.

PPENMe$_3$-Th

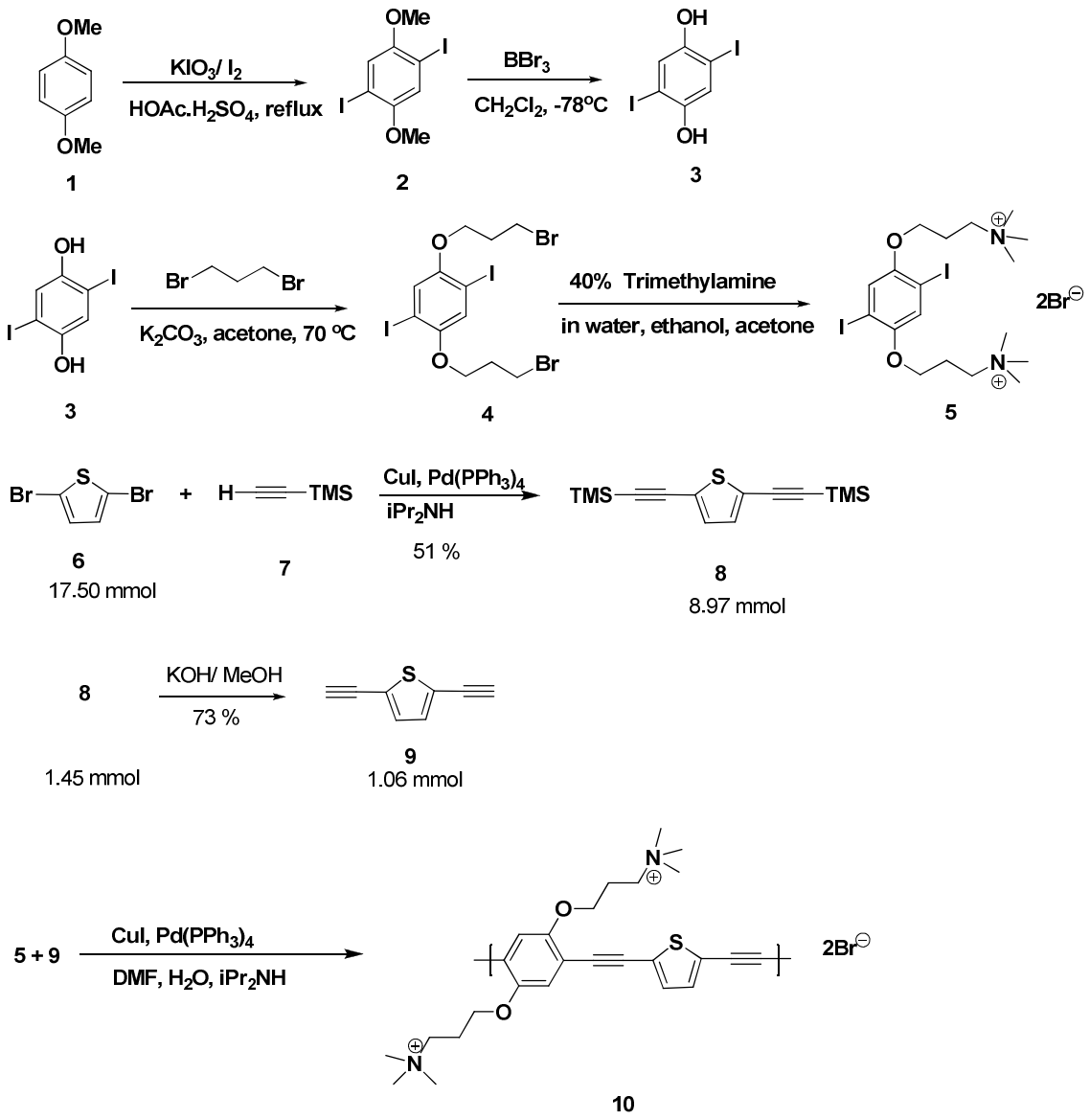

Scheme A-2. Synthesis of PPE-Th.

Oligomers

Scheme A-3 shows a typical oligomer synthesis. Condensation chemistry is much the same as for polymers, but requires step-wise protection/deprotection for some configurations. The diethynylbenzene molecule that functions as the central linker can also be substituted with various moieties

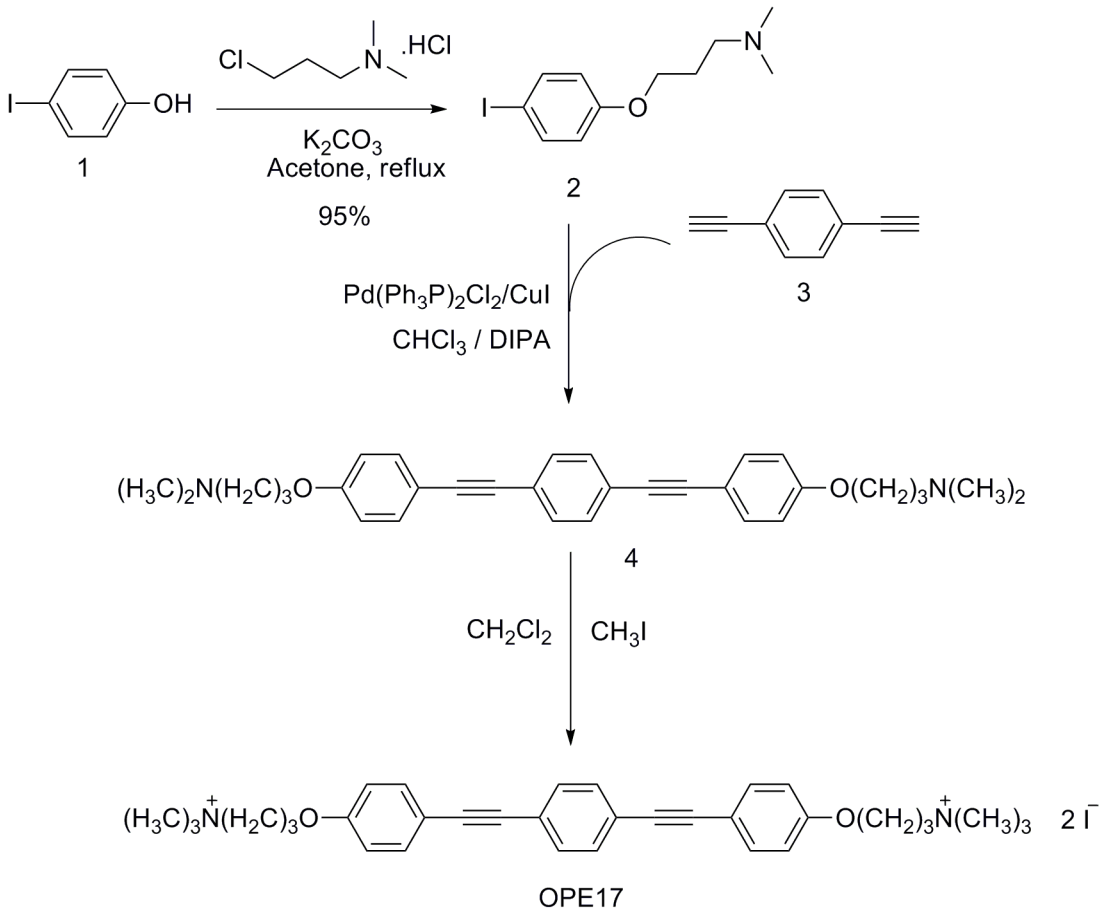

Scheme A-3. Synthetic route to OPE17.

Appendix B

Photophysical Characterization

The majority of the photophysical measurement and characterization of the CPE polymers was carried out at the University of Florida by K. Ogawa and E. Ji.

Methods

UV spectra

UV-visible absorption spectra were obtained either on a Perkin-Elmer Lambda 25 dual beam absorption spectrometer or on a Cary 100 UV-vis spectrophotometer using 1 cm quartz cells. Steady-state fluorescence emission and excitation spectra were recorded on either SPEX FluoroMax spectrophotometer or Fluorolog 3 spectrophotometer. Steady-state fluorescence emission spectra for particles were recorded on a SPEX TRIAX 180 spectrograph coupled with a Spectrum One CCD detector. Transient absorption difference spectra were collected using a 1cm path length cell on an apparatus described elsewhere.(212) Solutions were prepared in water or methanol and purged with argon for 1 hour before making transient absorption spectroscopy measurements. The 3rd harmonic (355 nm) of a Continuum Surelite II-10 Nd:YAG laser was used as the excitation source. Singlet oxygen quantum yields were determined in water or methanol according to the procedures described elsewhere.

Characterization of PPE-OR8 (1a)

Transient absorption spectroscopy

In previous studies, we have shown that direct excitation of PPE-type conjugated polymers affords triplet excited states (triplet excitons) with moderate efficiency.(212,

210, 46, 168, 61) The triplet state is typically detected by its characteristic long-lived transient absorption in the red of the visible region. Since the triplet state plays a key role in the production of reactive oxygen species (i.e., singlet oxygen), in the course of the present study we carried out transient absorption spectroscopy of **1a** in methanol and water solutions to confirm that direct excitation of the polymer affords a triplet excited state.

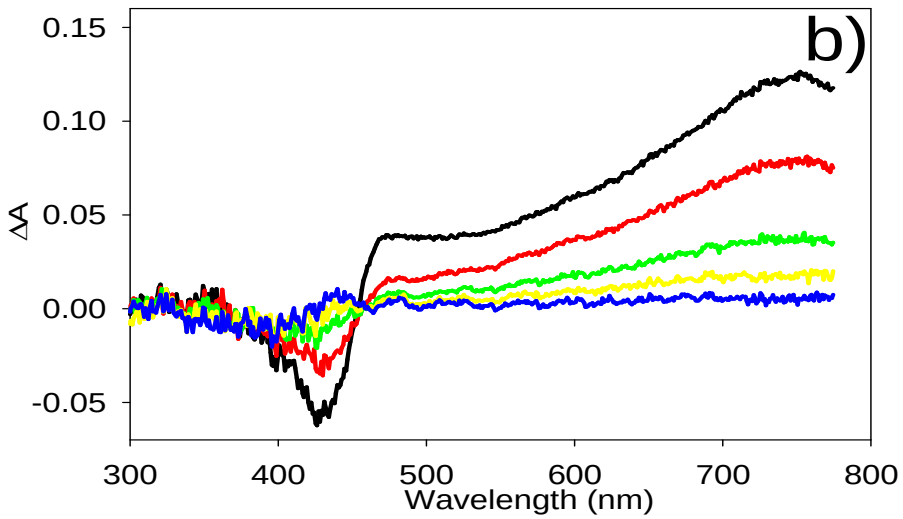

Figure B-1. Transient absorption difference spectra of **1a** in methanol. Delays: 50 ns (—), 1050 ns (—), 3050 ns (—), 5050 ns (—), 9050 ns (—).

As shown in Figure B-1, pulsed laser excitation (λ = 355 nm) of methanol and water solutions of **1a** affords a long-lived transient absorption that is characterized by ground state bleaching (400 – 450 nm) and an intense, broad transient absorption band with λ_{max} ~ 760 nm. The transient absorption decays with lifetimes of 57 µs in aqueous solution and 5.1 µs in methanol solution. Taken together, the spectral profile and long lifetimes provide strong evidence that the transient observed is due to the triplet excited state, and thus we conclude that direct excitation of **1a** in solution affords the triplet with moderate efficiency. Careful comparison of the amplitude of the transient absorption

observed for the polymer in water and methanol revealed that the triplet yield is larger in the latter solvent medium. This finding is consistent with the observation that the fluorescence of the polymer is reduced by aggregation in water. Apparently singlet quenching (by the aggregates) reduces the yield of the triplet state.

Singlet Oxygen Production.

On the basis of the transient absorption results which indicate that direct excitation of **1a** affords a triplet state in moderate yield, we anticipated that the cationic PPE-type CPEs might be able to sensitize the production of singlet oxygen ($^1O_2$). Thus, in order to explore this feature, near-infrared photoluminescence spectroscopy was applied to probe for the emission characteristic of $^1O_2$. As anticipated, excitation of a CD_3OD solution of polymer **1a** at 336 nm in the presence of oxygen gives rise to a moderately strong emission band at 1260 nm due to singlet oxygen phosphorescence (see supporting information). The concentration dependence of the $^1O_2$ emission was investigated by varying the polymer concentration and a linear correlation was observed between the polymer absorption at 335 nm and the $^1O_2$ emission intensity. The quantum yield of sensitized $^1O_2$ emission(148) by polymer **1a** in CD_3OD was determined as 0.13 ± 0.02 using 2'-acetonaphthone as an actinometer ($\Phi_\Delta = 0.79$).(216) This observation clearly indicates that PPE-type CPEs such as **1a** are able to sensitize $^1O_2$ with moderate efficiency.

Since the biocidal experiments were carried out in aqueous solution, we were interested in providing evidence that the cationic PPE-type CPEs will sensitize $^1O_2$ in water. However, near-infrared emission spectroscopy carried out with **1a** in D_2O in the presence of oxygen did not afford any detectable emission from $^1O_2$. This is likely due to

the fact that the quantum efficiency for $^1O_2$ emission is considerably less in D_2O, making it more difficult to detect in this medium. Thus, a second approach was used to detect for the sensitization of $^1O_2$ by the polymer. This method is based on the use of a water-soluble chemical trap, 1,3-cyclohexadiene-1,4-diethanoate (CHDDE), which forms a stable endoperoxide when it reacts with $^1O_2$. In these experiments disappearance of CHDDE was monitored by decrease of its absorption at 270 nm as a function of irradiation time (see supporting information for details). The quantum yields of singlet oxygen generation were determined following a literature procedure using 5,10,15,20-tetrakis(4-sulfonatophenyl)-porphyrin (TPPS) as an actinometer (Φ_Δ = 0.66) affording a value of 0.069 for $^1O_2$ generation by polymer **1a**.(148) This result confirms that the production of $^1O_2$ is sensitized in water, but with approximately 50% reduced efficiency compared to that in methanol. The decreased efficiency is consistent with the photophysical experiments which show that the triplet yield of **1a** is lower in water relative to methanol, presumably due to quenching of the singlet excited state by aggregation.

Oxygen gas was bubbled into CD_3OD solutions of polymer **1a** in the dark for 15 min with stirring. The oxygen-saturated polymer solutions were excited at 336 nm and steady-state near-IR phosphorescence spectra recorded on SPEX-2 fluorescence spectrophotometer equipped with an Indium-Gallium-Arsenide (InGaAs) detector. A long pass filter (LP850) was placed before the emission monochromator to eliminate UV and visible light. The singlet oxygen quantum yield of a sample can be calculated by the equation

$$\Phi_{\Delta s} = \frac{I_r}{I_s}\frac{I_{\Delta s}}{I_{\Delta r}}\frac{\tau_r}{\tau s}\Phi_{\Delta r} \qquad (6)$$

where I_s and I_r are the absorbed incident light, and $I_{\Delta s}$ and $I_{\Delta r}$ are the integrated singlet oxygen emission intensities of the sample (polymer **1a**)and the reference (2´-acetonaphthone), respectively. τ_s and τ_r are the singlet oxygen phosphorescence lifetime in the reference and the sample solvents and $\Phi_{\Delta r}$ is the singlet oxygen quantum yield of the reference compound. Quantum efficiency of sensitized singlet oxygen emission was determined following a literature procedure(148) using 2´-acetonaphthone as an actinometer ($\Phi_\Delta = 0.79$).(216)

Quantum Yields of Singlet Oxygen Generation by Chemical Trapping

Oxygen gas was bubbled into aqueous (D_2O) solutions containing CHDDE (100 µM), phosphate buffer (100 µM, pH 7.0), and polymer **1a** (2 µM) in the dark for 15min with stirring. Solutions were irradiated at 365 nm with stirring using a xenon short arc lamp equipped with a monochromator. Duration of irradiation was recorded and UV-visible spectra collected on Cary 100 UV-Vis Spectrophotometer. The disappearance of CHDDE was monitored as decrease in absorption at 270 nm. The quantum yields of singlet oxygen generation were determined following a literature procedure using 5,10,15,20-tetrakis(4-sulfonatophenyl)porphyrin (TPPS) as an actinometer (Φ_Δ = 0.66).(148)

The quantum yield can be calculated using equation 7.

$$\Phi_s = \Phi_r \times \frac{t_r}{t_s} \qquad (7)$$

where t_r and t_s are irradiation time to induce the oxidation of the same amount of CHDDE and Φ_r is the singlet oxygen quantum yield of the reference compound (TPPS). The irradiation time for 10 % loss of CHDDE was 48.7 ± 1.1 s (t_r) for TPPS and 467 ± 26 s

(t_s) for polymer **1a**. Thus, calculated quantum yield singlet oxygen generation by polymer **1a** is 0.069.

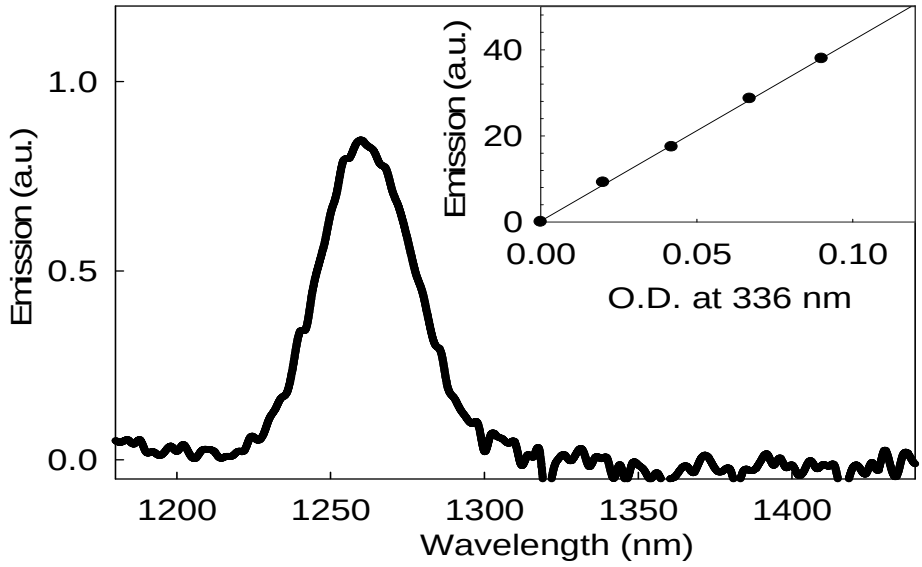

Figure B-2. Singlet oxygen emission sensitized by **1a** in CD_3OD. Inset: Integrated $^1O_2$ emission intensity versus optical density of the polymer solution.

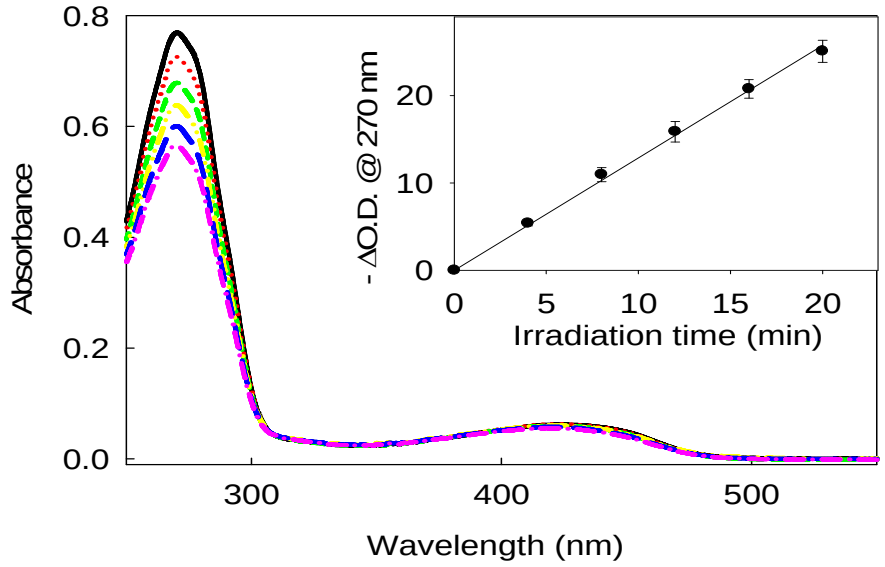

Figure B-3. UV-visible spectra of CHDDE (100 µM) and PPE-OR8 (**1a**) (2 µM) in D_2O solution containing phosphate buffer (100 µM, pH 7) as a function of the irradiation time (0 - 20 min). Inset: decrease of absorbance at 270 nm (%) as a function of irradiation time.

Characterization of PPE-Th (4)

The presence of the triplet excited state in **4** was confirmed by a broad intense transient absorption band centered at λ_{max} ~ 760 nm. As seen in Figure B-4, **4** exhibits a transient absorption band centered at λ_{max} ~ 760 nm quite similar to other PPE-based CPEs. The lifetimes of the transient absorption are 40 (± 10) µs in aqueous solution and 12 (±3) µs in methanol solution.

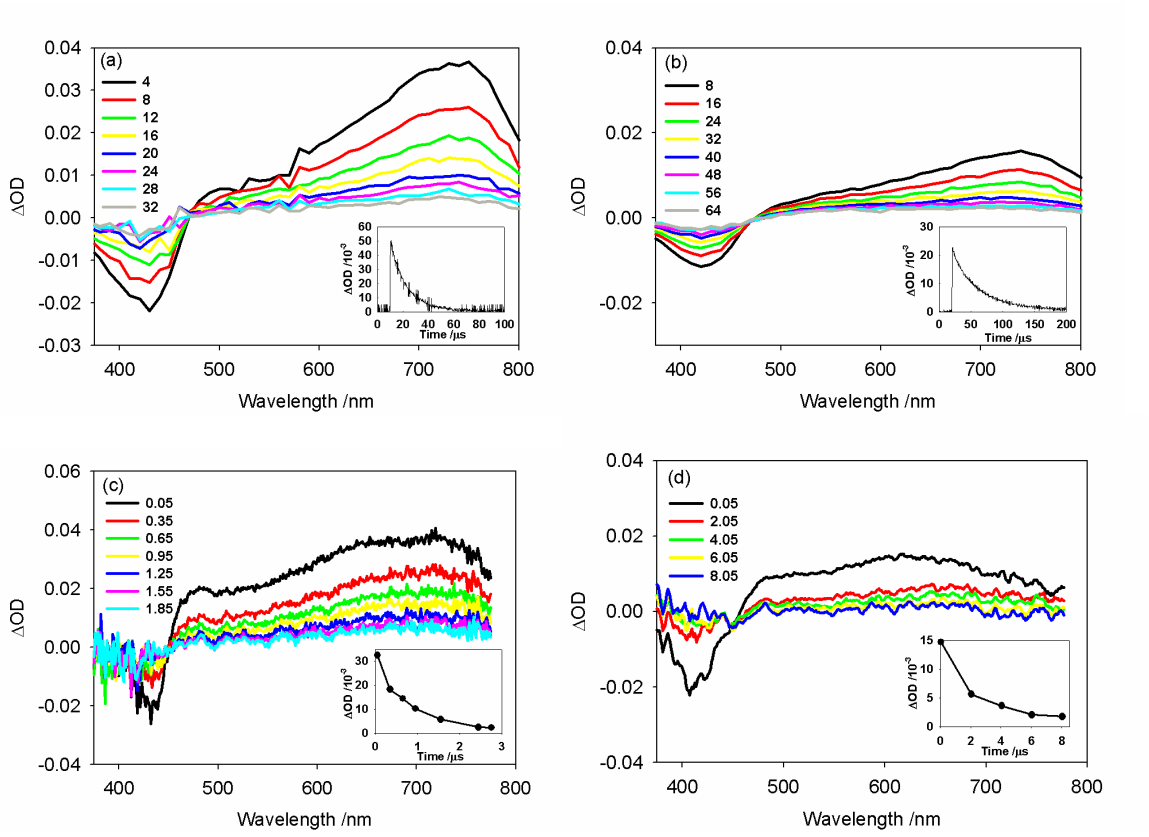

Figure B-4. Transient absorption difference spectra of **2** and **4**. (a) **4** in methanol, (b) **4** in water, (c) **2** in methanol, and (d) **2** in water. Insets: Transient absorption difference decay curves. All experiments were done with solutions having matched OD of 0.7 at 355 nm and excited with the same laser energy at 10 mJ. The spectra in (a) and (b) were obtained on the laser system described in ref. (212), and those in (c) and (d) were obtained on the system described in ref. (56).

The appearance of the spectra and lifetimes strongly suggest that the transient species is the triplet state of **4**. The lower intensity of the transient absorption in water

suggests that the triplet yield is lower in comparison to methanol solution. Such a lower triplet yield in water can be explained by aggregation of the polymer, which quenches the singlet excited state of the polymer. This is consistent with the reduced fluorescence intensity of polymer in water compared to in methanol.